2013

RESIDUAL STRESS RELIEF ANALYSIS ON LOW CARBON STEEL RINGS

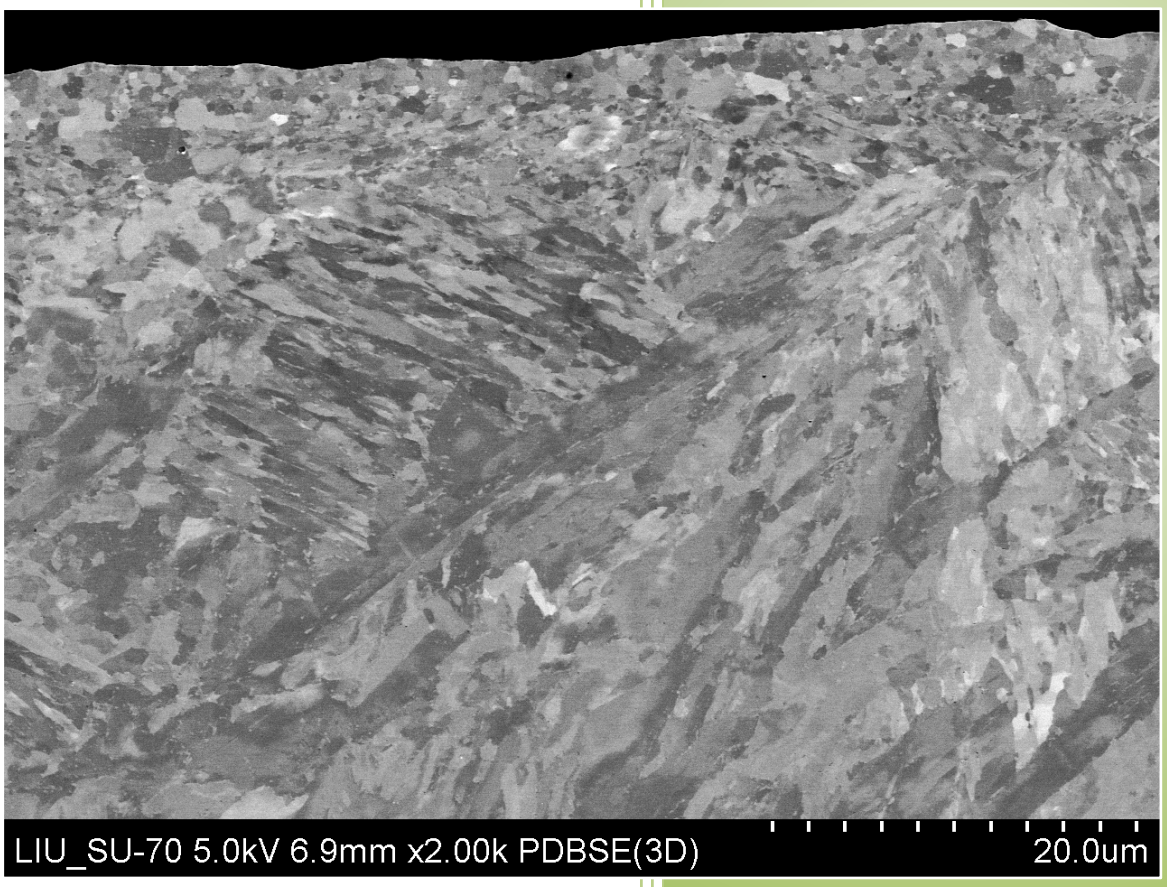

Daniel Lopez Gomez

Linköping's University

5/21/2013

ABSTRACT

The project carried out was based in analyzing which treatment was the finest to reduce the residual stress stored in the rings given after the machining was executed. Siemens A.B. sent three kinds of rings to analyze: the machined, the Heat Treated and the vibratory stress relieved (VSR). The aim was to compare the properties of them three and conclude which method was more suitable for the residual stress relief.
In order to get a conclusion, some tests were accomplished. First, small replicas of the real rings were given. The tests carried out were an X-Ray analysis, two microstructure analysis and two different hardness tests. Succeeding, new bigger rings were sent from Siemens A.B and some new tests were executed. First, the rings were cut using the sparkling method. Right after, the Hole Drilling technique and a X-Ray test were performed.

TABLE OF CONTENTS

1. INTRODUCTION

1.1 Background

A material can be yield to two kinds of stress. They are applied stress and residual stress. The first one is created by external forces acting on the material, which disappear when the action is over. However, residual stress remains in the material after the applied forces have been removed [1].

The main cause of the residual stress is the non-uniform plastic flow in consequence of the operations carried out in the material. Some of the causes could be welding, casting, quenching and cold working, such as bending, twisting, grinding and shot pending [1].

The residual stress might be decreased or even eliminated with special treatments. It is supposed that the residual stress is always harmful, but sometimes it is not. For instance, the residual tensile stress of the surface of a material is harmful as it is one of the most important causes of a brittle fracture. Nevertheless, compressive residual stress at the surface normally increases fatigue strength [1].

As it is mentioned above, residual stress can be introduced into metals by any process, such as mechanical, thermal or chemical processes [1].
In relation to mechanical processes, all cold working operations create residual stress. Examples of these operations are: the surface working, drawing, rolling, grinding, machining and assembling.
In thermal processes, there is a special classification when residual stress arising from thermal process is considered. This classification is divided in two groups: the residual stress arisen from a thermal gradient alone and the residual stress arisen from a thermal gradient in combination with a transformation phase [1]. Quenching and tempering are two examples; each one belongs to one of the groups respectively.
The chemical processes introduce residual stress into metals as well. For instance, oxidation, corrosion and electroplating are sources of residual stress [1].

1.2 Motivation and problem description

A local turbine manufacturer of Sweden (Siemens Industrial Turbomachinery AB in Finspång) is interested in knowing more about the Vibratory Stress Relief method. It is common in both gas and steam turbines to use forged rings that need to be machined to their final shape. Sometimes distortion of these rings can cause problems in the manufacturing of the components.

It is, therefore, often necessary to introduce an intermediate processing step involving residual stress relief. The conventional way is by a heat treatment. This can, however, cause other microstructural changes in the material. An alternative method is Vibratory Stress Relief (VSR).

1.3 Aim, Purpose and Method

The aim of this project could be divided in two different goals:

The first goal is to compare the residual stress profile (in depth from the surface) for three different conditions of the ring:

- As machined
- As Heat Treated
- As Vibratory stress relieved

The stresses are to be measured with the X-Ray diffraction technique and the Hole Drilling technique.
The second one will be to investigate if there are any microstructural differences between the different conditions listed above. It could include micro hardness measurements, degree of plastic deformation determined from X-Ray peak broadening analysis (from the measurements described above) and microstructural investigations using light microscope and Scanning Electron Microscope (SEM).

1.4 Structure of the essay

The essay will be divided into different sections. First of all, small replicas of the original rings would be analysed with the X-Ray diffraction method, microstructure analysis and two hardness testing methods. Some steps will be carried out so as to prepare the specimens for the tests. Two microstructure analysis will be executed, one using a light microscope and the other one using a Scanning Electron Microscope (SEM).
Once the tests are finished, bigger replicas will be sent by Siemens A.B. The aim of the new rings is to obtain a closer idea of the real behaviour of the rings. Those rings will be analysed with the Hole Drilling technique and the X-Ray diffraction as well.
Each chapter will contain the tests that will be executed and a conclusion of the results obtained.

2. SCIENTIFIC CONTEXT

The research carried out was based in mechanical problems occurred in the rings handling a kind of turbines in Siemens A.B. In order to analyse the problem and find a solution, a scientific context was studied. Once the physical properties and behaviours were analysed, there was an election of the appropriate tests to execute.

The rings given had diverse properties and, as a result, their behaviours differ. All the rings were machined and, afterwards, a heat treatment was given so as to increase their mechanical properties [7]. Another heat treatment was applied to one of the rings, a lower temperature treatment, as a method to reduce the residual stress created when machining it. There is another ring which was also modified. The treatment applied was a new technique designed to reduce the residual stress without a change of the properties of the material. It is the vibratory stress relief (VSR).

Residual stress has to be eliminated as it is a non-desirable circumstance. The consequences of leaving the stress are severe. It can accelerate corrosion and cracking of material fragments and, in combination with service loading, it may reduce the fatigue life and strength [4].

The traditional method practiced was annealing the material. The fatigue life was decreased by altering the material properties [3]. When the temperature is raised, the material yield stress becomes very low and it cannot support internal stresses. When cooling takes part, by avoiding the thermal contraction stresses, the material retains a non-stress state. Even if the method is effective, the cost is truly high and the modification of properties, such as plastic deformation [4], could not always be a desirable consequence. Moreover, an oxidation on the outside layer appears and, afterwards, it has to be removed [2].

As a substitution, the VSR method was created. It is based on the reduction of stress by a cyclic loading treatment. There are two procedures to reduce stress by vibrating the material, resonant and non-resonant vibrations. Applying the resonant method, the greatest vibratory stress appears at that amplitude and plastic deformation occurs. In the non-resonant method, the stress reduction is truly dependant on the vibration's amplitude [6]. The permanent deformation obtained makes the residual stress be relieved [5]. If the effectiveness could be proven, time, equipment and a high range of costs could be saved [2].

Some VSR researches were carried out. The results state that, with the appropriate vibration amplitude, the stress relaxation reached could be 40% [2]. The VSR treated material had an increase of the fatigue live of between 17% and 30%, although the thermal treated one experimented a decrease of the fatigue live of the 43% [3].

Another benefit of the VSR treatment in relation to the annealing process is that, while the thermal treatment makes the residual stress decrease to a thermal zero-stress point, VSR treatment reduces the residual stress to a structural zero-stress point. It implies that macro stresses could reappear in service if the treatment performed is annealing. It is because the VSR treatment is the one that relieves stress in active service, not by taking an advantage of the thermal change of properties [5].

3. THE STUDY

3.1 OLD DATA ANALYSIS

The lines that will follow are meant to show the results of the residual stress tests executed to three different kinds of rings. All of them were shaped by machining. They are equally sized, 430 mm of diameter, a thickness of 10 mm and 10 mm of width. They are also made of the same material, low carbon steel. The difference between them comes when talking about the treatment imparted to reduce the residual stress after machining them. The treatments chosen are: Heat treatment (H) and Vibratory Stress Relief (V). The one with no treatment will be appointed with an (M),
The measurements were taken, for each ring, in a portion of the whole ring in two different directions, as shown in the picture below.

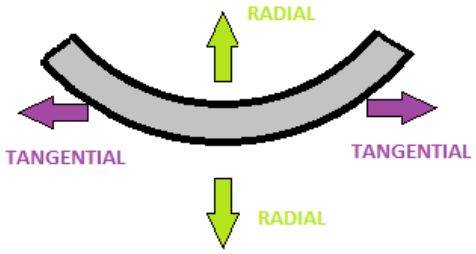

Figure 1.1 Description of the forces analysed in a piece of each ring

Before showing the graphics, a useful value, FWHM (Full width at half maximum), will be explained. It is the width measured in the middle of the peak of the maximum intensity of the diffraction peak obtained from X-Ray diffraction measurement [1]. The peaks measured in this test are 7 in depths from 200 µm to depths close to the surface, where the number of peaks measured increase to 11 (it is detailed in the Appendix). The FWHM value is the average of them. When the ring is machined, the dislocation density increases and the angle of diffraction of the X-Ray measurement as well. Consequently, the peak of maximum intensity decreases and the width increases, making this method a visible technique to measure the plastic deformation produced in the material. It is used to know if the properties of the material have changed after applying the treatments chosen.

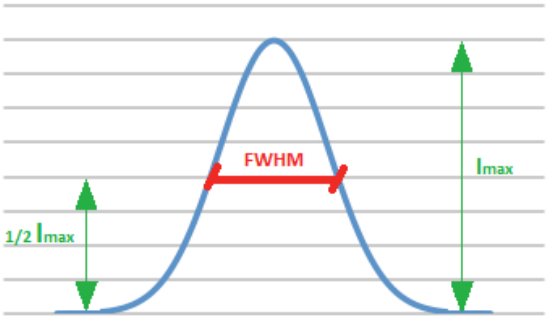

Figure 1.2 Explanation of the meaning of the FWHM

3.1.2 Analysis of each treatment

First, each one of the different treated ring results will be analysed so as to compare the residual stress within the ring along the depth from the surface from the two directions shown in figure 1. In addition, a comparison of the FWHM will be executed in order to understand if the direction of the measurements presents different values of the dislocation itself.

3.1.2.1 Machined Ring

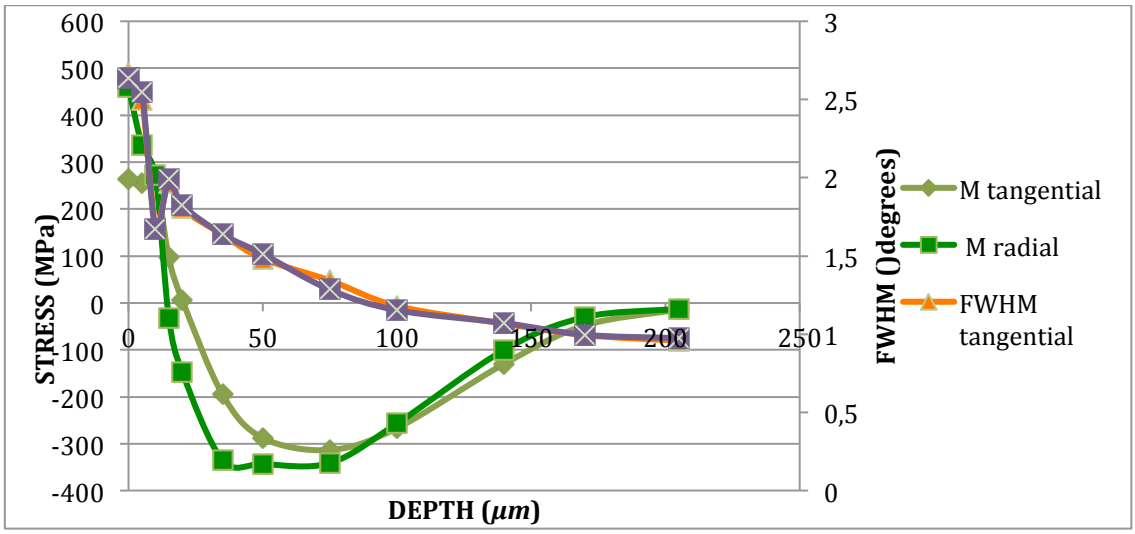

Figure 1.3 Residual Stress, in both directions, and FWHM values, along the depth measured in the machined ring

In this case, the ring has not been treated after been machined. As it is shown in figure 1.3, the residual stress values are very high and have both tensile and compression stresses along the measured length. It is found that, in the surface, there is a considerable difference of tensile stress in the directions measured. The radial stress is 460 MPa and 265 MPa in tangential direction instead. Taking a view to deeper measurements, it is revealed that both stresses tend to have closer values, reaching a peak of compression of 300 MPa in a depth of 50 μm and it decreased to zero at 200 μm.
Examining the FWHM values in the surface, it is explained that the dislocation density is very high in that point. It decreases until it comes to the value of one degree in a depth of 200 μm.

3.1.2.2 Heat Treated Ring

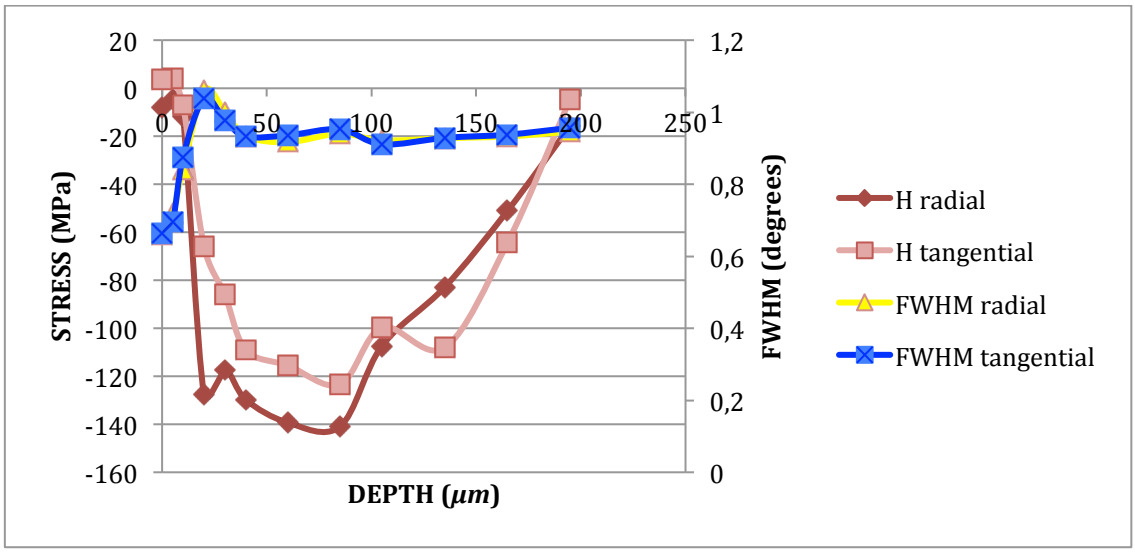

Figure 1.4 Residual Stress, in both directions, and FWHM value, along the depth measured after Heat Treatment

The Heat Treatment is based on raising the material's temperature above its critical one, and afterwards cooling it. That causes changes in its properties and also the decrease of the residual stress [1].
Examining the graph, it is shown that, in the surface, the ring has no stress. The two directions have similar shapes, showing the radial direction higher values in measurements under 100 μm and reaching a peak of 140 MPa. Besides, the FWHM value is mostly a fixed value around one degree.

3.1.2.3 Vibratory Stress Relieved Ring

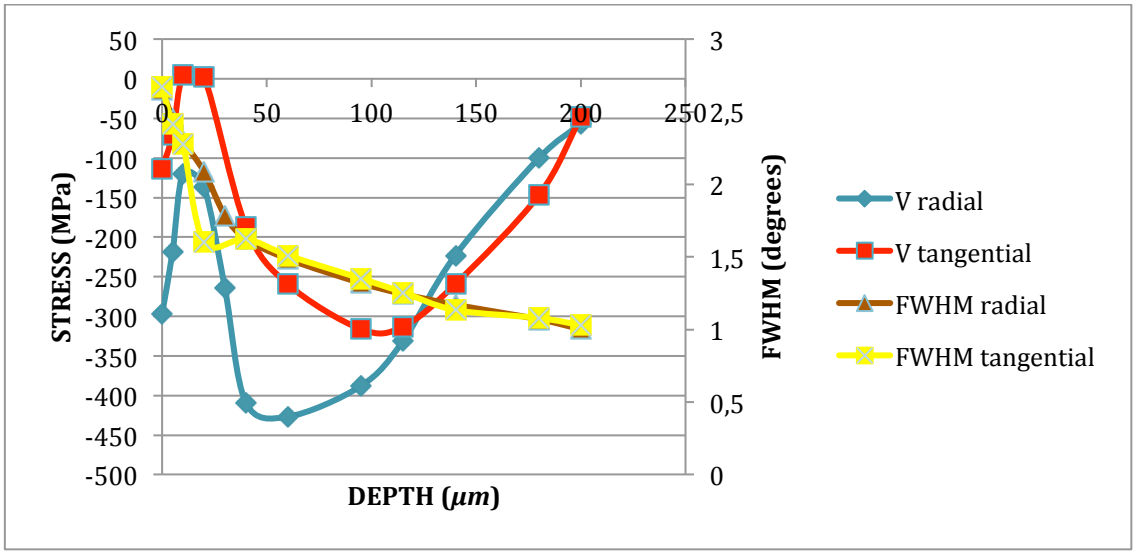

Figure 1.5 Residual Stress, in both directions, and FWHM value, along the depth measured after VSR Treatment

As it was explained before, the aim of the VSR treatment is the macro residual stress relief. The relief of the residual stress is proportional to the local plastic deformation value, which is proportional to the slid dislocations as well. These dislocations are associated with the level of vibratory stress. The stress relieve is achieved by adjusting different vibration's amplitudes to resonant and non-resonant vibrations [5].

In figure 1.4 it is displayed different stress values all along the measured depth in the directions analysed. At first, in the very surface, there is 114 MPa of compression stress in tangential direction, instead of 297 MPa in radial direction. Looking down to around 125 μm, the radial direction has higher stress than tangential one. Afterwards, both directions have almost the same stress values. The FWHM value consolidates around one degree and it is almost the same for both directions. The different values shown in the graphic are a result of statistical measurements.

3.1.3. Comparison of the residual stress

Comparing these three stress measurements, it is clear that both directions have the same tendency.

The Machining causes a high value of tensile stress in the surface. Going deeply, the stress on the ring starts shifting from tensile stress to compression. Once it reaches a value of around 350 MPa in compression in a depth of about 80 μm, the stress begins to decrease until it turns to be zero in a depth of 200 μm.

The Heat Treatment is the one that has the smallest values of stress all along the measured surface. It commences with no stress, increases until around 100 MPa of compression stress and finally it is established again with no stress slightly before 200 μm.

The VSR Treatment shows compression stress lengthwise the measured surface. It is noticed that both directions have slightly different curves, but equivalent trends. It first rapidly rises until the total stress relief, and before long it drops markedly down to 300 MPa in tangential direction and 400 MPa in radial of compression stress, rising to no stress when the 200 µm depth is reached.
In the two graphics below, it is worth mentioning that total area of compression stress is bigger in the VSR treatment than in the one machined. The greater difference is that tensile stress is eliminated around the surface when giving the ring a VSR Treatment.

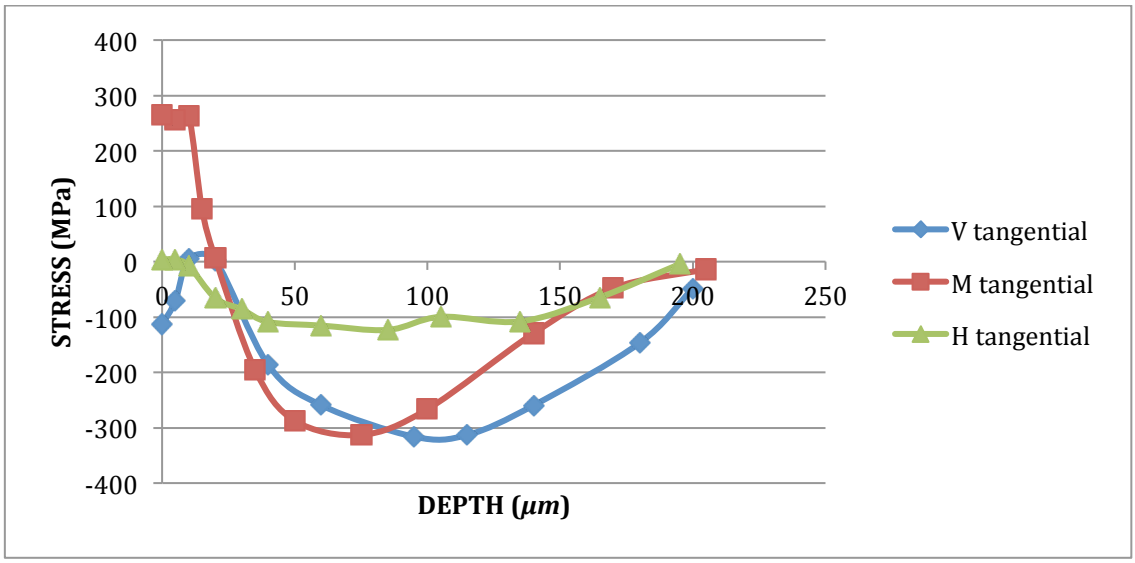

Figure 1.6 Comparison of the Residual Stress within the three treatments in tangential direction

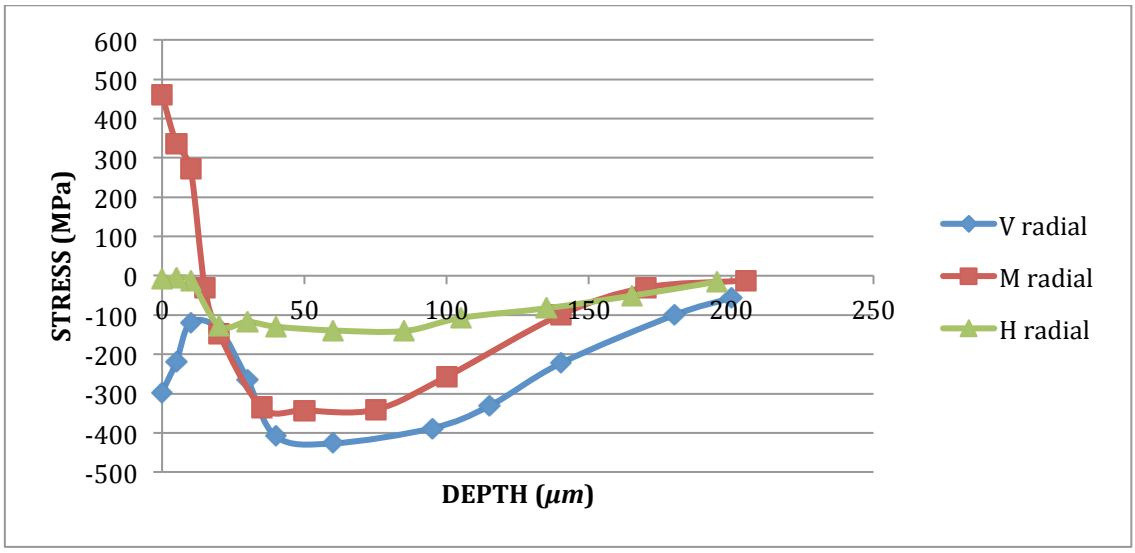

Figure 1.7 Comparison of the Residual Stress within the three treatments in radial direction

3.1.4. Comparison of FWHM values

As it is displayed in the figures below, an analysis of the FWHM values of X-Ray diffraction peaks has been performed. The result is that the peak width is much higher in the surface of the rings treated with Vibratory Stress Relief and Machined. The one Heat Treated, instead, has its minimum value on the surface, and the diffraction is lower all along the depth analysis. It means that Heat Treatment affects just to the very surface of the ring. On the other hand, Machining and Vibratory Stress Relief Treatment suffer a bigger change in dislocation density in higher depths. This is because residual stress is eliminated by provoking plastic deformation to the material.
The last fact that can be appreciated in Figure1.9 is that the three of the rings, when reaching a depth of 200 μm, tend to value 1°.

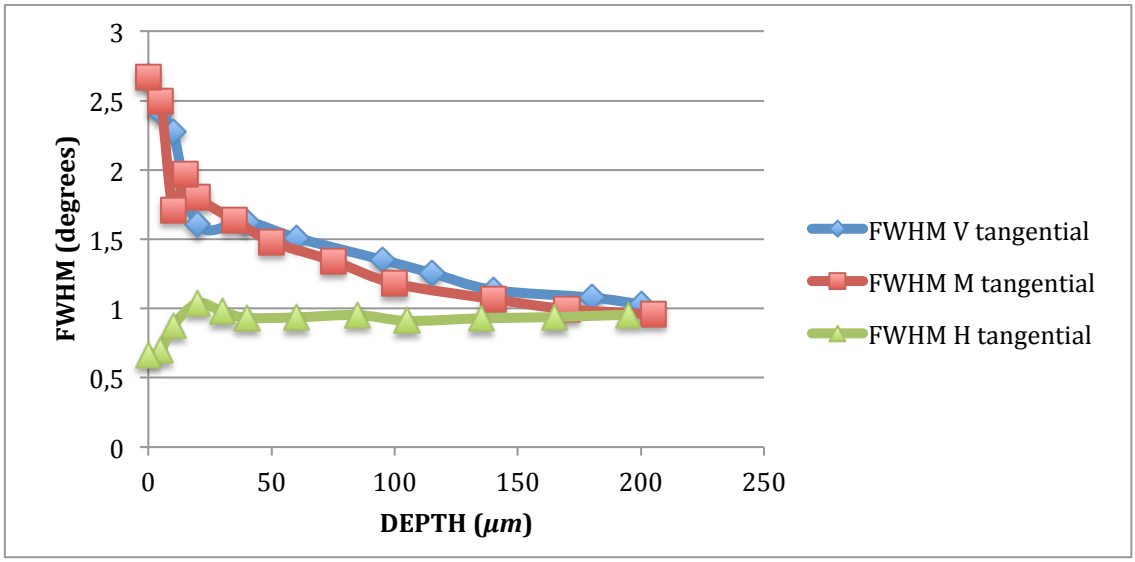

Figure 1.8 Comparison of the FWHM value within the three treatments in tangential direction

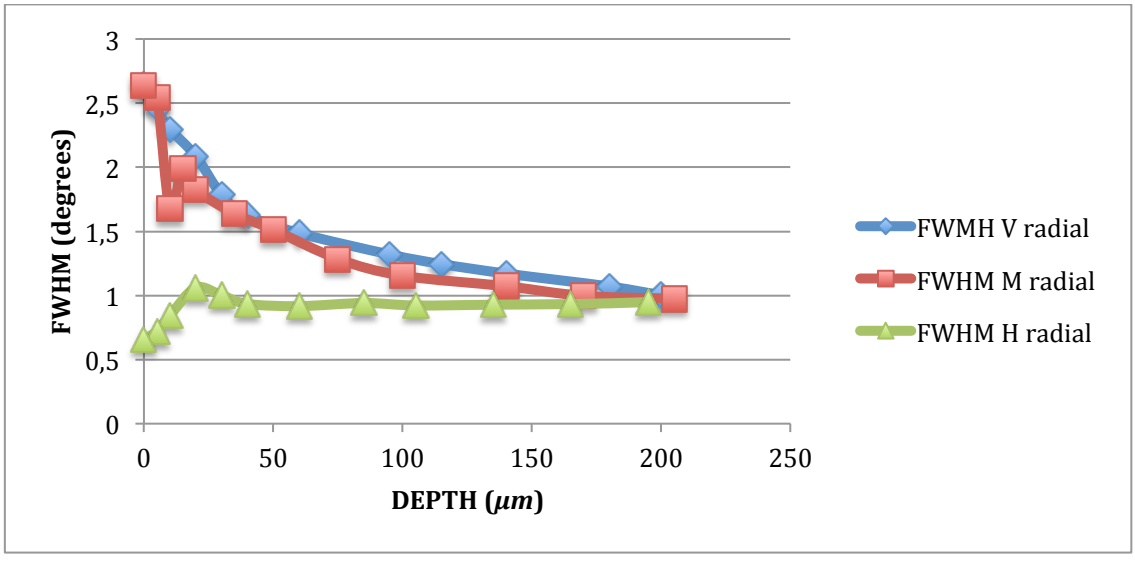

Figure 1.9 Comparison of the FWHM value within the three treatments in radial direction

3.1.5. Discussion

Comparing the Machining with the other two treatments shown above, it is manifested that the Heat Treatment is the one that relaxes more residual stress. However, it is the one that changes most the material properties. In addition, this treatment has some inherent high cost machines, making it a very expensive choice [2].

The VSR is less efficient; it leaves three times more stress than the Heat Treated ring. Comparing it with the Machined ring stress curve, it is displayed that the tensile stress close to the surface has been converted into compression stress with a lower value but, on the other hand, compression stress in deeper measures has become higher. VRS Treatment hasn't removed the residual stress in the depth of the ring measured. The analysed depth is not enough to conclude if the treatment is effective with the parameters given. This method is still on a development phase and a change of parameters could make the method more effective for the stress relief if a further analysis shows that is has not a satisfactory efficiency.

When a view is taken to the FWHM graphics, it is presented that plastic deformation is decreased when the depth is increased up to 200 μm. Once reached, the plastic deformation becomes inexistent. The graphic shows that Heat Treated ring is the one with a bigger change of properties near the surface. VSR treated ring has almost the same curve than the original one. This statement makes VSR Treatment a more reasonable method to remove the stress without high changes in the properties of the material.

3.2. TREATMENT OF THE SPECIMENTS

3.2.1 Background of the rings

The rings were made of a material called X22CrMoV12-1 (1.4923).
The nominal chemical composition is 0.22%C, 0.3%Si, 0.65%Mn, 11.5%Cr, 1.0%Mo, 0.6%Ni, 0.3%V, remaining is Fe.

All the rings were Heat Treated in order to obtain the hardness required for the purposed production. It was also performed to remove the stress generated in the machining [2]. The conditions of the heat treatment were: hardening at 1120degC, oil quenching and tempering at 700degC (approximately 2 hours).

After the heat treatment, a second heat treatment was applied to one of the rings. The purpose was to analyse if a substantial stress relief could be achieved by applying this heat treatment. It was performed at 660degC for 5h.
The second annealing temperature has to be lower than the first one not to modify the properties achieved by applying the previous one. Increasing the metal's temperature, the solidified molecules turn into austenite. The cooling velocity is the one that modifies the austenitic molecules and the properties of the material. The duration of the annealing influences in the austenitic grain size. As the time goes longer, the grains go greater [7].

3.2.2 Cutting

Once the X-Ray tests have been executed and analysed, it is time to take a view to the microstructure and the hardness of the different rings.
It is hoped to know if the same peculiarities will appear in the image of the ring in the microscope as they appear in the analysis of the X-Ray tests.

Some steps have to be accomplished in order to obtain the specimens. The first step is to cut each ring into smaller pieces so as to put them into a plastic form in order to polish them afterwards.

When cutting the rings, some stresses appear as a consequence of mechanical deformation of the ring while going through it [1][7]. This is why several polished will be applied after the cutting. The first polish removes most part of the stress created when cutting and the rest of the following polish will remove the stress originated by the polished performed before [7].

The interesting surfaces to study are the ones marked in the picture below. The green line shows the interesting surface in radial direction and the red line was performed to analyse the grains in the middle of the thickness of the ring in the tangential direction.

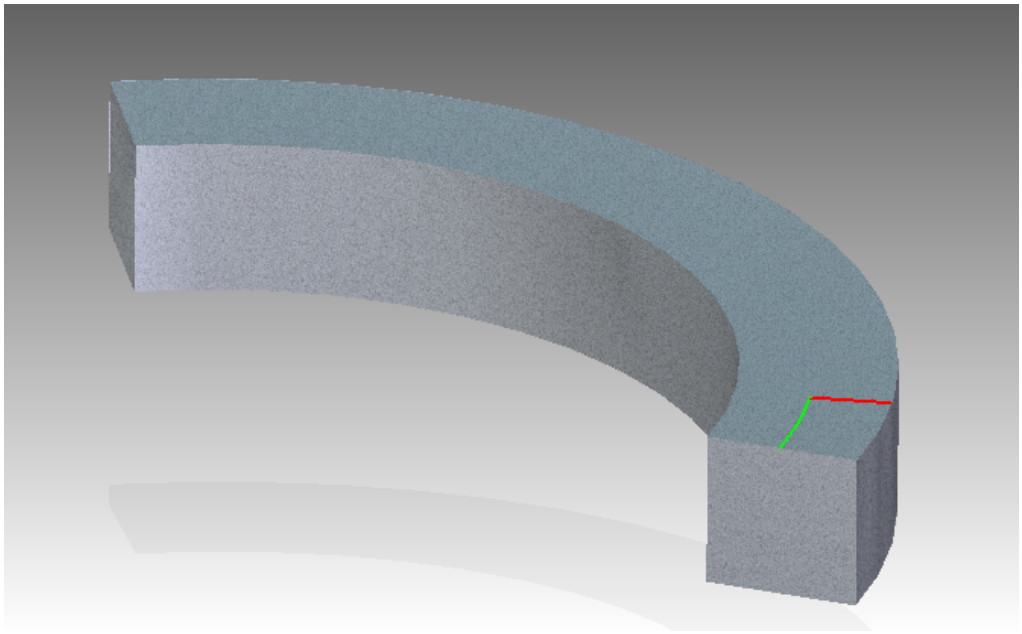

Figure 2.1 Cuts performed to the rings in order to obtain the specimens

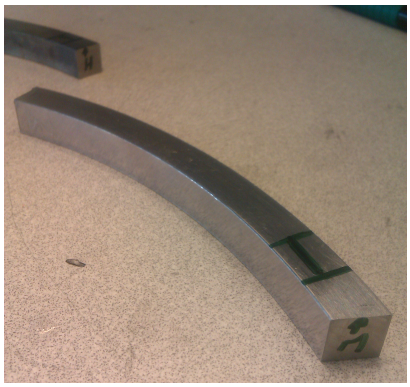

Figure 2.2 Cuts performed to the rings in order to obtain the specimens

Three specimens will be created. Each one will have both radial and tangential surfaces. In order to differentiate them, a green mark will be added to the radial piece of the ring. The middle surface in between the pieces coincides with the red and green lines explained above. Once the specimens are created, they will look like the picture below.

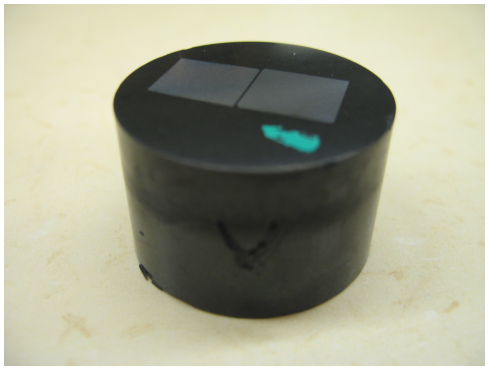

Figure 2.3 VSR specimen showing the 2 surfaces of interest in radial and tangential directions.

For the hardness testing, a different specimen will be created.
In order to operate as close as possible to the surface of interest, the metal piece will be cut in an angle of 45 degrees as it is shown in the following picture.
The surface of interest is the one situated in the middle of the specimen and it is indicated by a green spot.

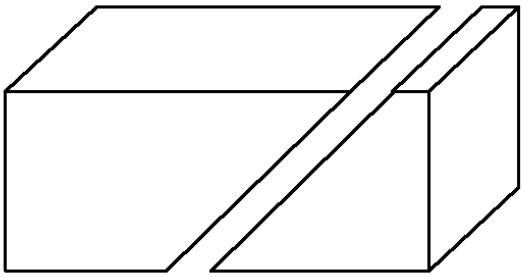

Figure 2.4 Image of the cut performed to the ring so as to create a specimen for the hardness testing.

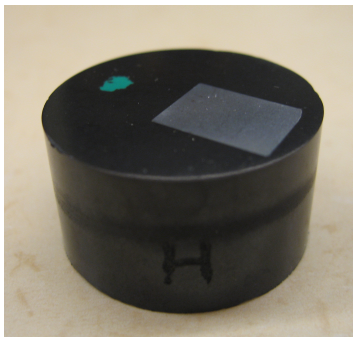

Figure 2.5 Heat Treated specimen created for the hardness analysis.

The whole cutting process was accomplished by the equipment lent by the Materials department of Linköping's University.

The first cut was carried out by the machine shown in the picture below. It provokes a quite big mechanical deformation within the ring so this machine will be appropriate just for the first approximation based on the cut of a small piece out of the whole ring.

Figure 2.6 Big cutting machine

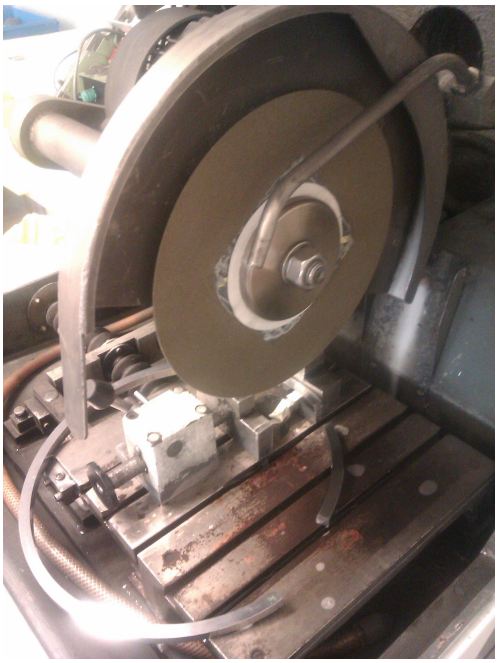

Figure 2.7 Closer view of the cutting tool

For higher approximations, a second cutting machined will be used. Once a small piece is obtained, the next step will be executed with this second cutting machine named above and shown in the picture below. This one will be a more precise cut and the final one.

Figure 2.8 Small cutting machine (1)

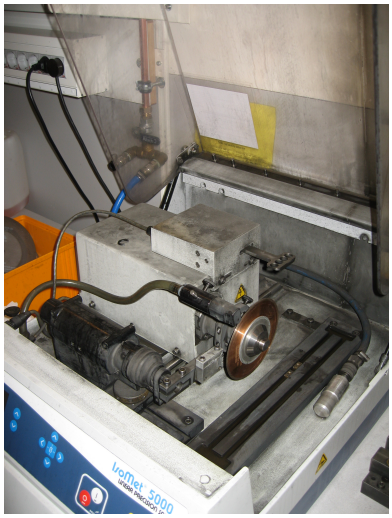

Figure 2.9 Small cutting machine (2)

3.2.3 Creating the specimens (Mounting)

In order to polish the specimens and analyse them in the microscope, the pieces of the ring previously cut have to fit in a plastic cylinder. This process is called mounting.

Mounting is based on the application of heat and a high pressure to a special mix of resin in order to melt it and stick both the resin and the metal pieces into a standard cylindrical specimen [7] as it is shown in the pictures above in figures 2.3 and 2.5.

The mix selected to create the cylinder depends on the use of the specimen. As both light and electron microscopes will be used to analyse the microstructure, a special mix of phenolic hot mounting resin with carbon filler will be selected. The black resin allows electricity go through the specimen in the electron microscope. Also the utilization of an etchant to reveal the microstructure will influence the type of mix used for the mounting [7].

The cut pieces of the ring will be introduced in a machine (see picture 2.10). The surface of interest will lie against the cylinder base of the machine and once the ring pieces are set, the cylinder will be sent inside the machine and 4 cups of the resin powder will be added in order to create a cylinder. Just after the resin is inserted, the cover is set and the process is started. The metal pieces and the resin will be heated and exposed to a 10 MPa pressure. The process of melting the resin will last 7 minutes and right after, the specimen will be rapidly cooled for three minutes.

Figure 2.10 Mounting machine

Figure 2.11 Mounting resin

The same process will be executed for all the pieces of the three rings. At the end, 6 specimens will be obtained. Three will be used for the microstructure analysis

comparing both directions, radial and tangential; and the other three will be for the hardness testing.

3.2.4 Polishing

Right after the specimens are created, they have to be polished before the microstructural analysis is executed. As it has been mentioned earlier, many different polishes have to be performed so as to remove the stress created in the cutting process.

The techniques used for the polishing depend on the microstructure. For instance, a specimen in which the ferrite grain boundaries are to be etched would require longer polishing times and an etching after each polishing [7].

The steps followed for the polishing process were:

1. Two minutes of polishing with a paper number 500. It removes 30μm of layer using a pressure of 20 N. The liquid used is water. The paper and the specimens rotate in the same direction.
2. Analyse if all the plastic have been removed from the surface of interest. If not, repeat step 1 until the surface is completely cleared.
3. Clean the specimens with water and alcohol and dry them with compressed air.
4. Two minutes of polishing with a paper number 1200. It removes a layer of 14μm, with a pressure of 20 N. The liquid used is also water. Both paper and specimens rotate in the same direction.
5. Clean the specimens as in step 3.
6. Three minutes of polishing with a paper number 4000. It removes a layer of 5μm, with a pressure of 20 N. Using water as liquid for the polishing. Same rotation direction.
7. Clean the specimens as in step 3 again first and then clean the specimens with an ultrasonic machine for 1 minute and right after clean them again with water and alcohol before drying them with compressed air.
8. 8 minutes of polishing on a hard cloth using 3μm diamond drops, with a pressure of 30 N and water under the cloth as a coolant. Same rotation direction as well.
9. Clean the specimens as in step 7.
10. 15 minutes of polishing with a softer cloth using 1μm diamond drops, with a pressure of 15N. The bottom part of the cloth is cooled with water as in step 8. Same rotation direction.
11. Clean the specimens as in step 7.
12. Last polishing: two and a half minutes with the same cloth but, in this step, cloth and specimens rotate in different directions. The liquid is now a non-crystallizing colloidal silica. The cloth is cooled by water coming from the bottom of the cloth.
13. Clean the specimens with ultrasonic as in the previous steps.

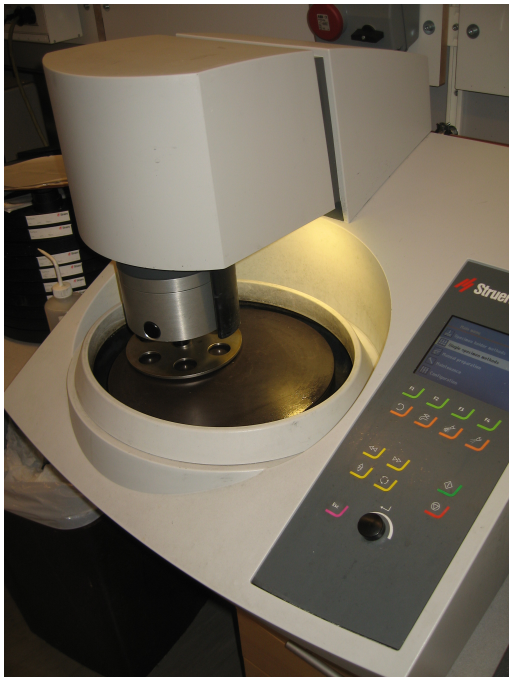

Figure 2.12 Polishing machine

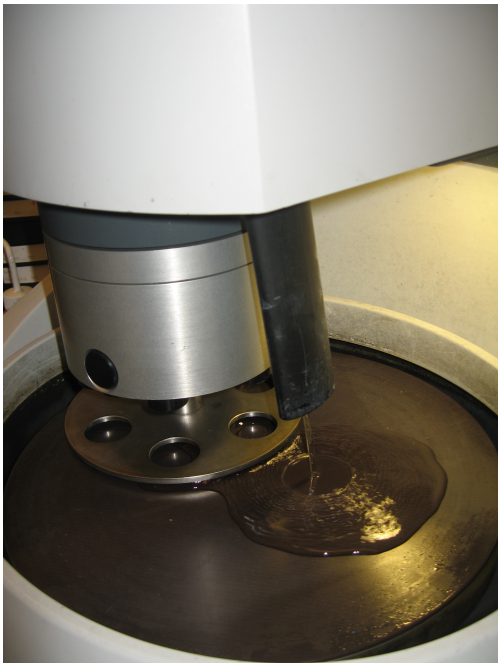

Figure 2.13 Closer view of the polishing machine

3.2.5 Specifications of cleaning after each polishing

Once each step of polishing has been executed, perhaps the surface could have small impurities or diamond bits. In order to remove them, the specimens are cleaned with a water flow and right after with alcohol steeped in natural cotton, flushed with alcohol after and finally dried with compressed air.

However, when finer polishing is to be achieved, it is necessary to clean the specimens with an ultrasonic machine. This device uses ultrasounds (between 20 and 400 Hz) and a cleaning solvent. This procedure is based on an ultrasonic generator that creates ultrasonic waves in the fluid. The cavitation phenomenon is produced by these waves. Millions of bubbles are generated in the fluid and when they go across the surface and holes of the material, the surface is cleaned. The higher frequency is, the deeper and exigent the cleaning is [8][9].

The specimens are introduced in a glass filled with alcohol and put in the ultrasounds machine (see picture 2.15). For around 30 seconds, the ultrasonic waves remove the impurities of each specimen.

Figure 2.14 Cleaning sink

Figure 2.15 Ultrasonic machine

3.2.6 Micro etching

The last step is the micro etching. The specimen should be etched immediately after the final polishing is carried out. Otherwise, a layer of rust could be grown on the surface of the specimen and the last step of polishing would be needed to be executed once again. If the rust layer is not removed, the etching would not attack the specimen's surface [7].
There are different etching solutions depending on the composition of the specimen, such as the type of carbon and alloy steels that are used. Nital and picral are the most widely used etchants for carbon and alloys steels. They both give maximum contrast between pearlite and a ferrite or cementite network. Besides, it reveals ferrite boundaries and differentiates ferrite from martensite [8].

Due to the components of the rings, the acid chosen was Clorhidric acid (HCl). It was mixed with water, with a proportion of 75 ml of water and 25 ml of acid [8].

The mix was heated up to 90 degrees. Once this temperature was reached, the surface of the specimen was put in contact with the mix for 25 seconds. Straightaway, the etching was stopped by placing the specimen under the water flow as the mix was based on water. It was cleaned with alcohol right after and dried with compressed air.

3.3. ANALYSIS OF THE MICROSTRUCTURE

3.3.1 Introduction

Another way to analyze the characteristics and properties of the material is by analyzing its microstructure. Once the specimens have been mounted, polished and etched, a microscope is used to take a view to the microstructure.

Right after this introduction, some pictures of the rings will be shown. They were taken with an optical microscope owned by Linkoping's University.

A wide range of constituents can be found in carbon and alloy steels. Single-phase constituents such as austenite, ferrite, δ-ferrite, cementite, various alloy carbides and martensite. Additionally, two-phase constituents such as tempered martensite, pearlite and bainite can also be found [7].

In the analysed rings, the predominant structure is martensite. It is a resultant of a heat treatment performed after machining them. The annealing procedure is base in the transformation of the austenite obtained when the ring is heated up, into martensite when the cooling takes place [7]. Martensite is not an equilibrium phase in steels. Formation of this constituent depends on the chemical composition and the cooling velocity from the high-temperature austenite region. Once the specimen is cooled below a specific temperature called martensite start (M_s), the martensite is formed instantly. This temperature (M_s) depends on the carbon and alloys content of the parent austenite phase. The transformation is completed when the specimen reaches a lower temperature, the martensite finish temperature (M_f). By applying this method, an increase of the hardness and mechanical strength is achieved [7].

In order to acquire an idea of what has been explained above, a figure will be attached below, figure 3.1.

T_t is the tempering temperature, V_c is the minimum velocity a material can be cooled in order to obtain just martensite instead of a combination of martensite and other softer transformations of the austenite.
The C.C.T. (continuous cooling transformation) curve shows the beginning of the transformations of the austenite.
These graphic curves vary depending on the content of carbon and alloys on the material; the aim of displaying the figure was to get an idea about how the tempering process works [11][12].

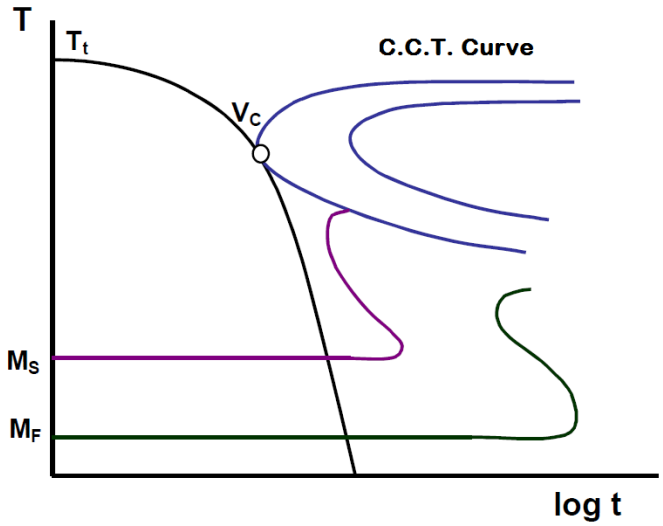

Figure 3.1 Tempering cooling process temperature

Carbon and alloys content has influence in the hardness of the martensite originated as well. Hardenability is increased when carbon and alloy contents are increased and by enlargement of the austenite grain size [7].

In low carbon content metals, the most common martensite's structure is lath martensite. It is formed in all low-carbon and medium-carbon steels. This kind of substructure's crystal structure (low-carbon steel) is bcc [7]. A figure of the bcc structure is displayed right below, in figure 3.2.

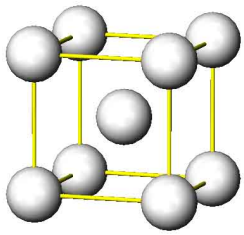

Figure 3.2 BBC structure

The properties of martensitic structure steels are strongly conditioned by the grain size of the martensite [7]. In consequence, the main goal is to reduce the grain size. The critical grain size for martensitic steels is the prior austenite grain size. This comes to mean that the grain content, the austenitic structure, is the one that changes, not the size of it.

As it was mentioned above, both martensitic hardness and strength are so related to the content of carbon. So, by increasing the carbon content percentage, these properties are increased. Nevertheless, the material becomes more fragile [7]. As it was declared before, all the rings studied were Heat Treated in order to obtain the hardness required for the purposed production. The tempering was performed for two hours at a temperature of 700 degC. A slump of the strength of the martensite was noticed after tempering the rings, but an increase of its toughness as well. However, tempering alloy steels might also reduce the toughness due to the embrittlement. Nonetheless, tempering permits the achievement of a wide range of useful strengths and toughness.

3.3.2 Light microscope analysis

3.3.2.1 Introduction

As it will be proven in the images that will follow this report, just two things came up clear with the light microscopes analysis. The first fact is that there is deformation layer in all the specimens due to the heating conditions of the machining process. The second fact analysed was a bending formed due to the heat transferred from the machining tool to the ring while the process of machining was carried out. It is noticeable in the whole edge of the tangential surfaces of the specimens.
In order to examine if some carbides were formed as a result of the heat treatment, and also to get a closer pictures of the deformation layer to examine its behavior, a second microstructure analysis was carried out with an electron microscope (SEM).

3.3.2.2 Machined ring

In figures 3.3, 3.4, 3.5 and 3.6 it is shown the microstructure of this specimen. These pictures present the microstructure in both radial and tangential directions. Moreover, there are two amplifications of the microstructure, 40 and 100 times.

It is easy to appreciate, in both directions, that the predominant microstructure is lath martensite, shown as white stripes. There is some ferrite as well, shown by black grains. The main characteristics of these microstructures are shown in part 3.1.

Ferrite is a dominant component in low content of carbon steels. It constitutes a soft low-strength phase. Good ductility and formability are obtained when the ferrite grain size is fine. If the temperature decreases or the strain rate increases, the ferritic steel will shift from a ductile to a brittle behaviour.

In radial direction, the microstructure presents 5μm width deformation layer alongside the edge of the specimen. A clear view of the lath martensite could be appreciated in the image below.

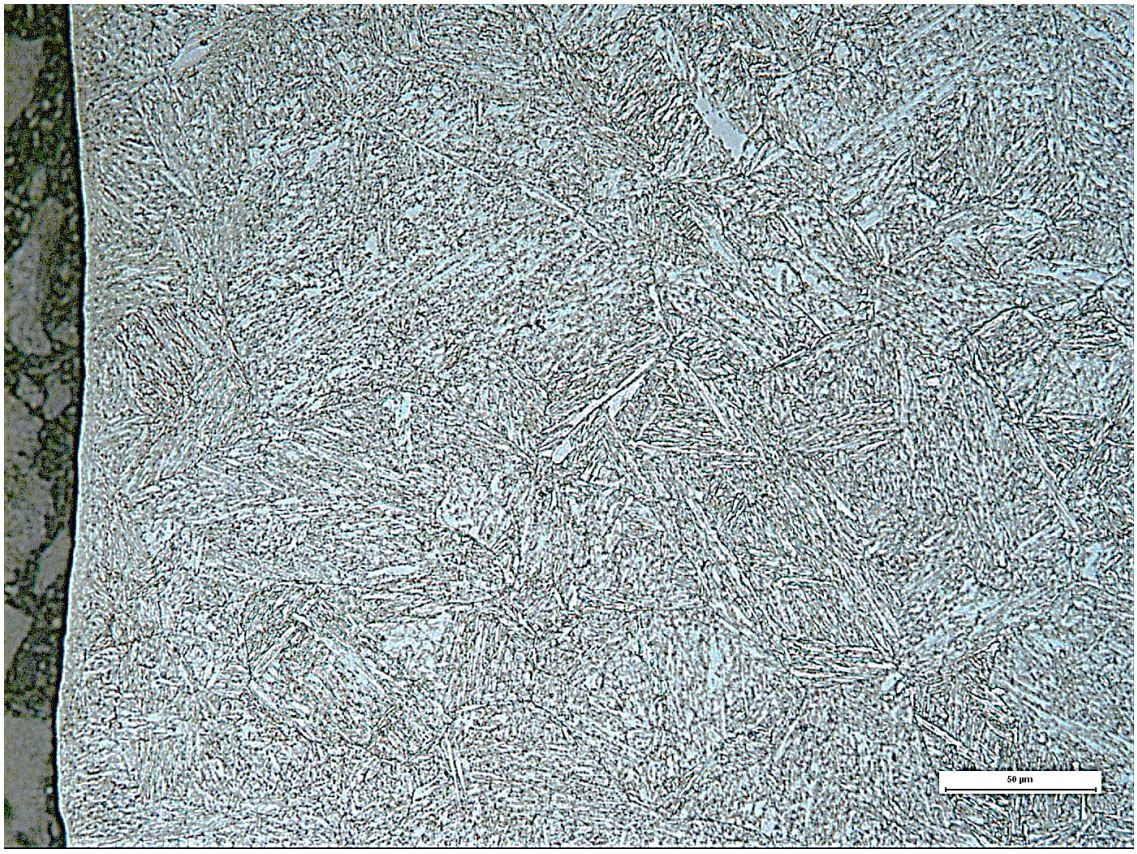

Figure 3.3 Picture of the specimen in radial direction amplified 40 times.

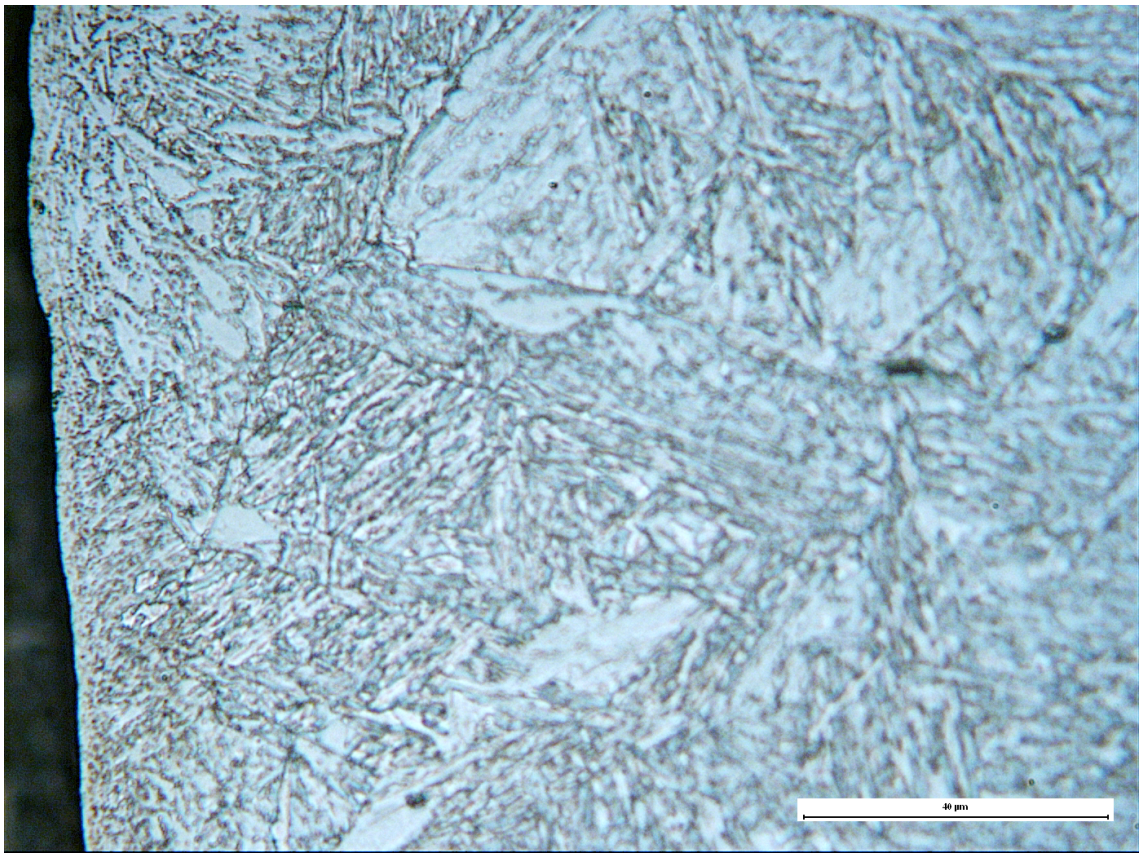

Figure 3.4 Picture of the specimen in radial direction amplified 100 times.

Taking a view to the tangential direction pictures, shown below in figures 3.5 and 3.6, a deformation layer of 5μm of width could be appreciated as in radial direction's pictures. There is a quite noticeable bending of the microstructure in one direction as well.

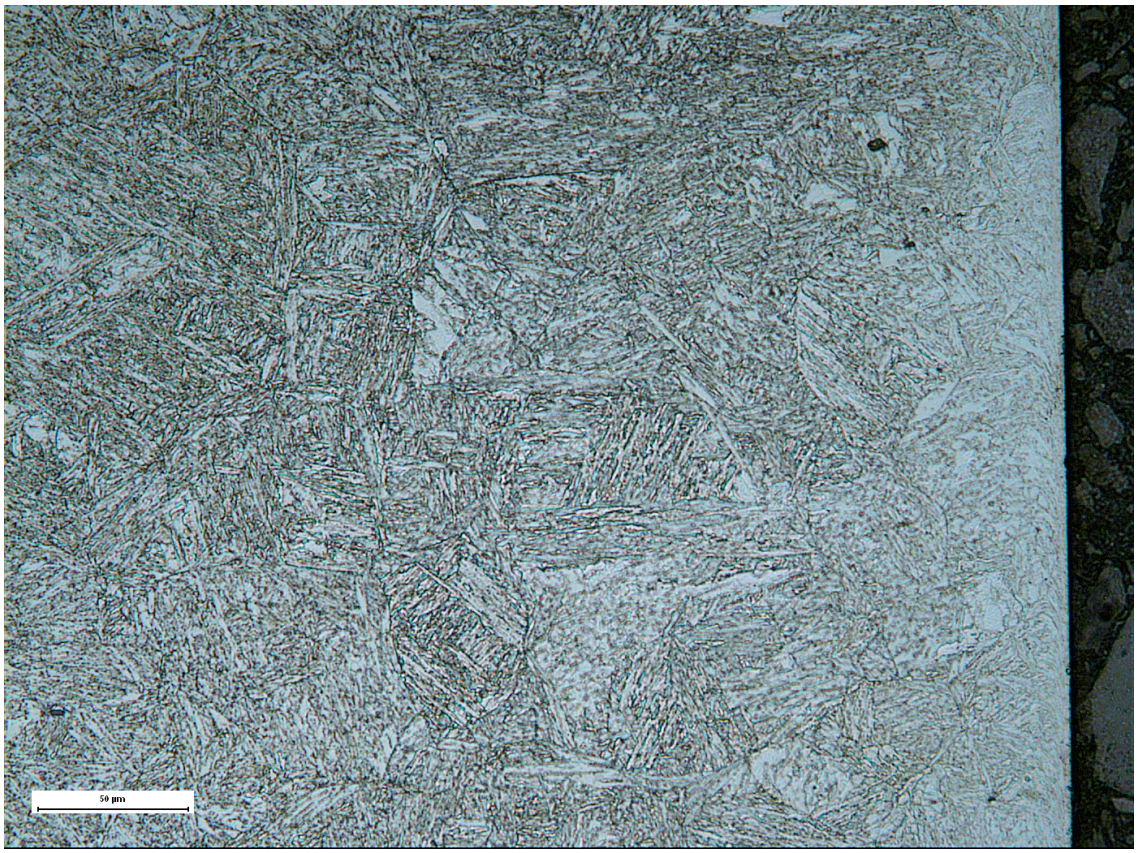

Figure 3.5 Picture of the specimen in tangential direction amplified 40 times.

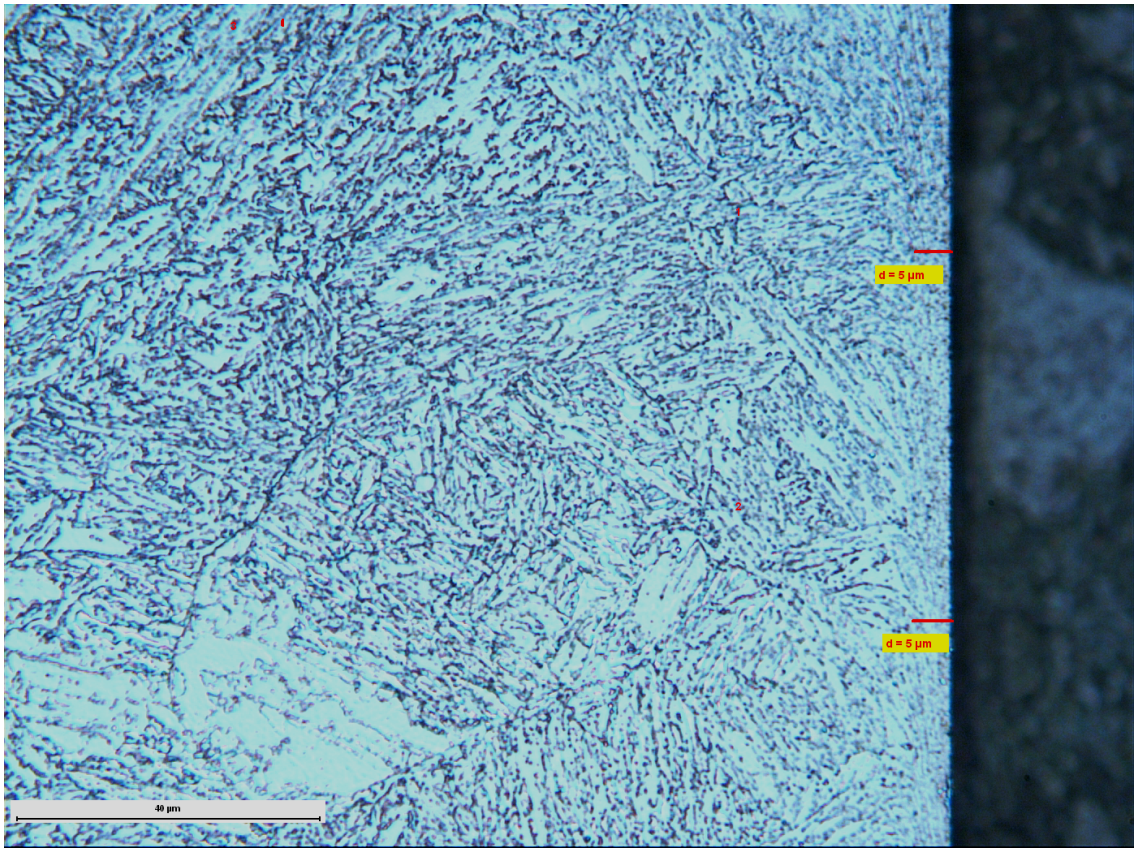

Figure 3.6 Picture of the specimen in tangential direction amplified 100 times.

3.3.2.3 Heat Treated ring

As in the machined specimen, the predominant microstructure of the ring is martensite. In figure 3.7, it is very clear to recognize lath martensite as a major component.

There is a clear layer in the radial direction images, which swings between 5 µm and 13 µm. Likewise, in tangential direction, there is also a bended structure close to the edge.

In pictures 3.8 and 3.10 it is also possible to recognize the grain boundaries of the microstructure.

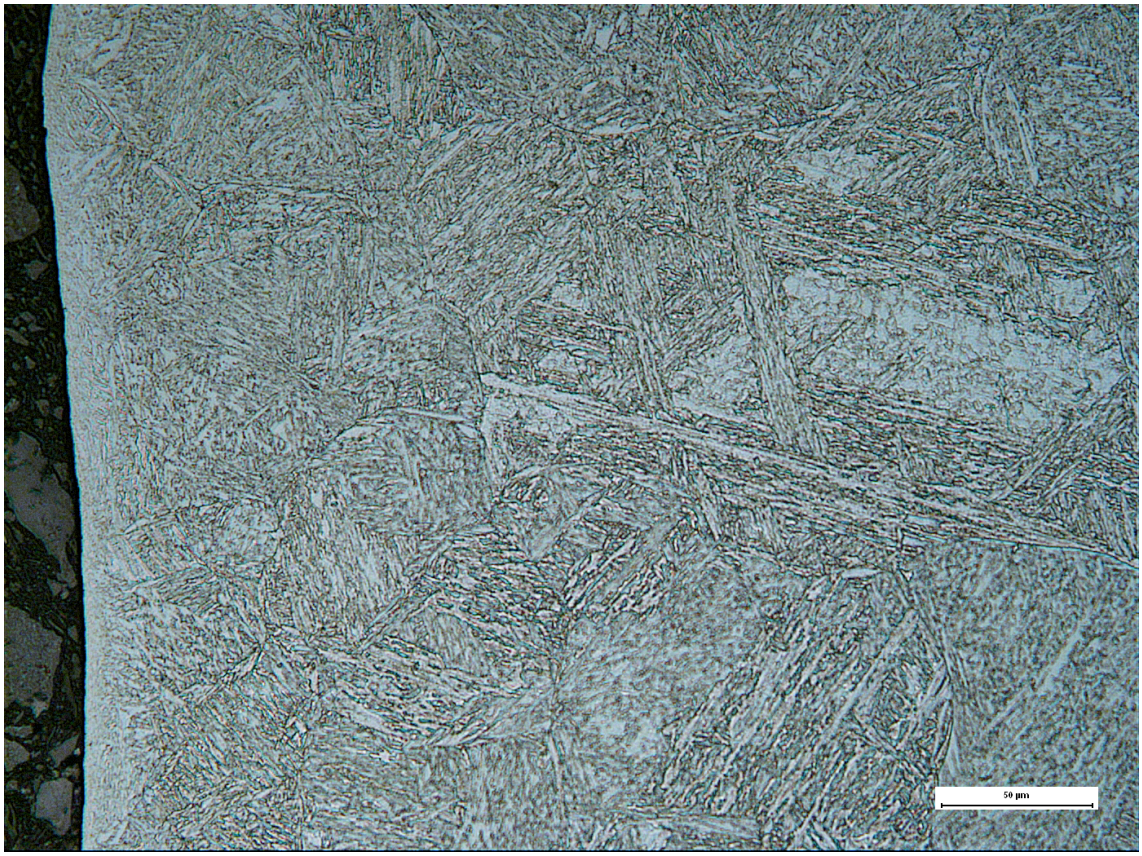

Figure 3.7 Picture of the specimen in radial direction amplified 40 times.

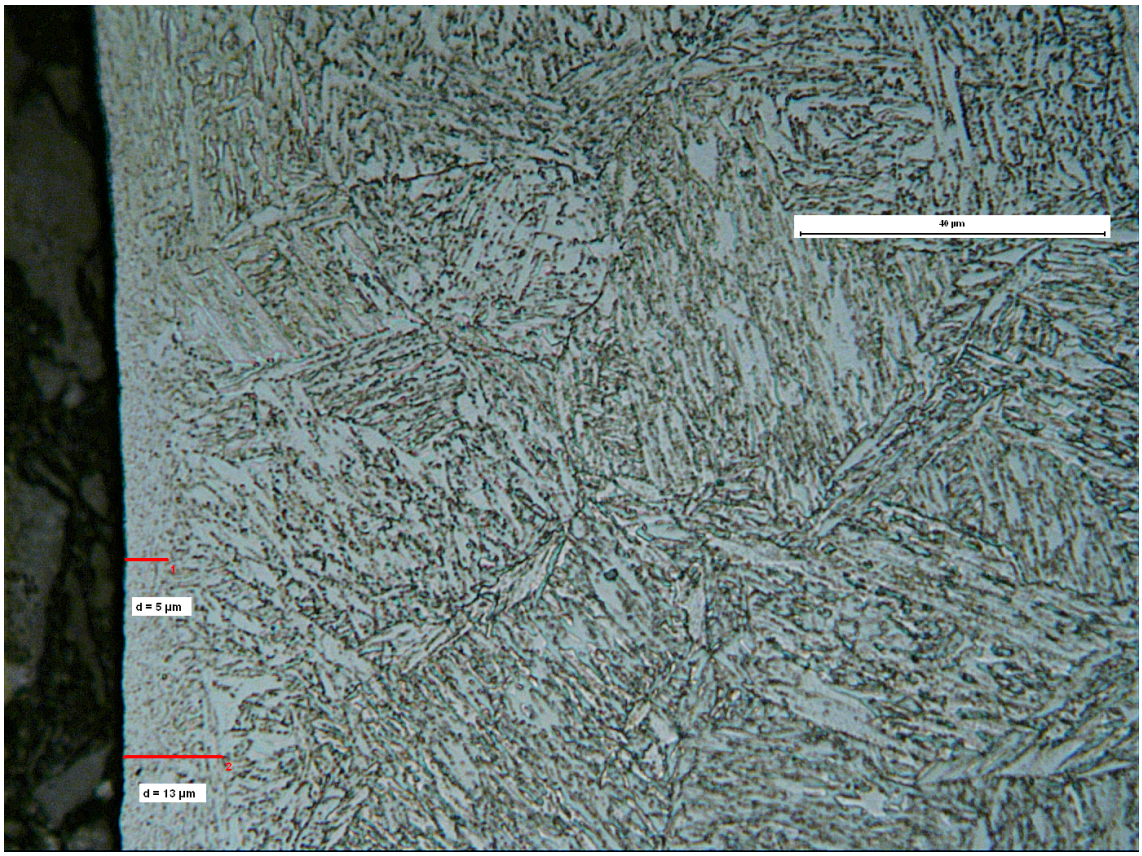

Figure 3.8 Picture of the specimen in radial direction amplified 100 times.

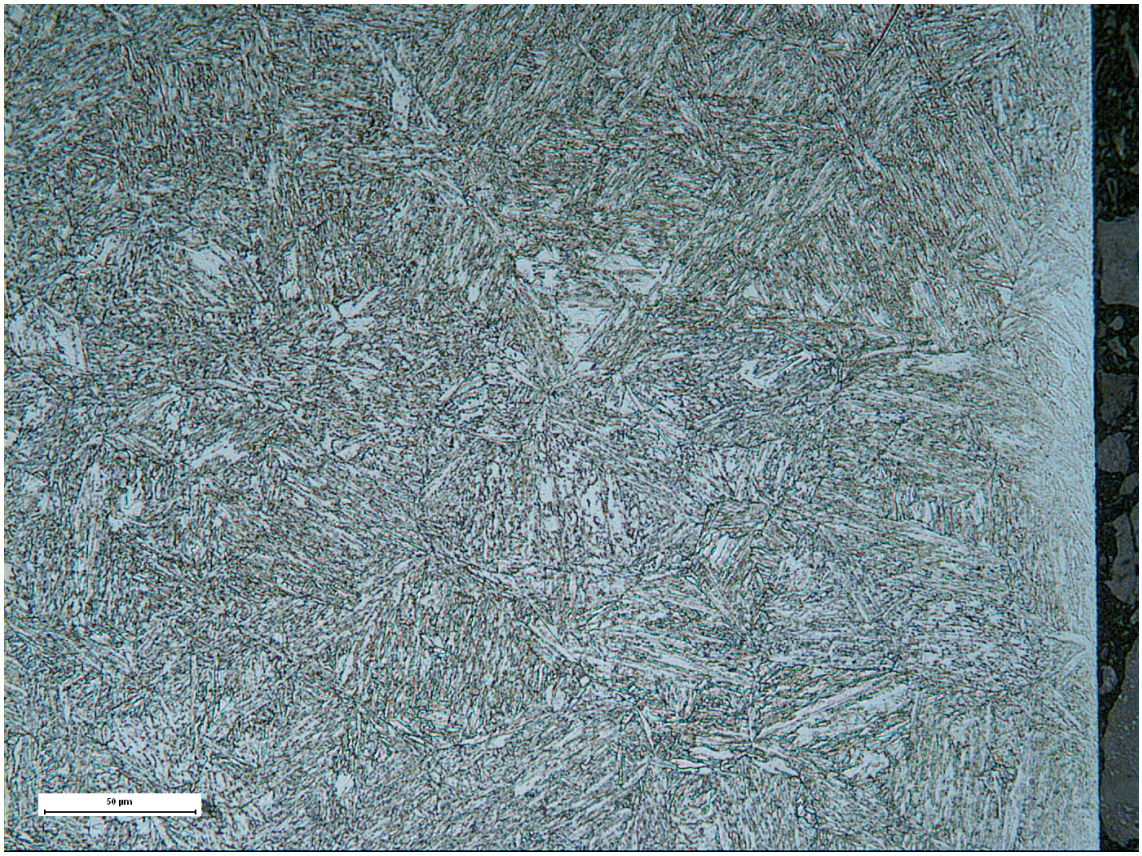

Figure 3.9 Picture of the specimen in tangential direction amplified 40 times.

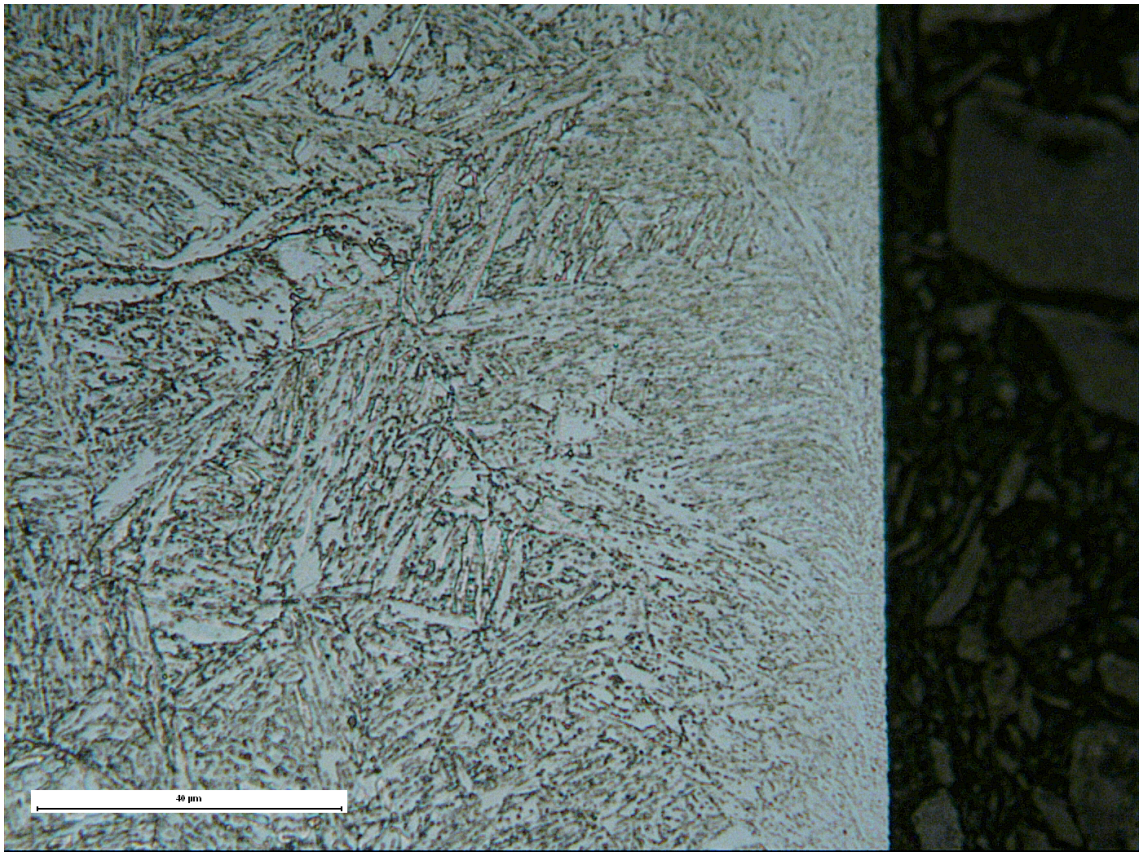

Figure 3.10 Picture of the specimen in tangential direction amplified 100 times.

3.3.2.4 VSR ring

The etching executed for this specimen was slightly different, so the contrast of the following images will be different, but the microstructure is based on martensite and ferrite too.

The measured layer on the edge is between 4 µm and 7 µm in radial direction. A quite noticeable bending could be appreciated in the tangential direction pictures as it was shown in the other two methods in the preceding pages.

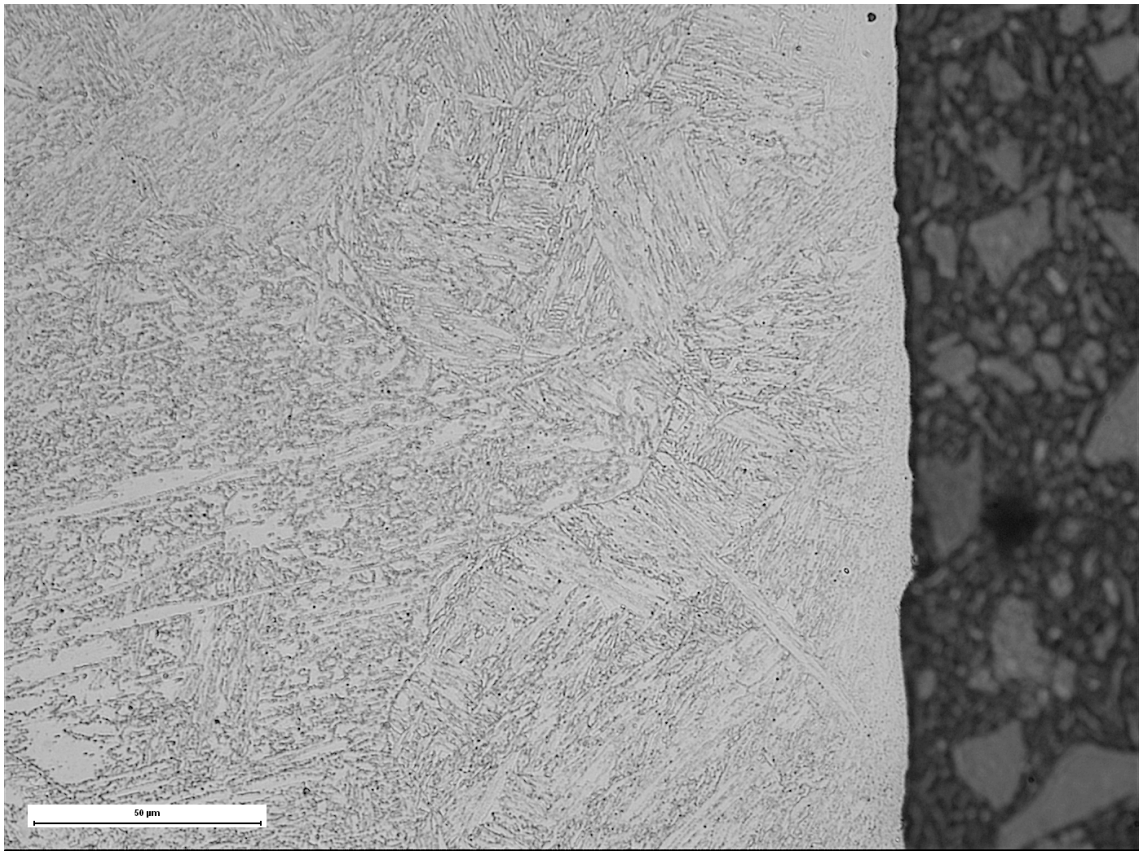

Figure 3.11 Picture of the specimen in radial direction amplified 60 times.

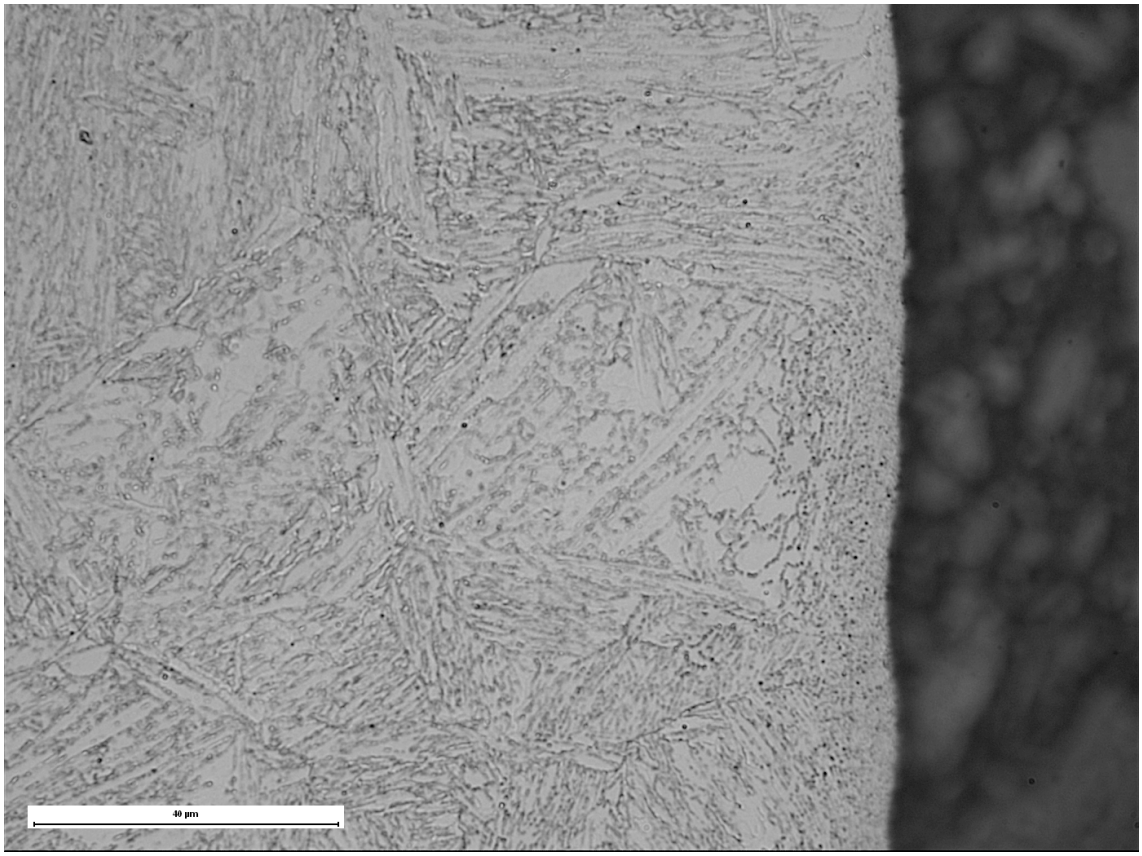

Figure 3.12 Picture of the specimen in radial direction amplified 100 times.

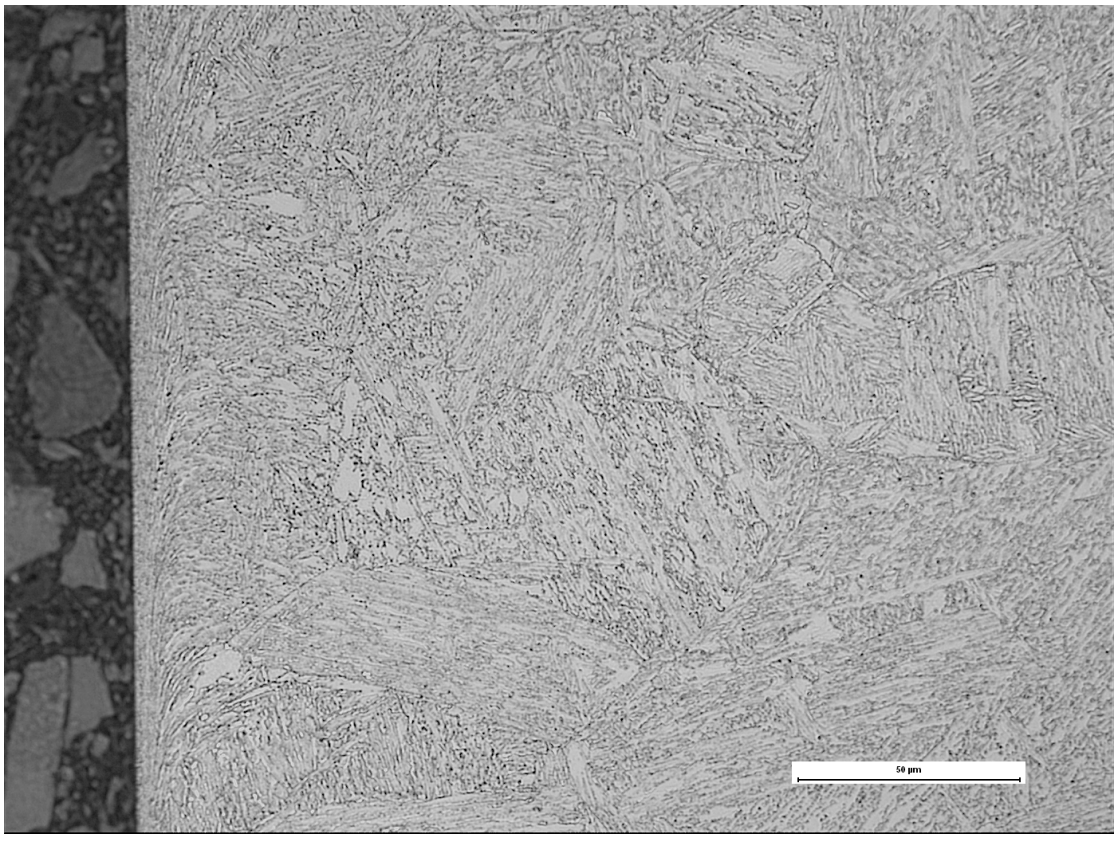

Figure 3.13 Picture of the specimen in tangential direction amplified 60 times.

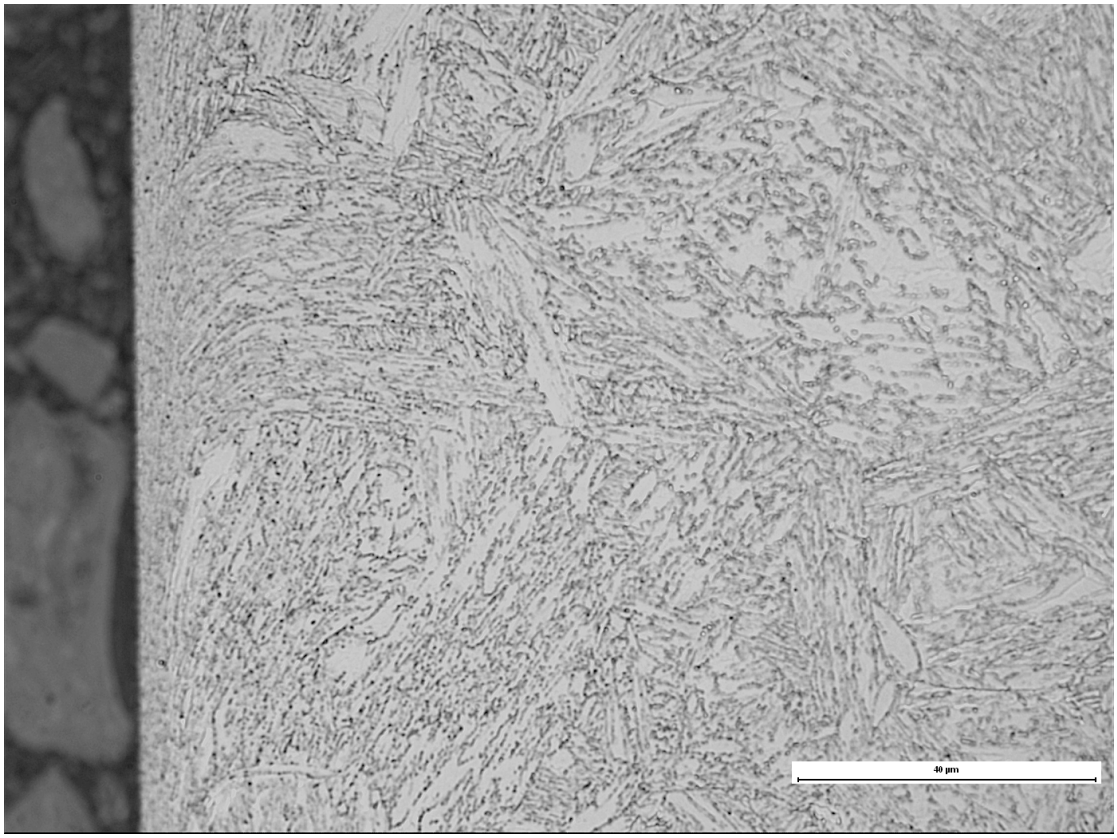

Figure 3.14 Picture of the specimen in tangential direction amplified 100 times.

3.3.3 SEM analysis

3.3.3.1 Introduction

The aim of this analysis was explained in previous pages. It is the examination of carbides on the specimen's surface and a closer analysis of the deformation layer.

Some images will follow exhibiting, in different magnification pictures, each specimen on each of the two directions studied.

3.3.3.2 Analysis of the rings

In order to get a finer analysis of the different microstructures of the rings and a clear difference between the specimens, the same magnification pictures were executed for each ring and displayed below.

Additionally, two lower magnification pictures were taken from the machined specimen on both radial and tangential directions so as to show the roughness of the surface on the radial one and the flat surface on the tangential direction. They are presented on figures 3.15 and 3.16.

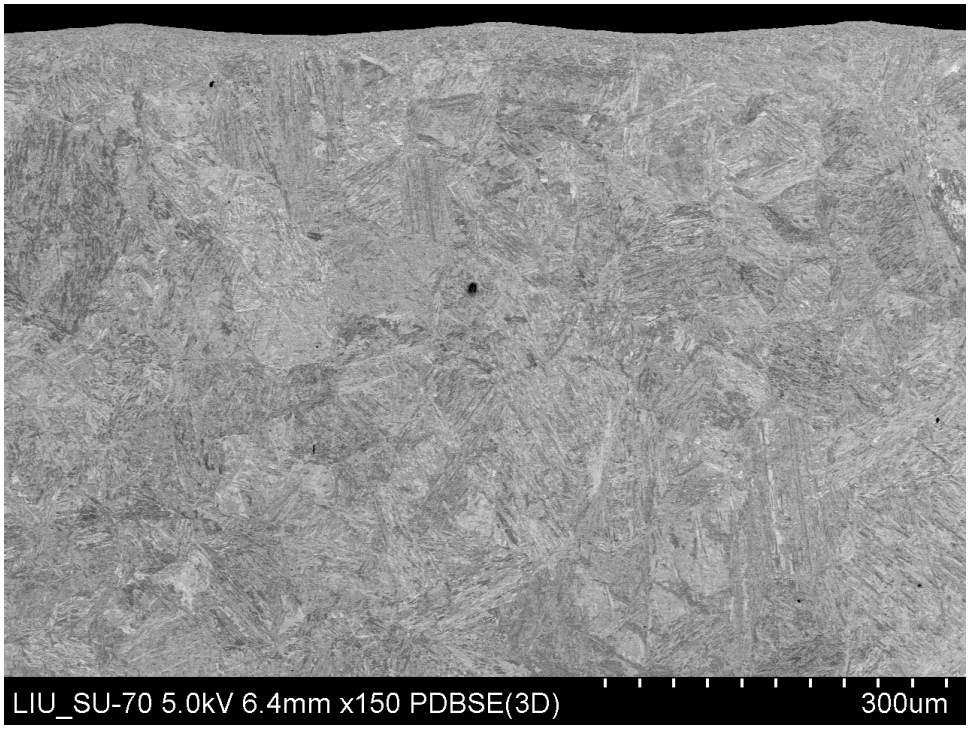

Figure 3.15 Picture of the machined specimen in radial direction, 150 magnifications

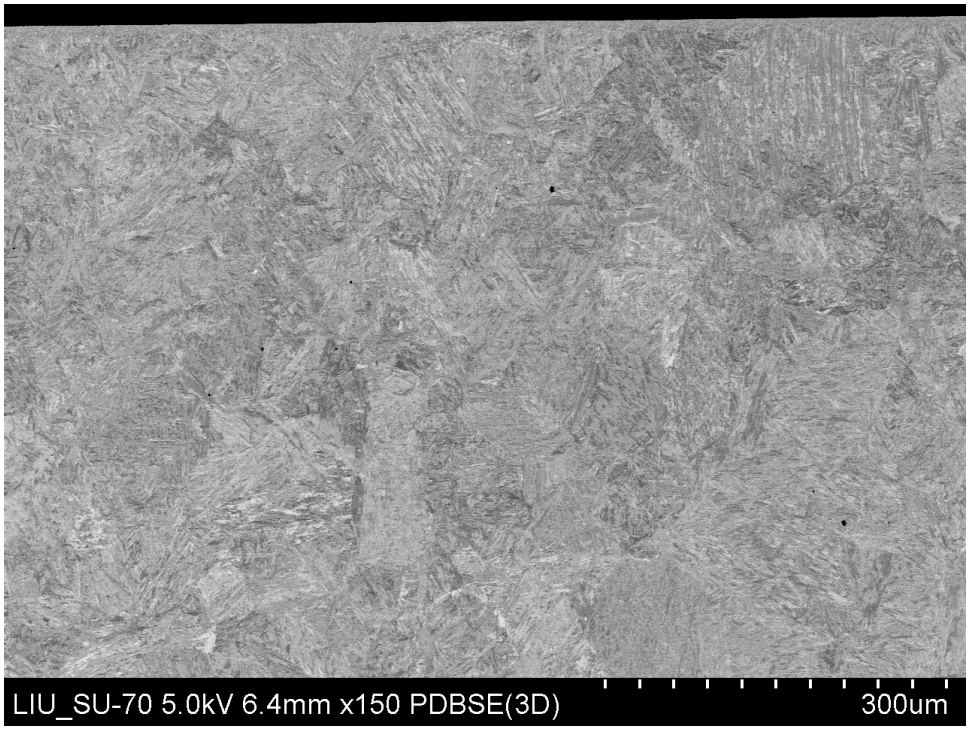

Figure 3.16 Picture of the machined specimen in tangential direction, 150 magnifications

3.3.3.3 Machined ring

First, an analysis of the radial direction images will be executed.
In the image shown in figure 3.17, not clear information can be perceived, just a rough sense of different components. The black spots could be carbides due to the heat treatment or holes left by some impurities when the polishing was performed. An analysis of the carbides will follow with some VSR ring's pictures.

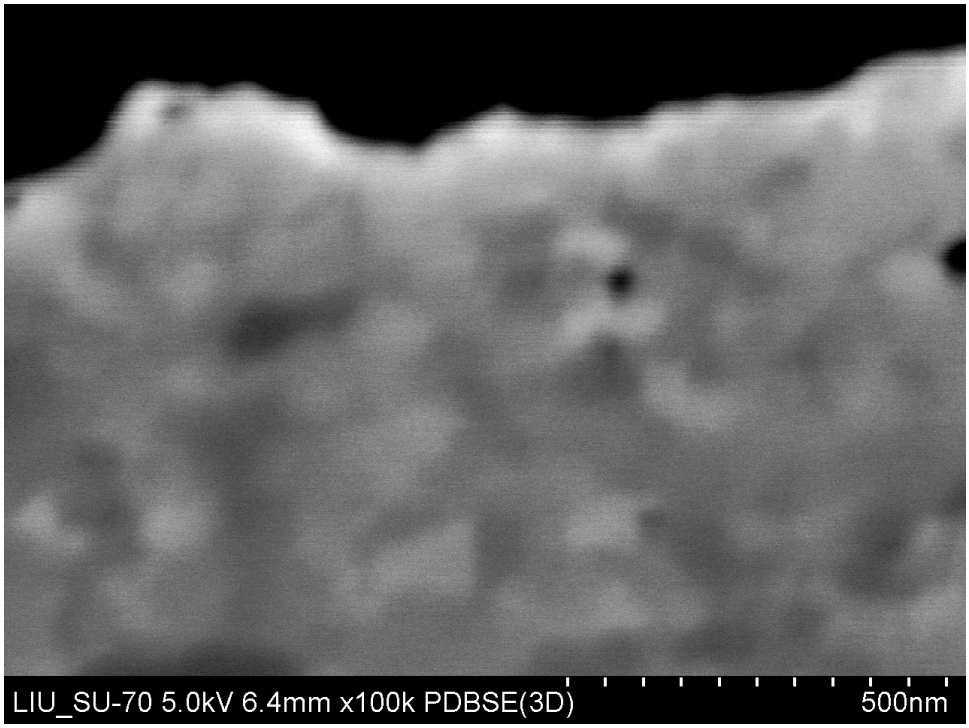

Figure 3.17 Picture of the machined specimen in radial direction, 100K magnifications

The picture taken with a 50.000 magnification, figure 3.18, shows a quite small distribution of grains situated in the surface. The image shows the deformation layer. However, a lower magnification would be useful to perceive if the deformation layer has a different grain size or even an alteration of the direction.

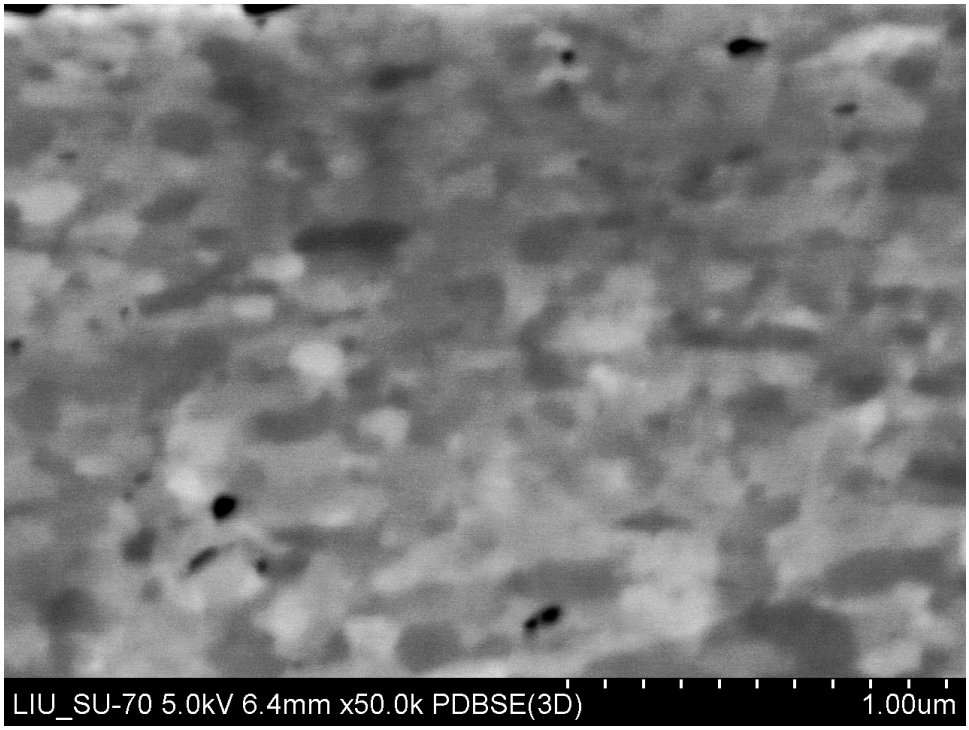

Figure 3.18 Picture of the machined specimen in radial direction, 50K magnifications

In the next picture, figure 3.19, a growth of the grain size with the depth increase can be appreciated. The black dots are still unrevealed.

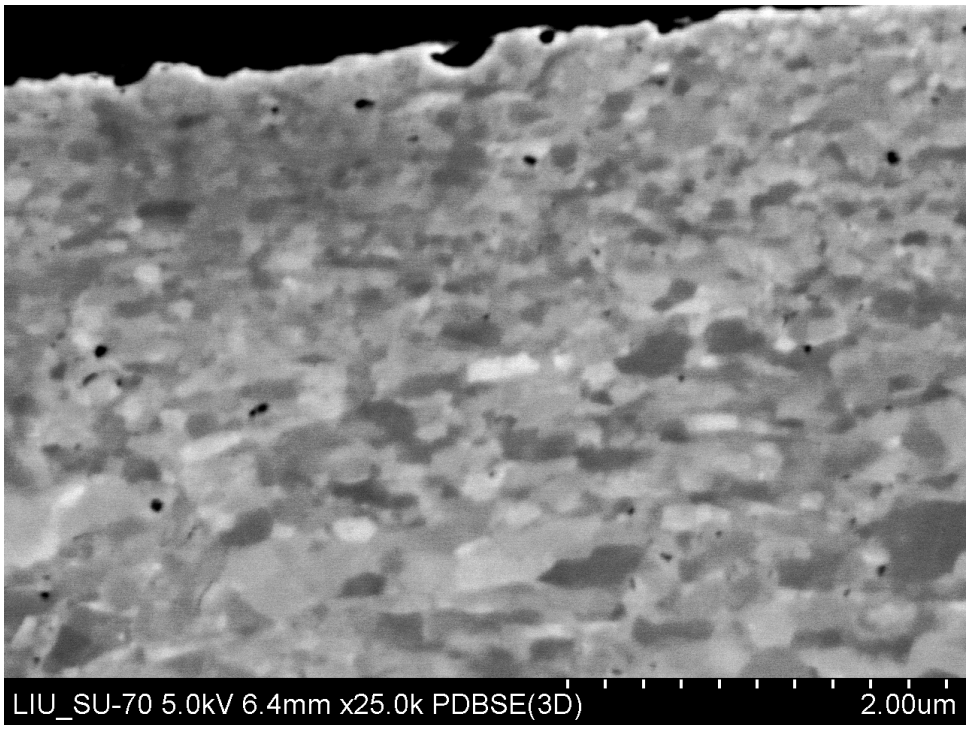

Figure 3.19 Picture of the machined specimen in radial direction, 25K magnifications

The 10k magnifications, figure 3.20, shows a plain view of the growth of the grain size in the layer surroundings and a possible orientation of the grains of the deformation layer.

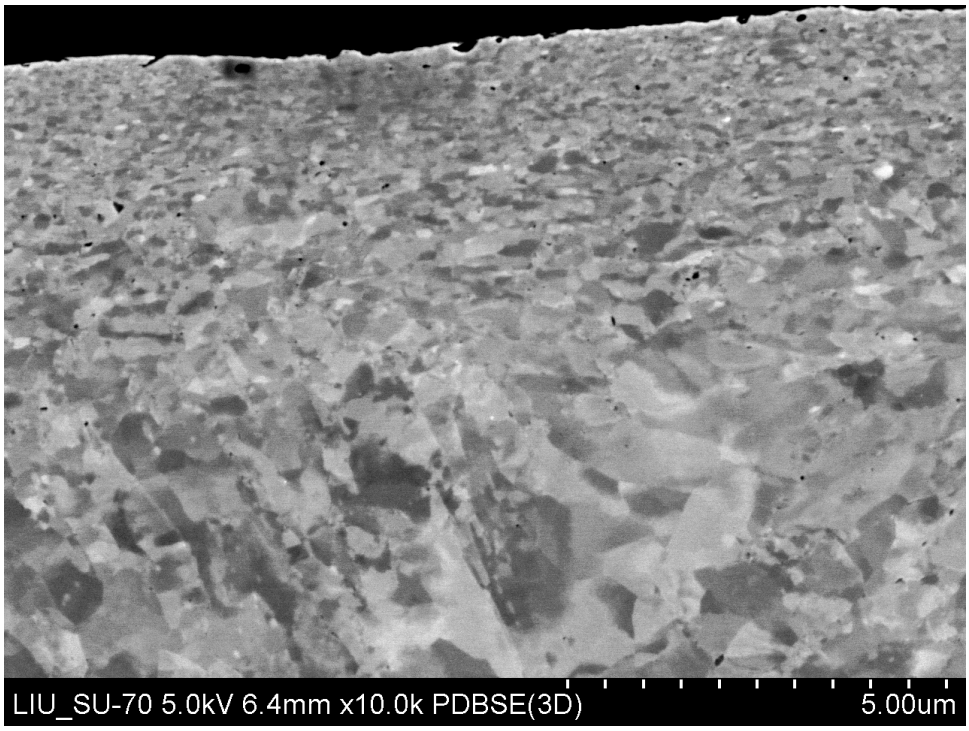

Figure 3.20 Picture of the machined specimen in radial direction, 10K magnifications

A clear difference in the deformation layer can be appreciated in this picture, figure 3.21. The grain size is greater in the core of the specimen and a possible recrystallization due to the heat obtained while the machining procedure is displayed in the edge of the surface.
The deformation layer seems to be quite homogeneous, at least in radial direction.
The last picture of the radial direction analysis is an image of a 2000 magnification, figure 3.22, and shows faultlessly what has been analysing, the grain size and orientation difference between the deformation layer and the rest of the specimen.

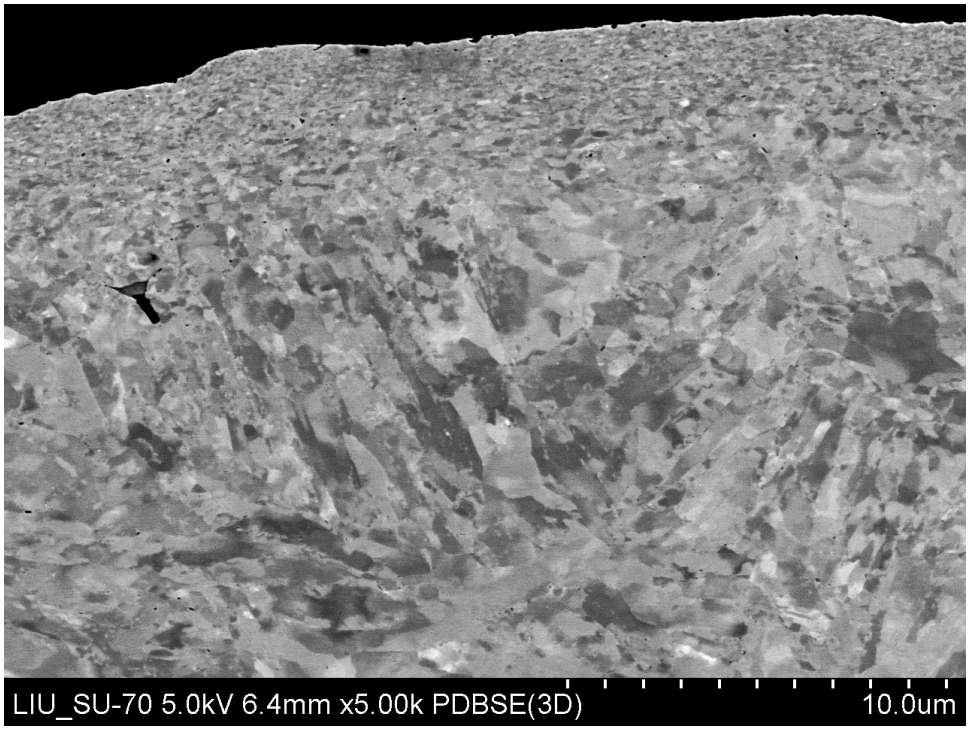

Figure 3.21 Picture of the machined specimen in radial direction, 5K magnifications

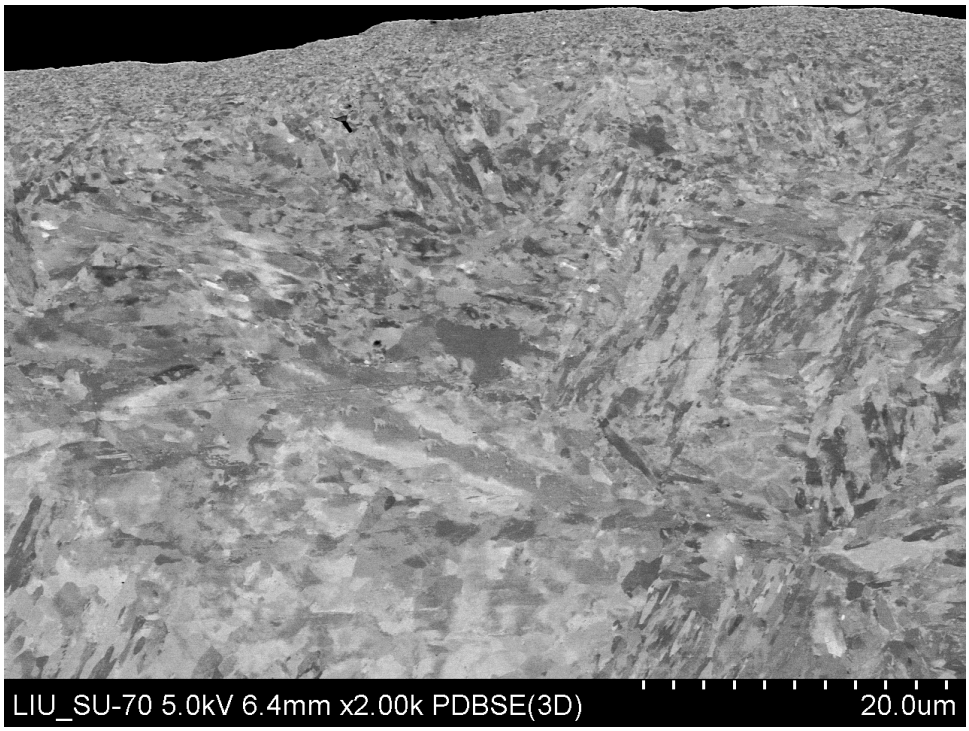

Figure 3.22 Picture of the machined specimen in radial direction, 2K magnifications

Right below, an analysis of the tangential direction images will be carried out.
The 100k times magnification image, figure 3.23, shows a not very focused grain distribution of the deformation layer. However, the small size of the grains could be appreciated.

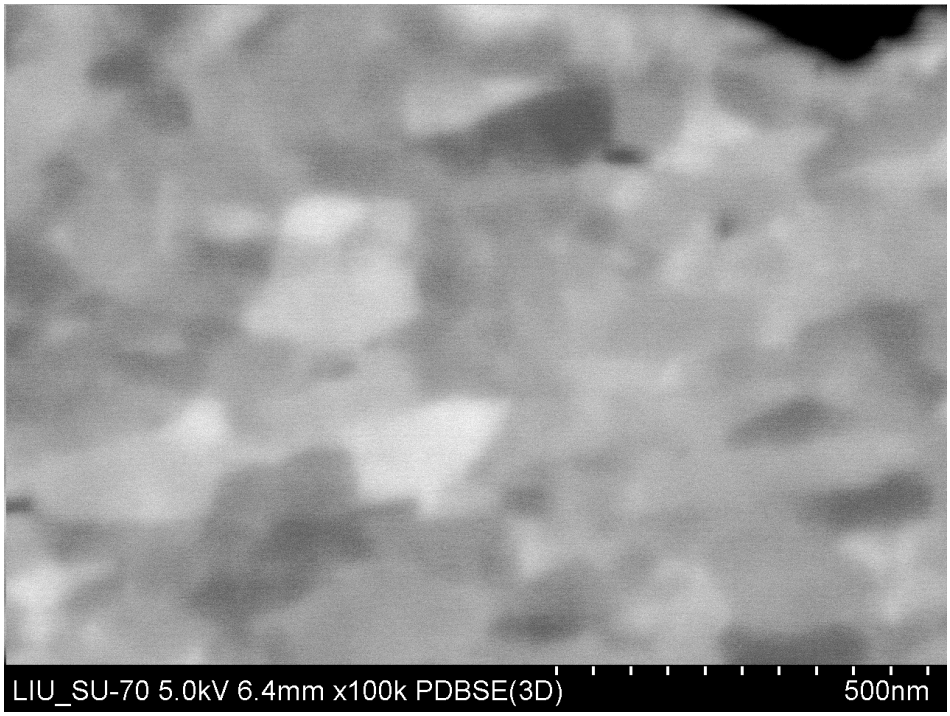

Figure 3.23 Picture of the machined specimen in tangential direction, 100K magnifications

Figure 3.24 shows a possible orientation of the layer grains along the edge of the surface. The small size of the grains can be noticed as well. Figure 3.25 settles what is perceived in figure 3.24. Thanks to the lower magnification pictures, a better view of the orientation can be acknowledged. Additionally, in figure 3.25, a slight growth of the grain size is displayed.
In both figures, 3.24 and 3.25, some black spots could be recognized but nothing so clear so as to state where they are coming from.

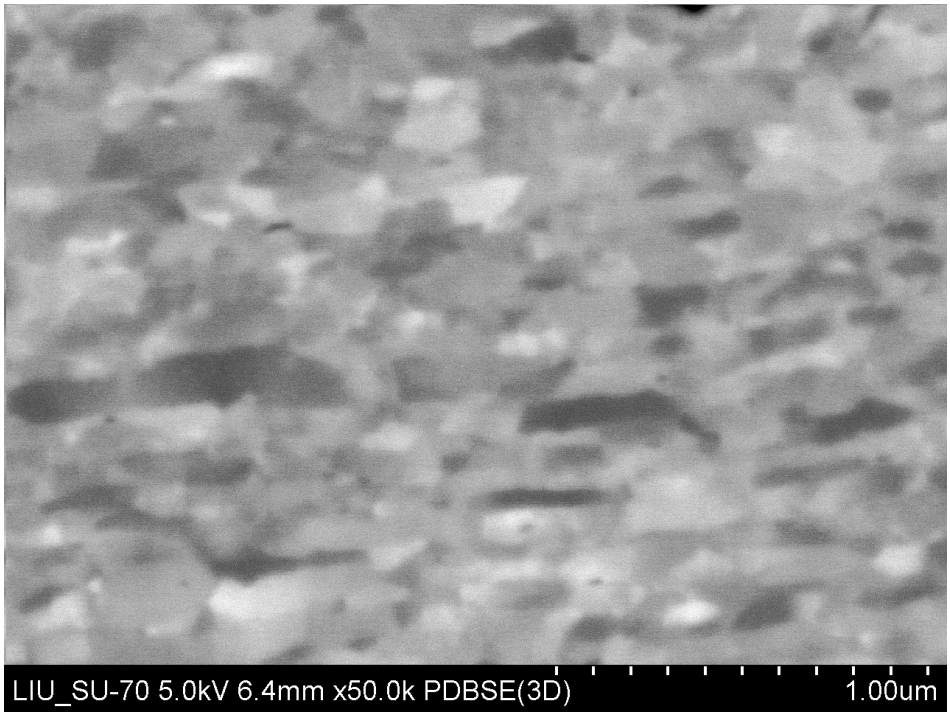

Figure 3.24 Picture of the machined specimen in tangential direction, 50K magnifications

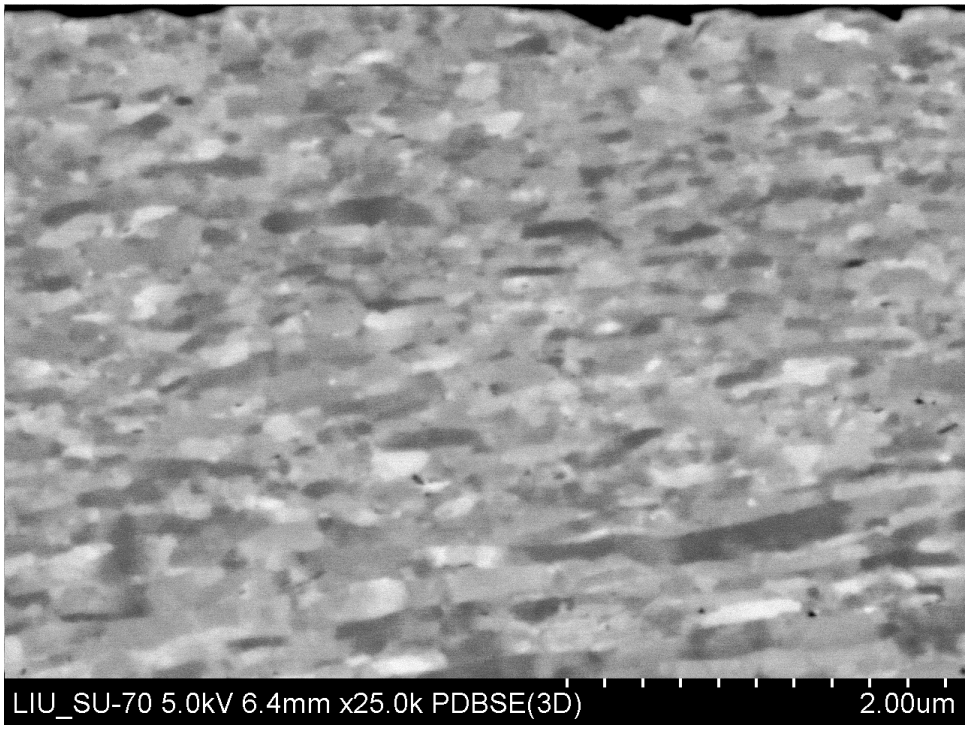

Figure 3.25 Picture of the machined specimen in tangential direction, 25K magnifications

Same deformation layer can be identified in tangential direction as well, shown in figures 3.26 and 3.27. However, the width of the layer differs in several parts of the edge of the specimen.
As another fact, a quite noticeable bending can be appreciated in the following two pictures. The reason of this bending was explained when the light microscope's analysis was executed. Anyway, figures 3.26 and 3.27 are a nice demonstration of the existence of the bending and also the recrystallization on the tangential direction.

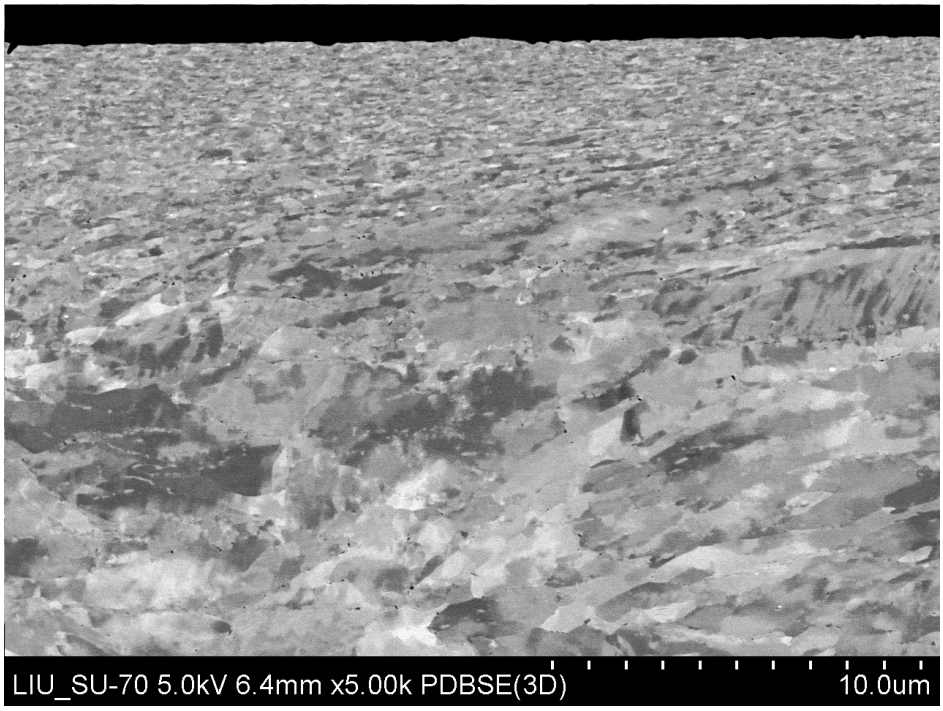

Figure 3.26 Picture of the machined specimen in tangential direction, 5K magnifications

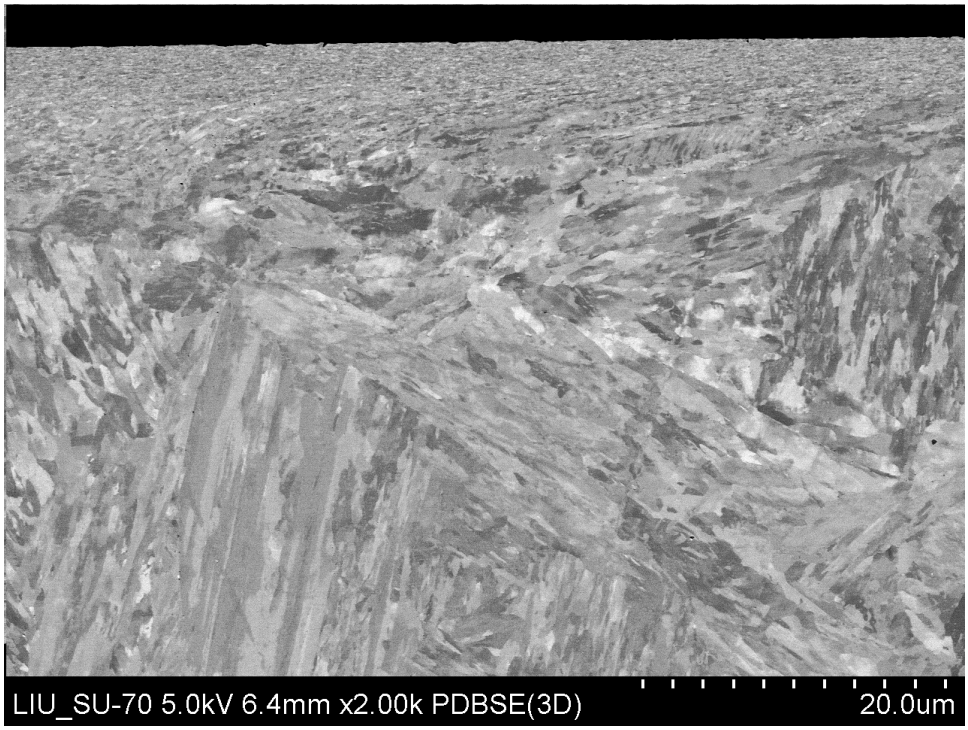

Figure 3.27 Picture of the machined specimen in tangential direction, 2K magnifications

Once the edge is studied, a view to the core of the specimen will be accomplished so as to acknowledge how the grain size and shape look like.
In the following pictures, figures 3.28, 3.29 and 3.30, some white and some black dots were detected.
It could be possible that the white ones have a harder composition and the black ones are still unknown. The difference between them is that the white ones can be seen in every picture and in quite many magnifications. On the other hand, black spots are not so spread.

Diverse shapes and orientations of the grains can be appreciated in pictures 3.29 and 3.30. Both pictures have 25k times amplification and really different shapes.

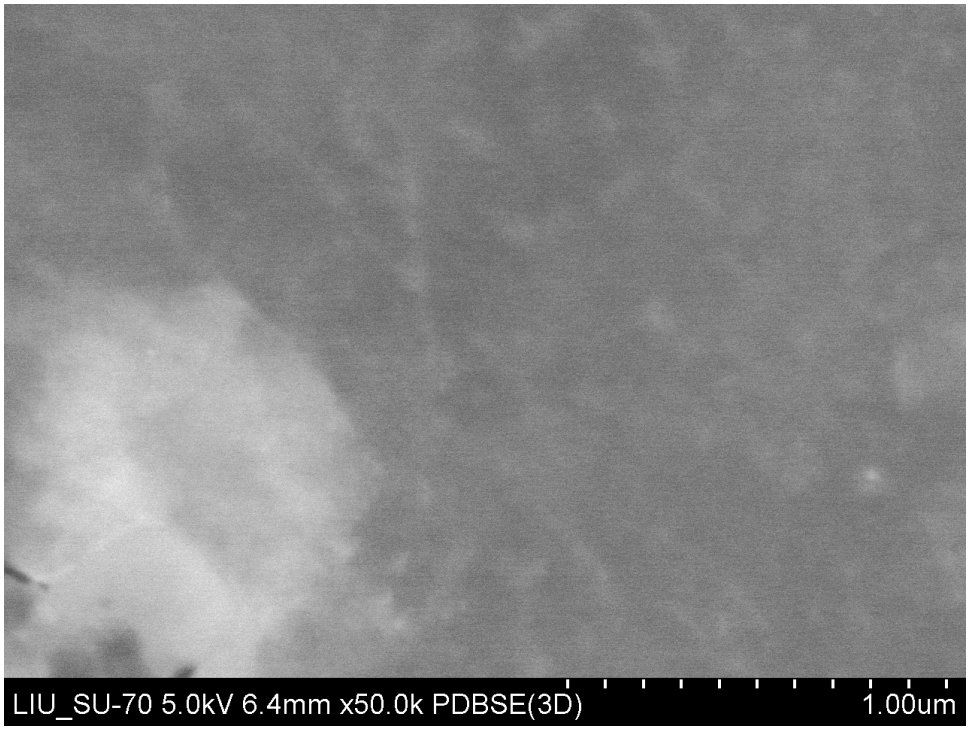

Figure 3.28 Picture of inside surface of the machined specimen in radial direction, 50K magnifications

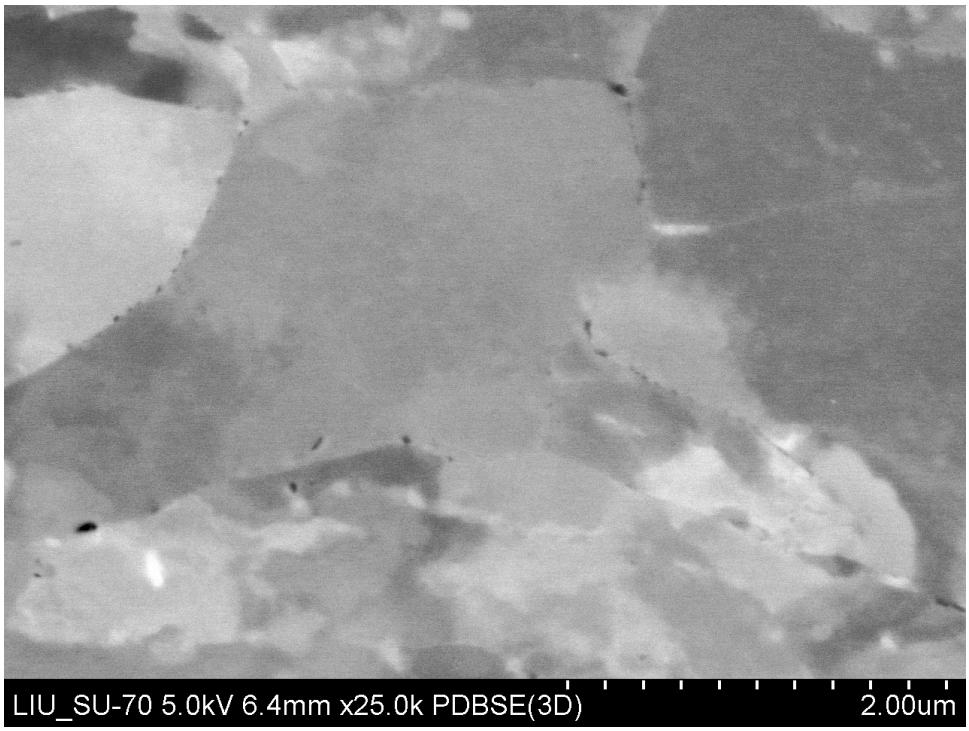

Figure 3.29 Picture of inside surface of the machined specimen in radial direction, 25K magnifications (1)

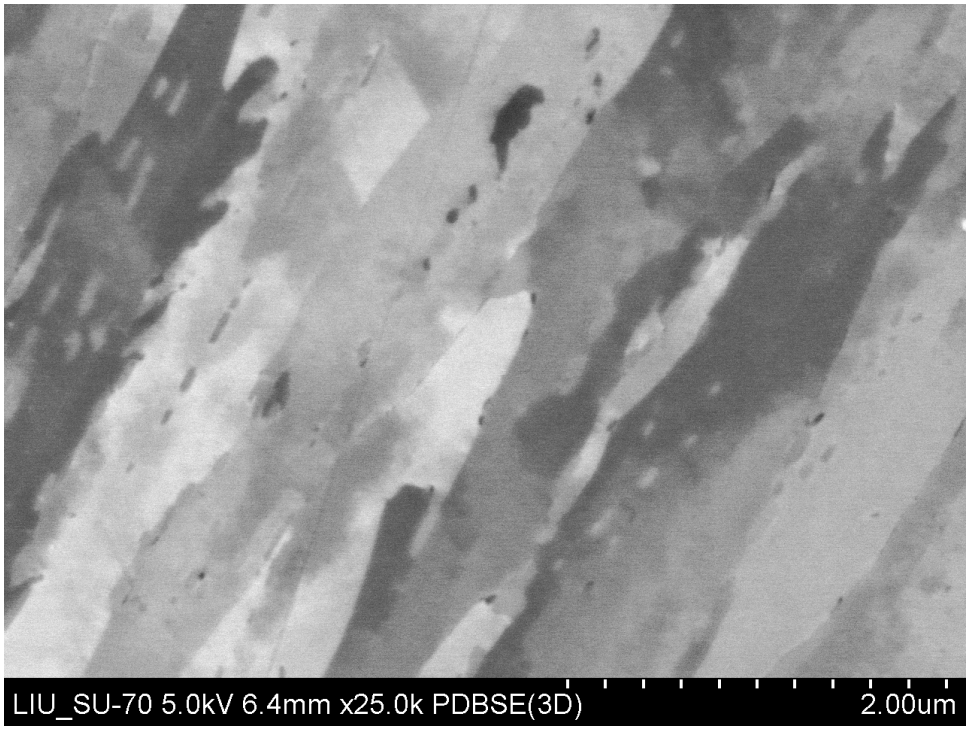

Figure 3.30 Picture of inside surface of the machined specimen in radial direction, 25K magnifications (2)

3.3.3.4 Heat Treated ring

Same procedure will be carried out for the Heat Treated ring. First, some images analyzing the radial direction specimen will be shown and, right after, tangential direction images. The figures displayed for this two analysis are from 3.31 to 3.36 and from 3.37 to 3.42, respectively.

A higher amount of white spots is noticed in this ring. A reason for them to appear could be that they were created during the heat treatment. In order to refresh the process carried out with this ring, just mention that two heat treatments were executed. The first one was given as the other two rings so as to obtain the strength and hardness required. The second one, in the other hand, was performed to relief the residual stress stored in the ring as a result of the machining.

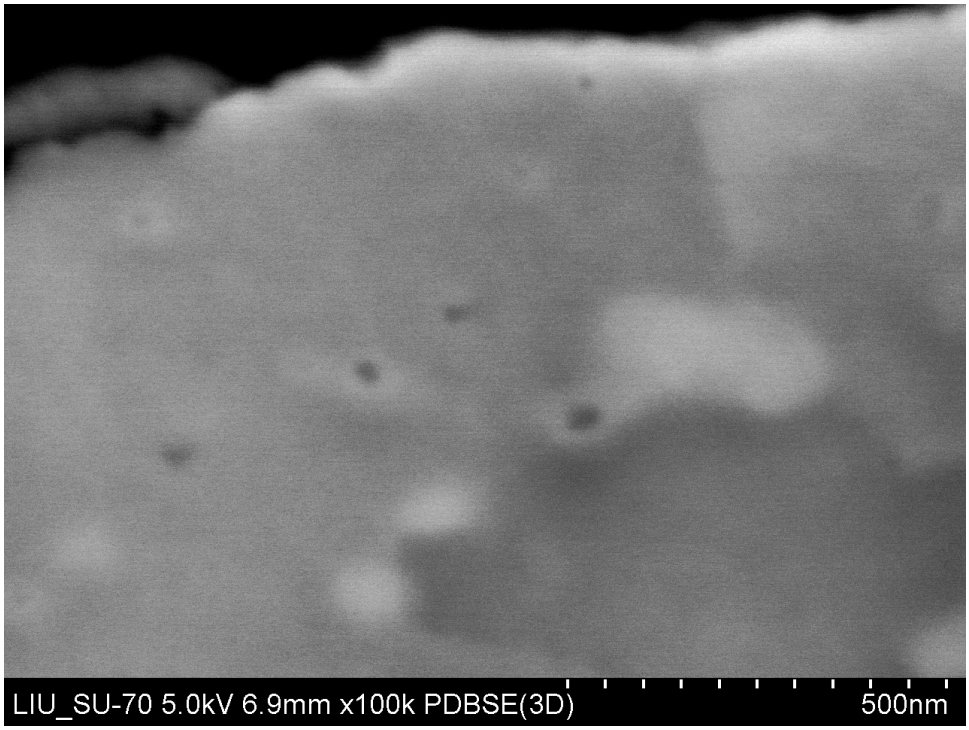

Figure 3.31 Picture of the Heat Treated specimen in radial direction, 100K magnifications

In every figure it can be noticed that, in the Heat Treated ring, greater grains are displayed. A quick comparison can be performed between the machined ring shown in figure 3.20, for instance, and figure 3.34. Both pictures were taken with a 10k magnification, so a clear view of the edge can be glanced.

It can be stated that the second heat treatment changed the properties of the ring. A totally altered layer could be peeked in the lower magnification images, such as figures 3.35 and 3.36.

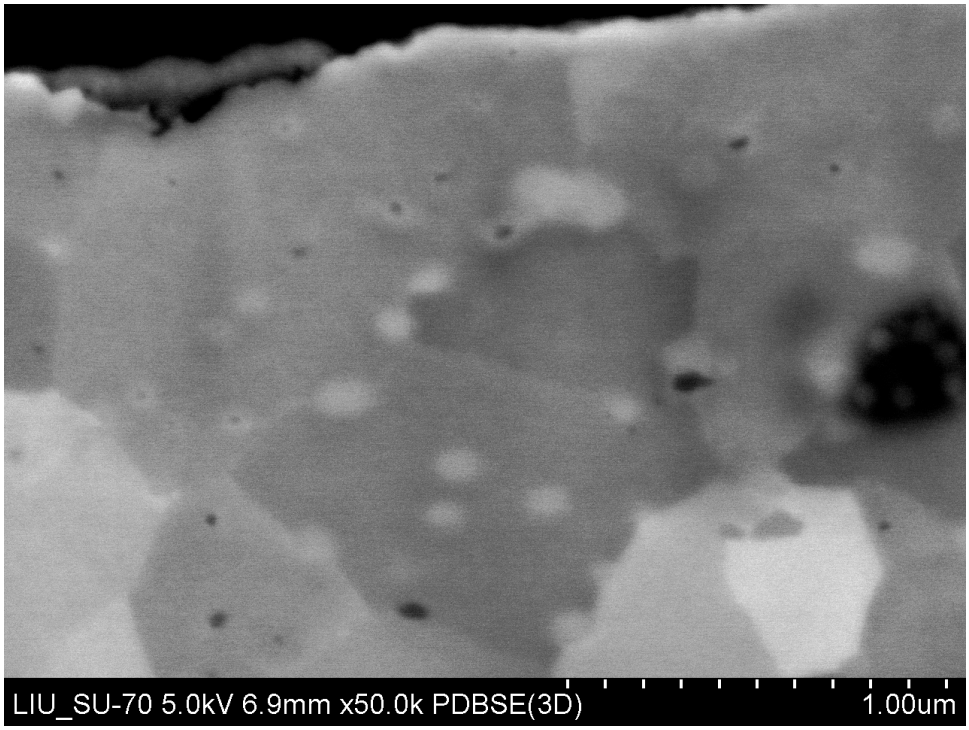

Figure 3.32 Picture of the Heat Treated specimen in radial direction, 50K magnifications

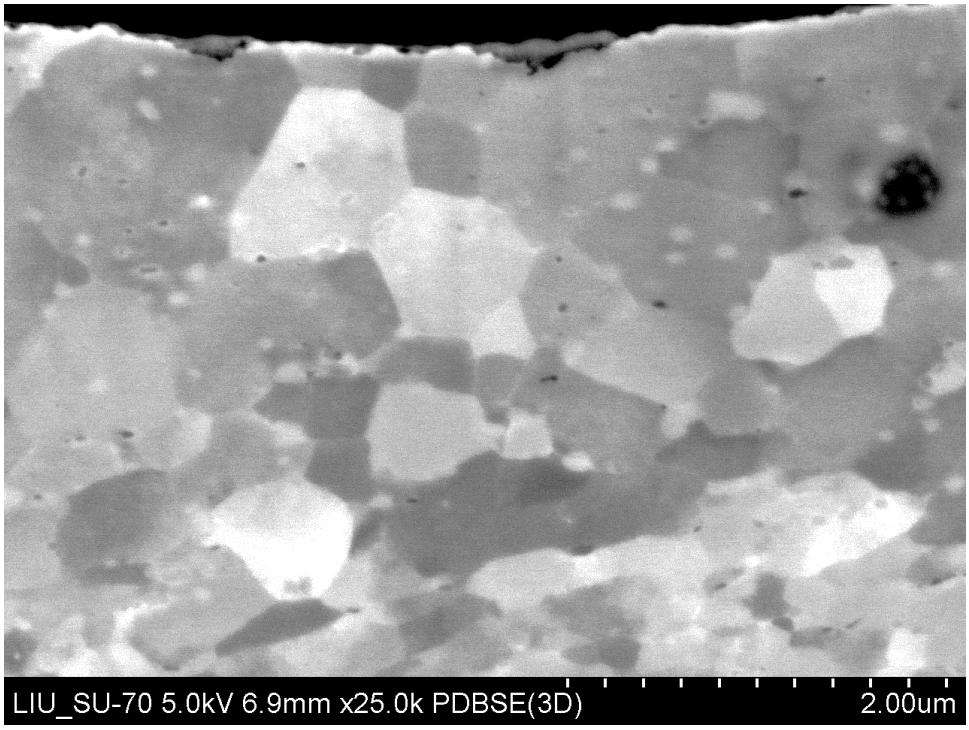

Figure 3.33 Picture of the Heat Treated specimen in radial direction, 25K magnifications

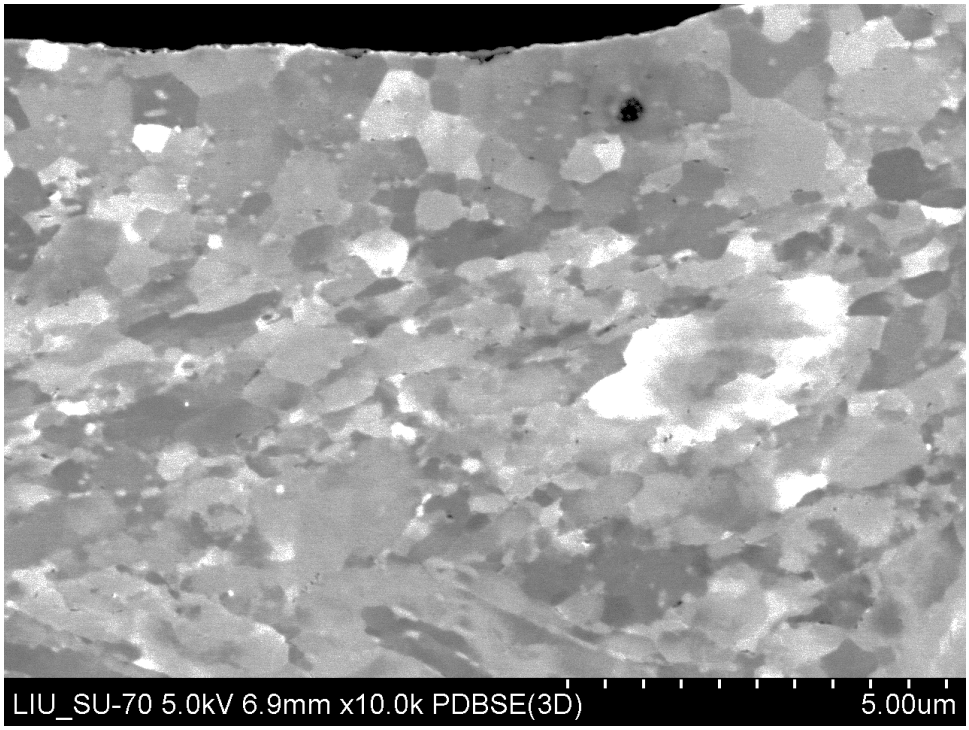

Figure 3.34 Picture of the Heat Treated specimen in radial direction, 10K magnifications

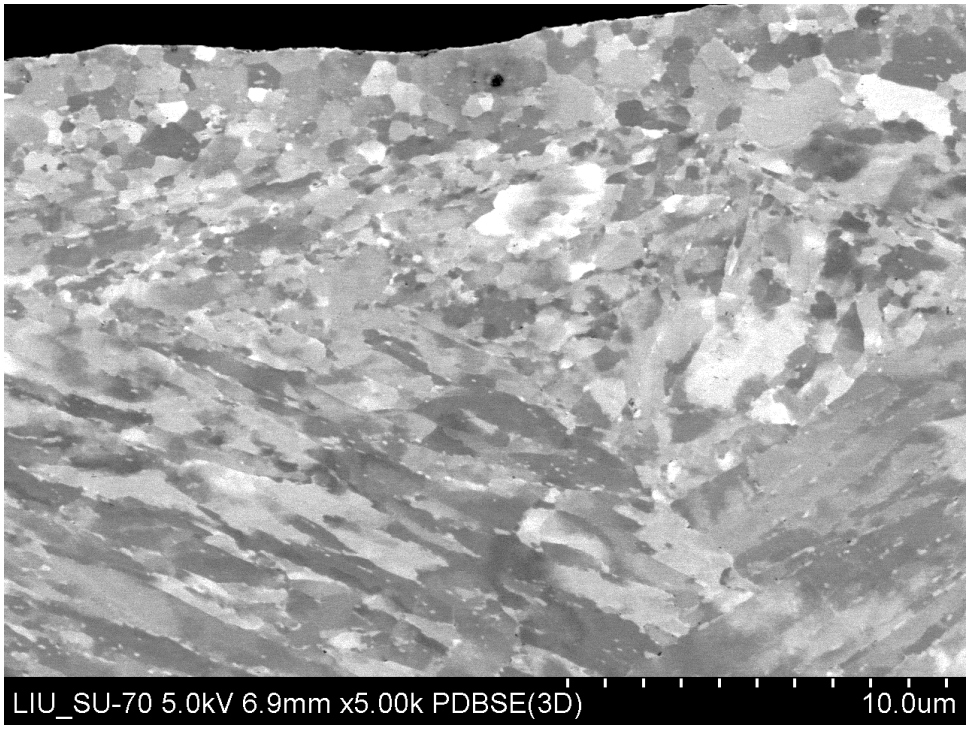

Figure 3.35 Picture of the Heat Treated specimen in radial direction, 5K magnifications

As it is affirmed in previous pages, there is a substantial difference between the machined and the Heat Treated microstructure. Just a rapid view of the picture below, figure 3.36, in comparison with image 3.22 shows it.

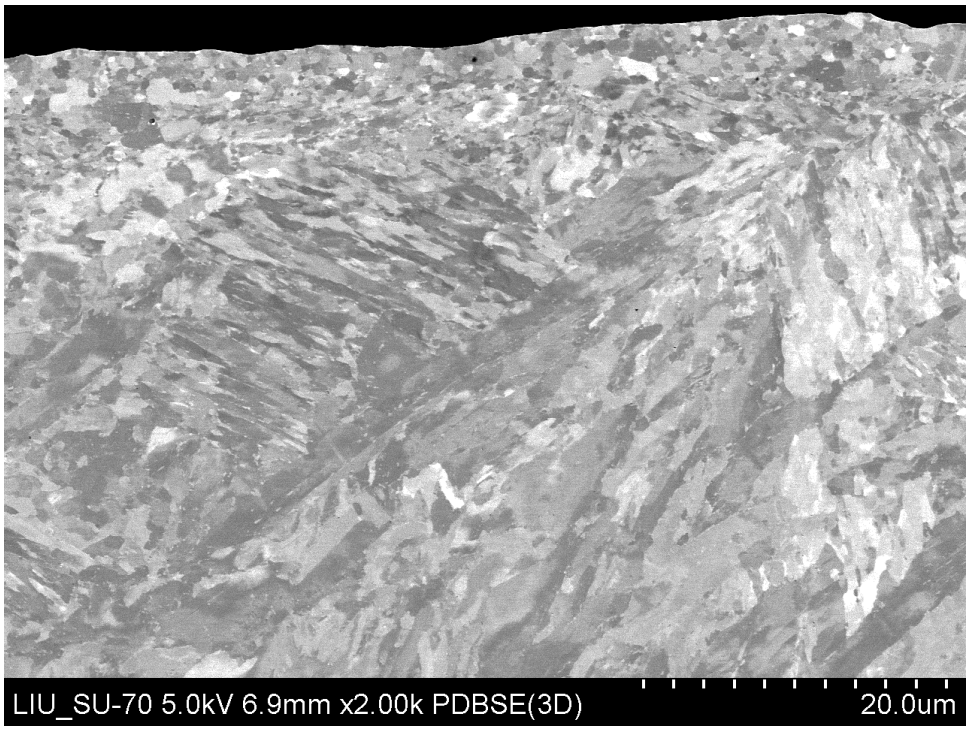

Figure 3.36 Picture of the Heat Treated specimen in radial direction, 2K magnifications

The tangential direction images show differences as well if they are compared to the machined ones.
The white spots appear in all the images. Besides, a clear difference on the bending was noticed too. In the following pages a deeper analysis will be executed.

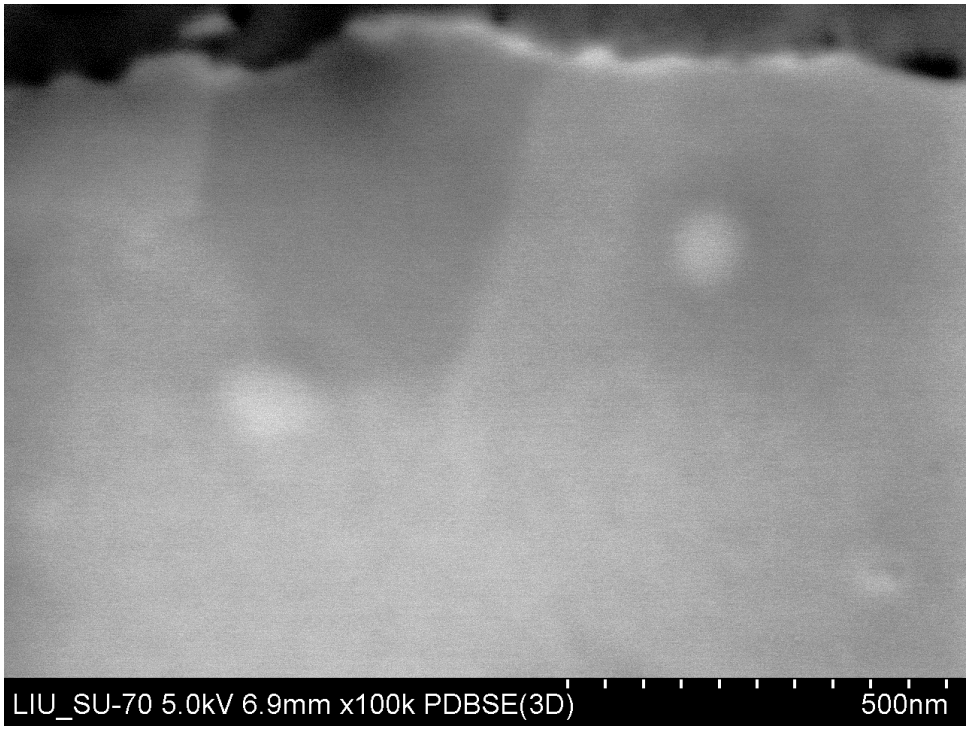

Figure 3.37 Picture of the Heat Treated specimen in tangential direction, 100K magnifications

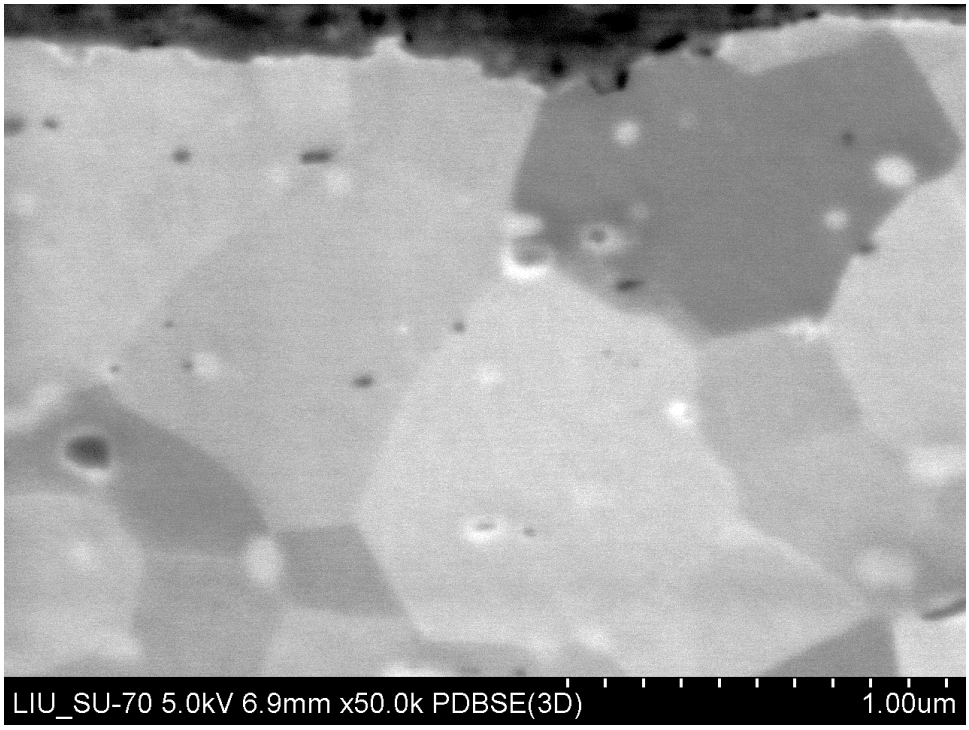

Figure 3.38 Picture of the Heat Treated specimen in tangential direction, 50K magnifications

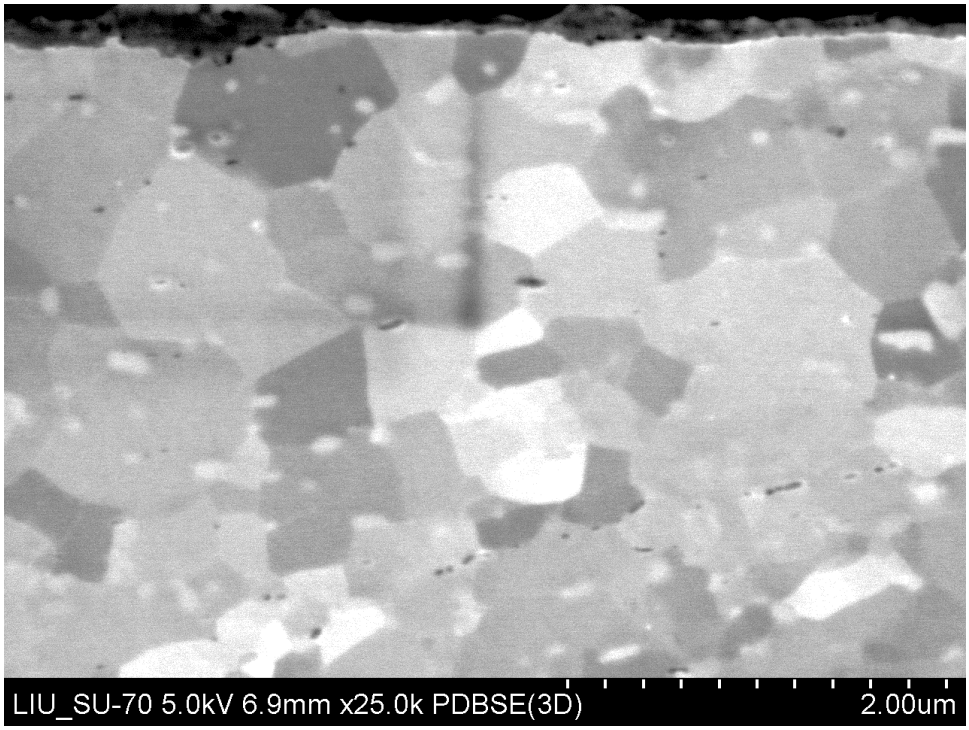

Figure 3.39 Picture of the Heat Treated specimen in tangential direction, 25K magnifications

In the image right below, figure 3.40, it is noticed a peculiar behavior of the microstructure. The grains are bended as the ones on the machined ring, but, on the other hand, there is a small layer on the edge that presents a really different behavior. Instead of appearing the grains bended, they are geometrically located. Same conduct could be appreciated in figures 3.41 and 3.42.

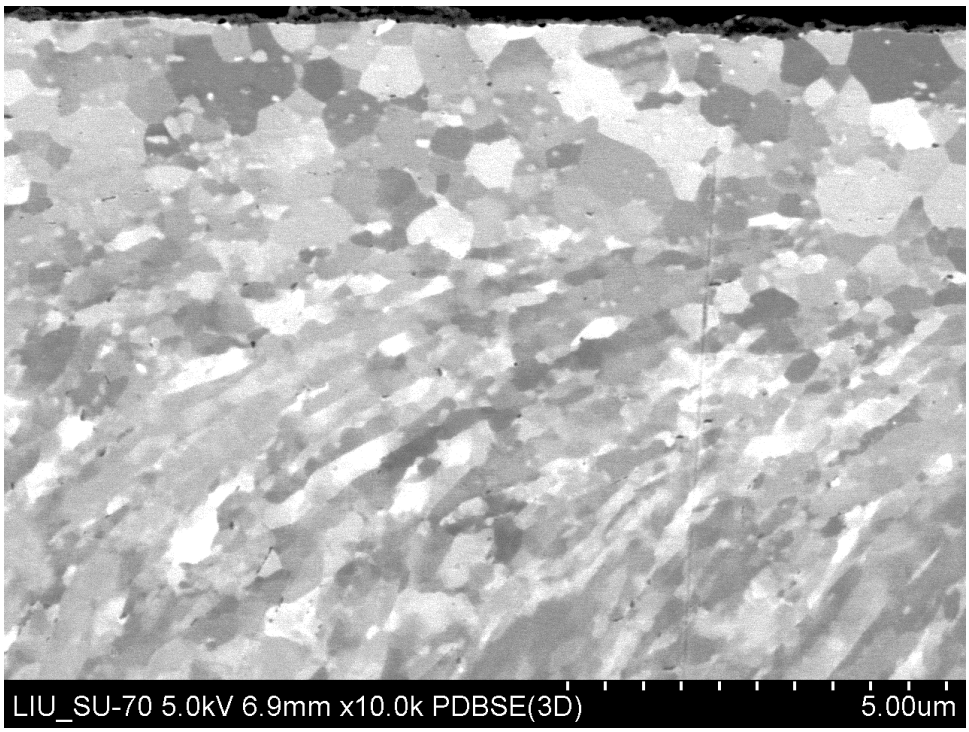

Figure 3.40 Picture of the Heat Treated specimen in tangential direction, 10K magnifications

Clear long grains are bended in one direction in the whole surface but not in the very edge. The growth of the grain size along the edge of the specimen's surface is an undesirable situation and it was a clear consequence of the heat treatment performed to the ring.

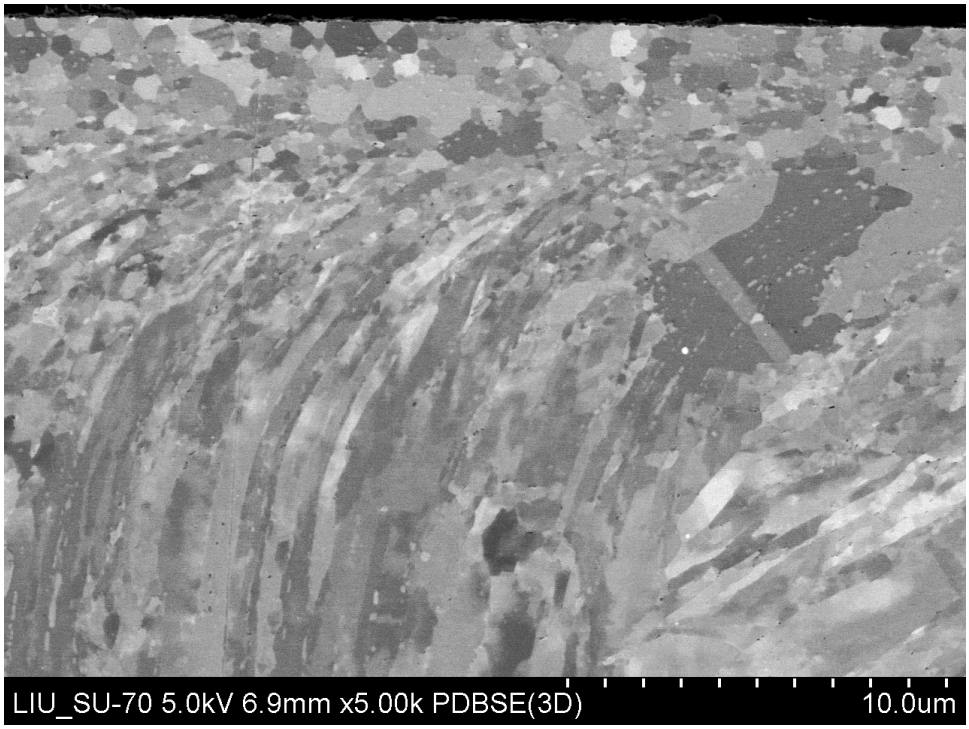

Figure 3.41 Picture of the Heat Treated specimen in tangential direction, 5K magnifications

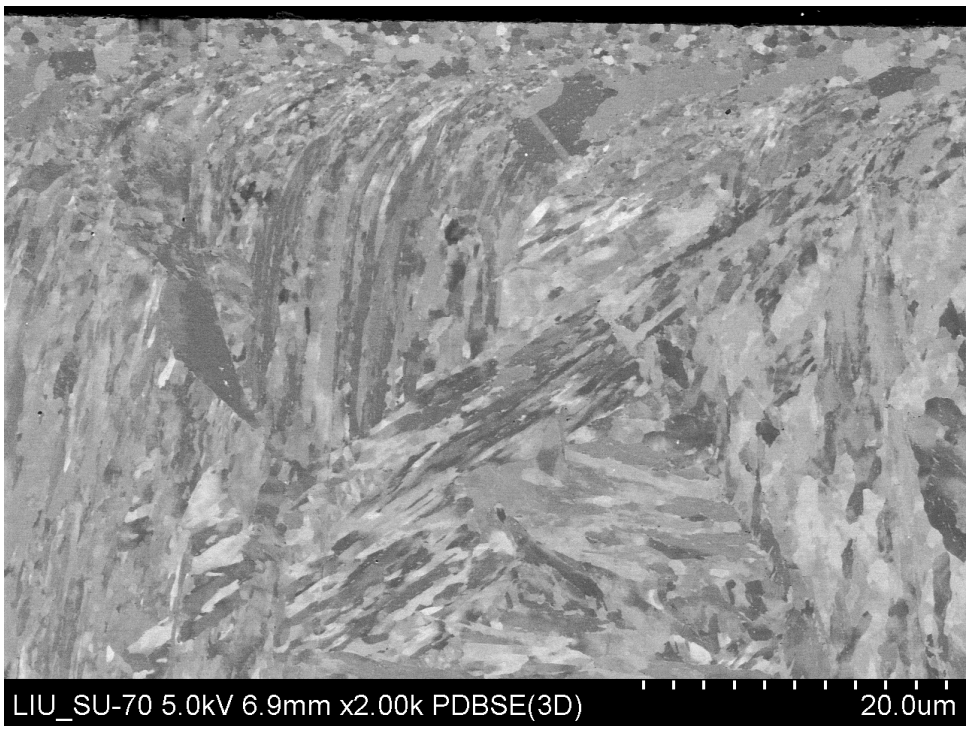

Figure 3.42 Picture of the Heat Treated specimen in tangential direction, 2K magnifications

3.3.3.5 VSR ring

Taking a view to the radial direction images captured with the VSR specimen, an obvious similarity of the grain size was noticed with the machined specimen. It can be spotted when figures 3.43 and 3.44 with figures 3.17 and 3.18 are compared.

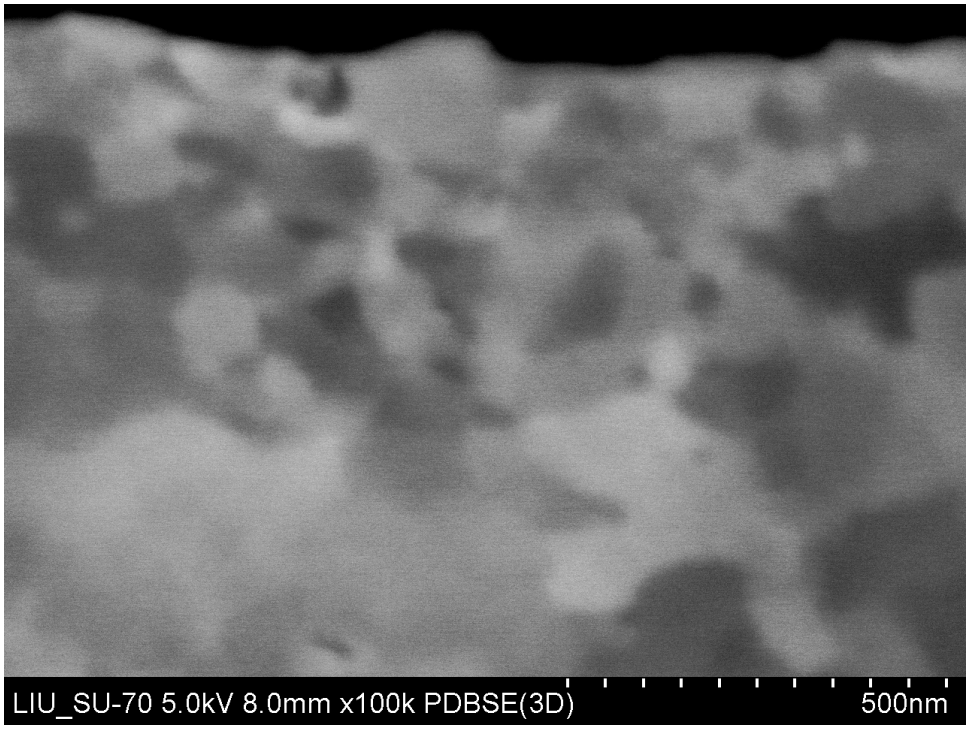

Figure 3.43 Picture of the VSR specimen in radial direction, 100K magnifications

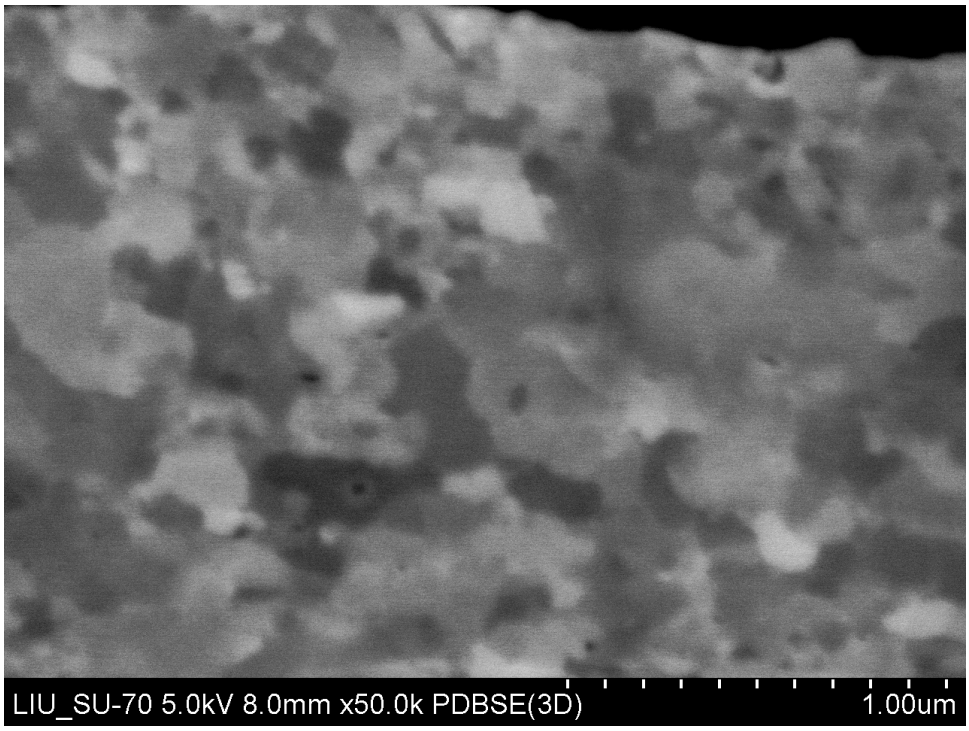

Figure 3.44 Picture of the VSR specimen in radial direction, 50K magnifications

Analyzing lower magnification images, the same similarity is found between the radial direction microstructures. 25k to 2k times magnifications displayed in figures 3.19 to 3.22 and 3.45 to 3.48 show the same size, shape and a homogeneous deformation layer on the edge of the specimen.

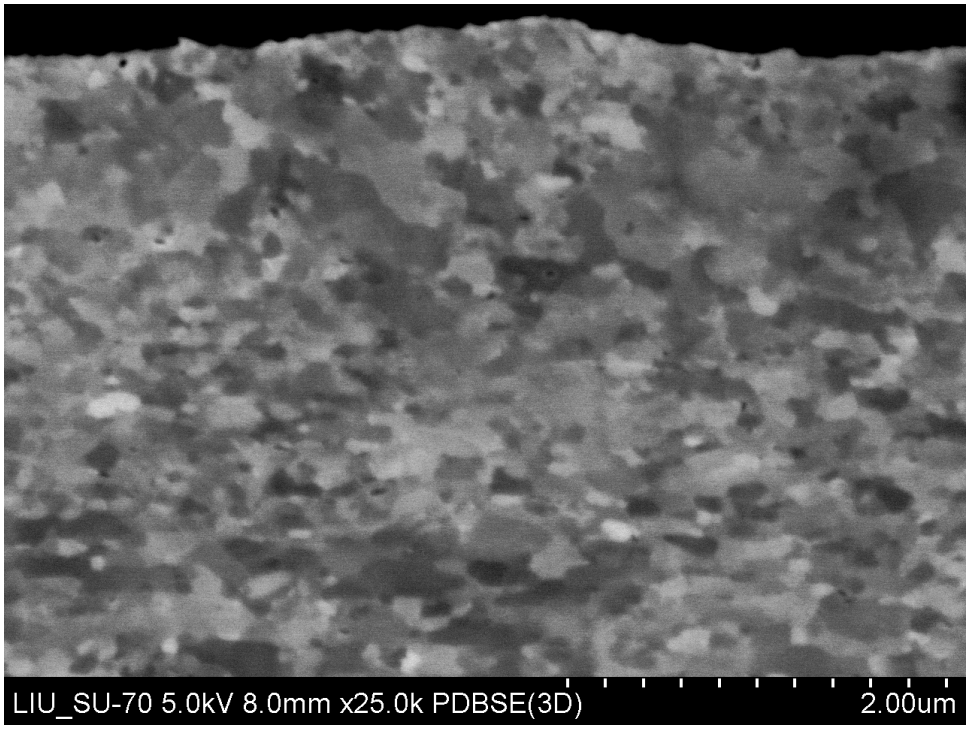

Figure 3.45 Picture of the VSR specimen in radial direction, 25K magnifications

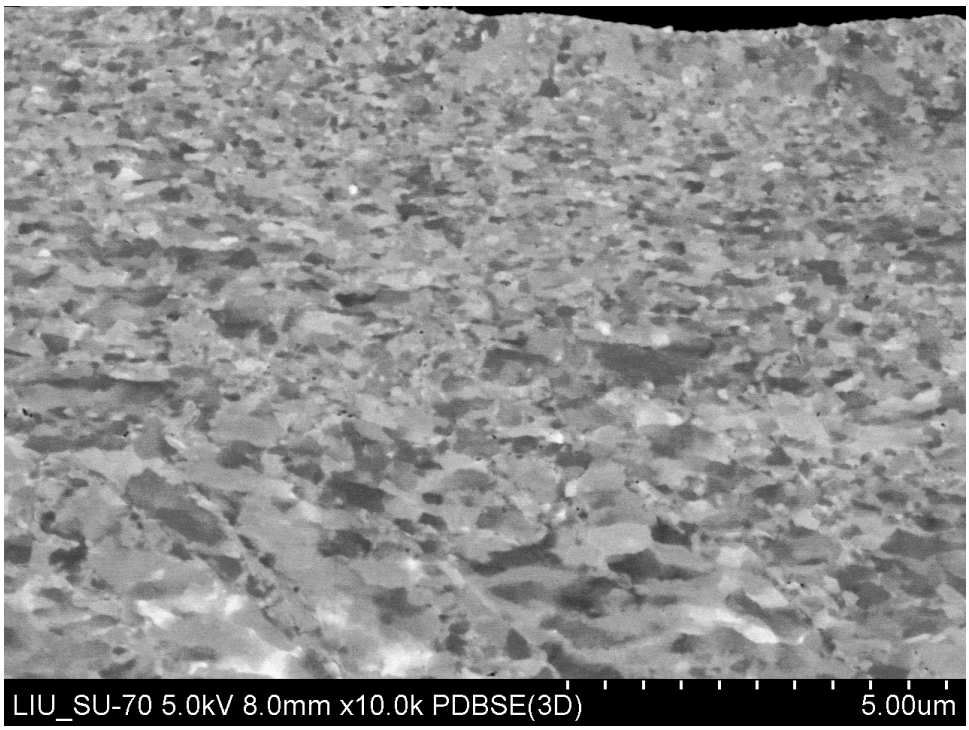

Figure 3.46 Picture of the VSR specimen in radial direction, 10K magnifications

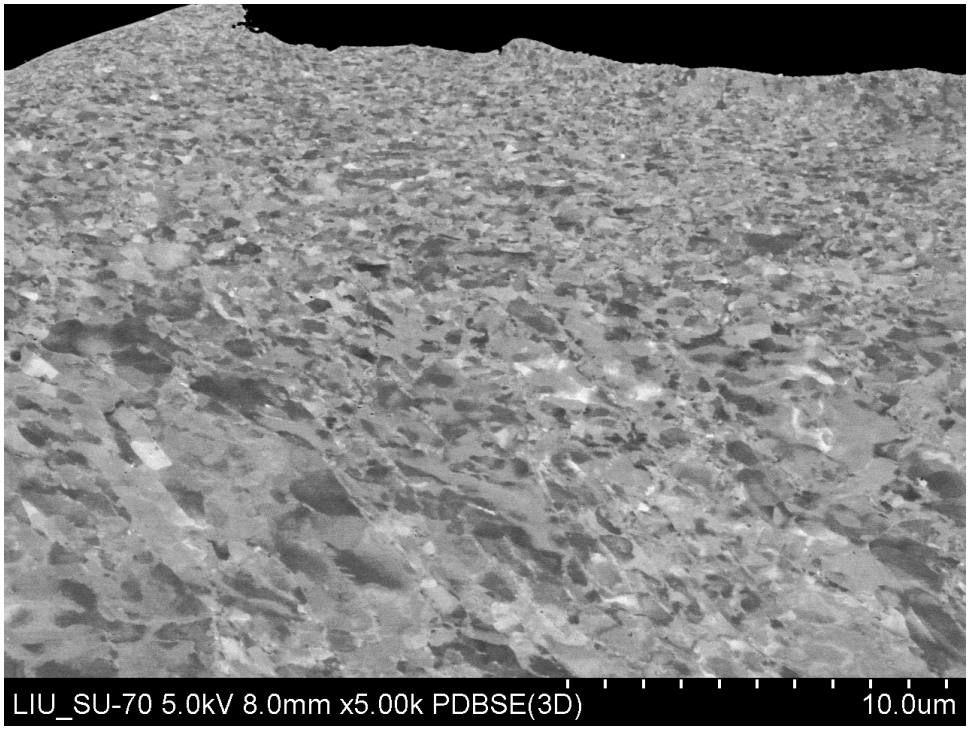

Figure 3.47 Picture of the VSR specimen in radial direction, 5K magnifications

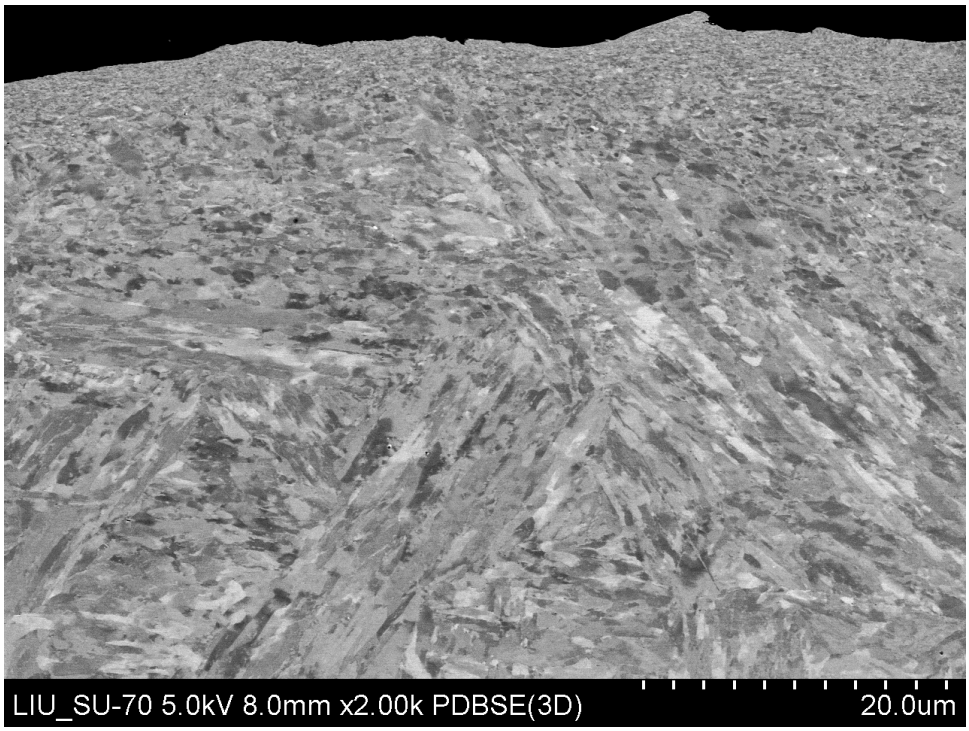

Figure 3.48 Picture of the VSR specimen in radial direction, 2K magnifications

In the following pages, an analysis of the tangential direction images will be carried out. The focus of the figure 3.49, located right below, is not enough to take out any conclusion. The only fact that could be appreciated is a small grain size. It is necessary to take a glance to figure 3.50, to recognize that the microstructure has definitely a small size grain size and a possible bended orientation.

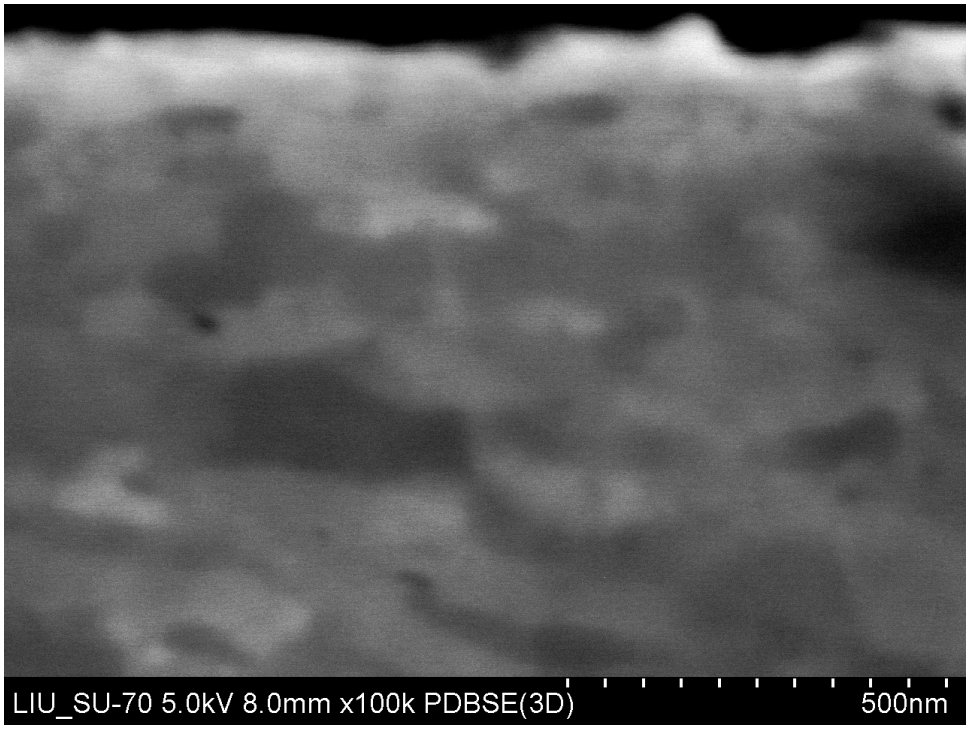

Figure 3.49 Picture of the VSR specimen in tangential direction, 100K magnifications

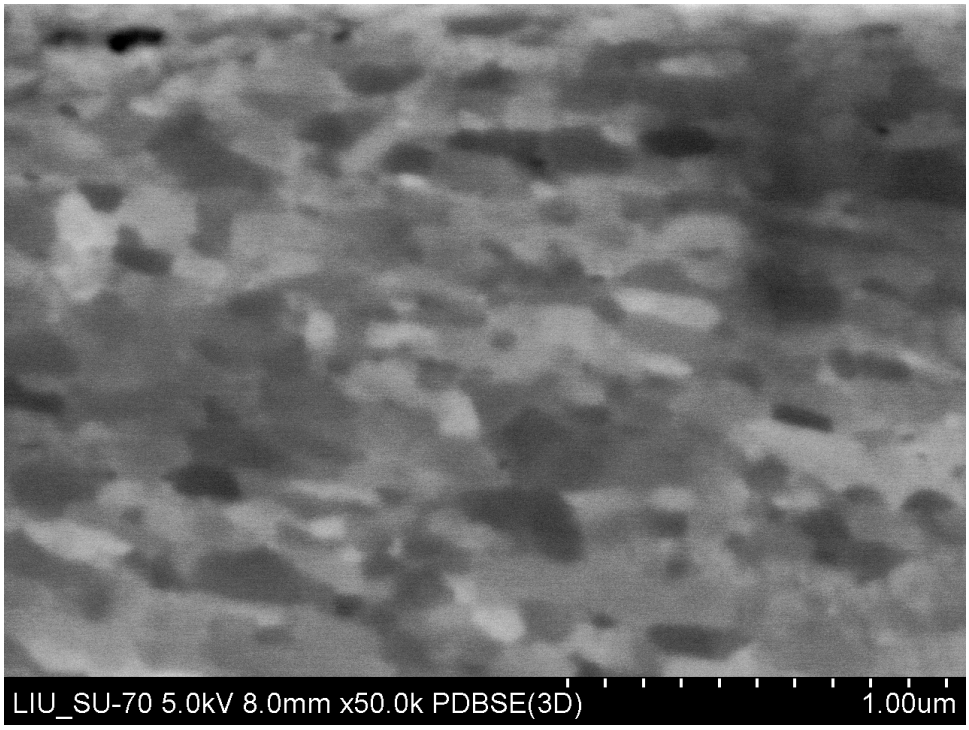

Figure 3.50 Picture of the VSR specimen in tangential direction, 50K magnifications

Taking a look to figures 3.51 and 3.52, the thoughts of the grain size and orientation are cleared. Additionally, a growth of the grain size could be detected as in the machined specimen.

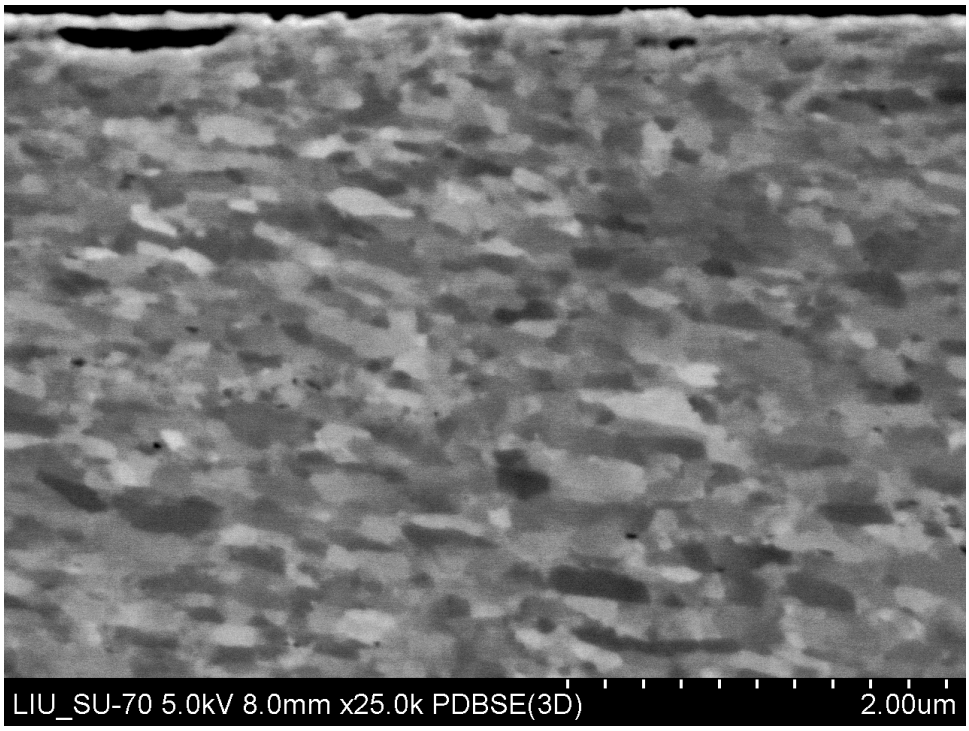

Figure 3.51 Picture of the VSR specimen in tangential direction, 25K magnifications

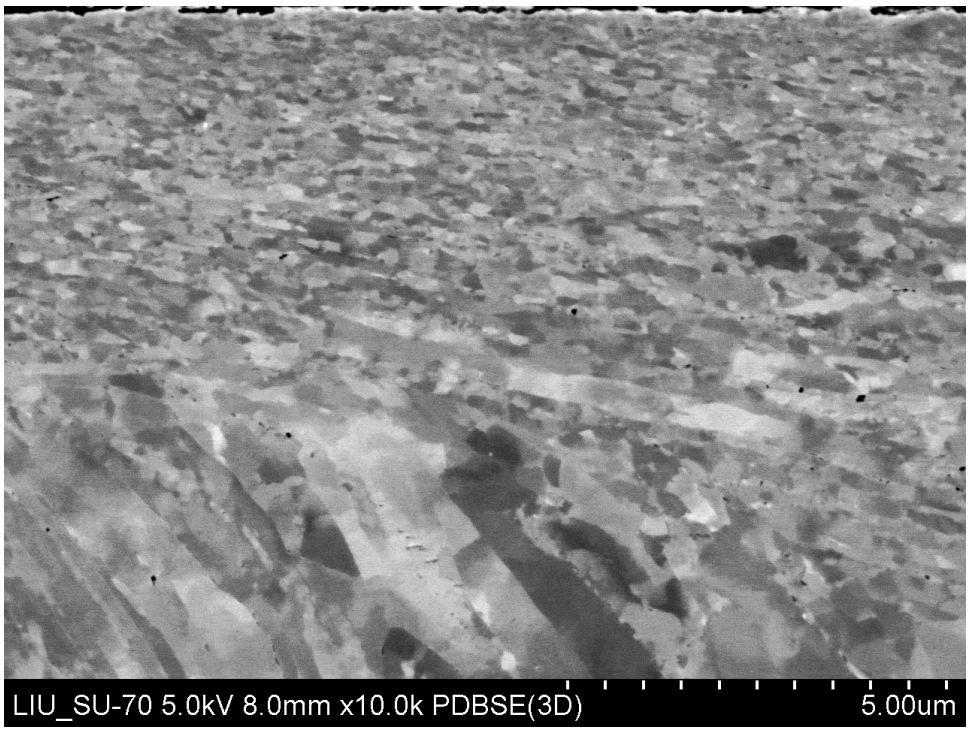

Figure 3.52 Picture of the VSR specimen in tangential direction, 10K magnifications

The successive pictures, figures 3.53 and 3.54, show discernibly a quite homogeneous deformation layer and an obvious bending. Executing a comparison between figures 3.54 and 3.27 (image of the tangential direction in the machined ring with a 2k magnifications), there is a quite similar bending and grain size but, on the other hand, also a less homogeneous layer can be detected in the machined ring.

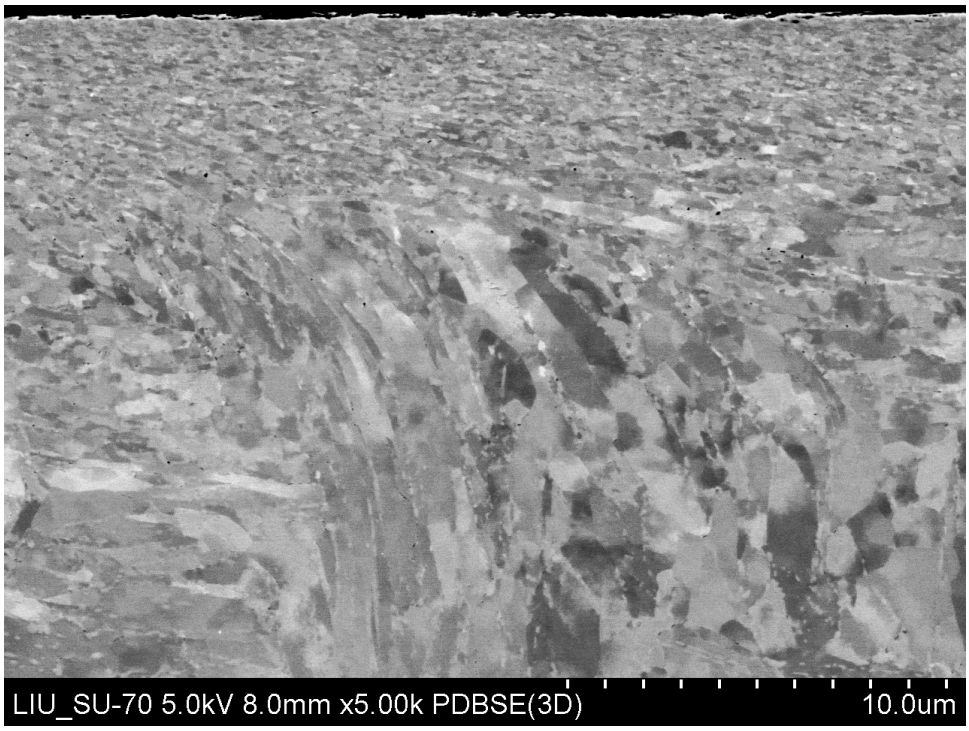

Figure 3.53 Picture of the VSR specimen in tangential direction, 5K magnifications

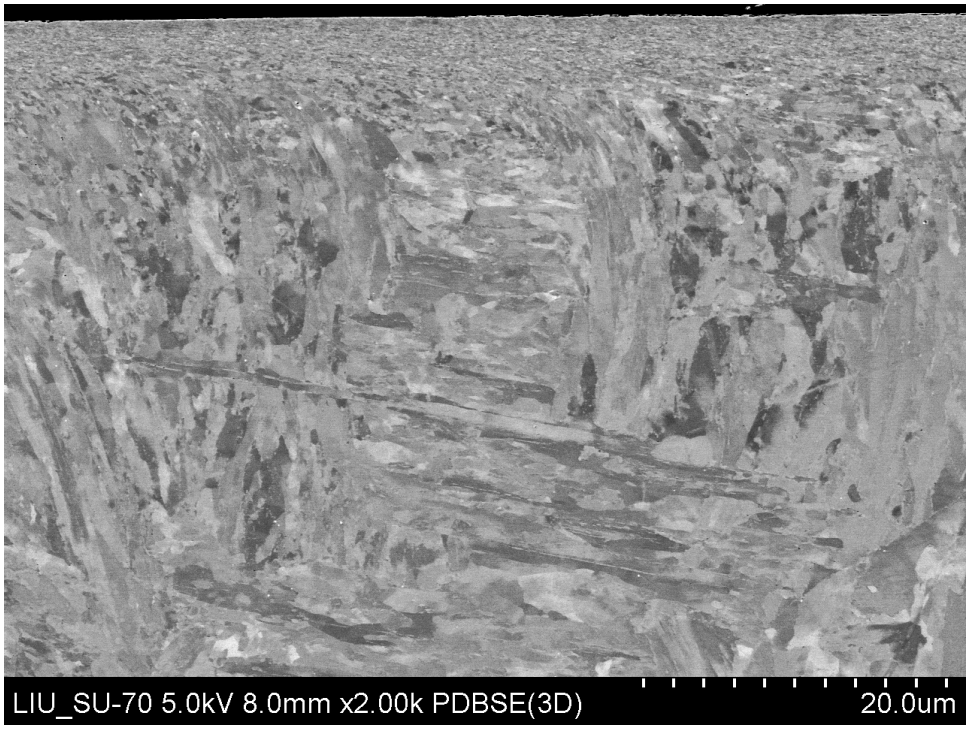

Figure 3.54 Picture of the VSR specimen in tangential direction, 2K magnifications

Some pictures captured the core of the VSR specimen in order to analyze the microstructure. Same conclusion was carried out, lath martensite and ferrite were found. They are displayed in figures 3.55 to 3.57.

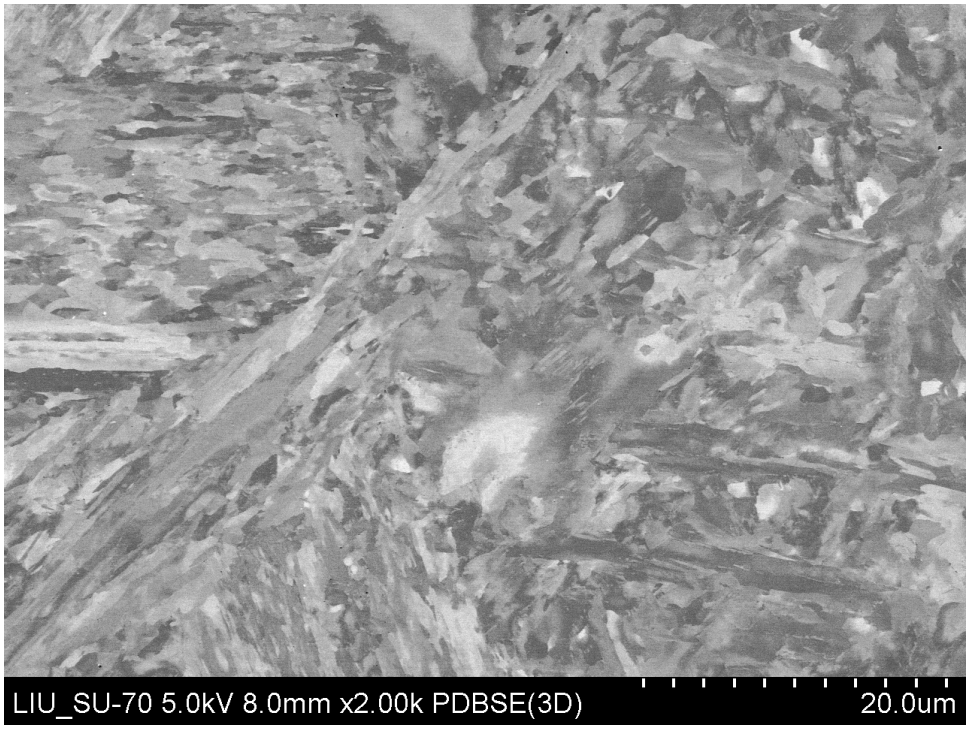

Figure 3.55 Picture of the inside of the VSR specimen in tangential direction, 2K magnifications (1)

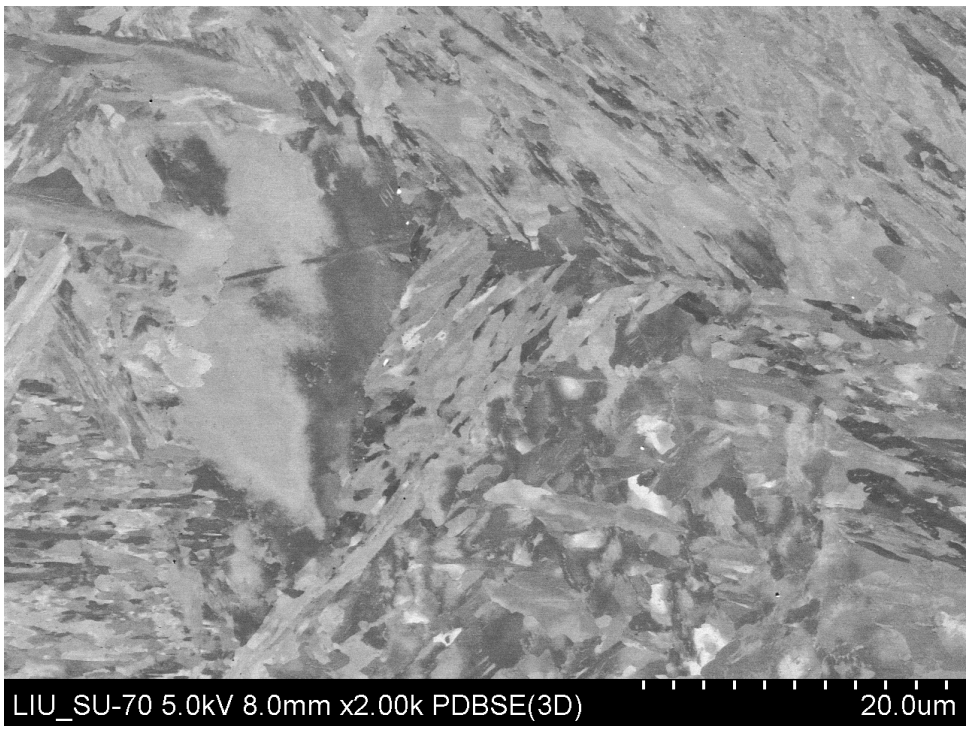

Figure 3.56 Picture of the inside of the VSR specimen in tangential direction, 2K magnifications (2)

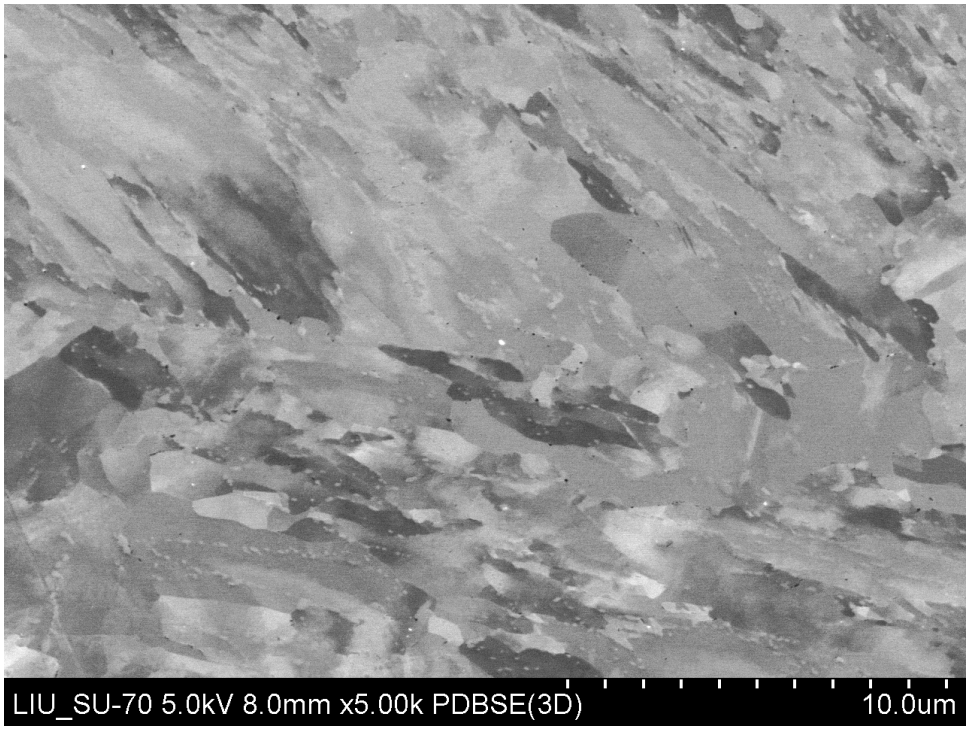

Figure 3.57 Picture of the inside of the VSR specimen in tangential direction, 5K magnifications

The possible carbides wanted to be analysed more carefully, hence some pictures were taken utilizing two detectors. PDBSE detector, used in the rest of the analysis performed, and SE detector, used to compare the images captured with the other detector.

In the picture shown below, figure 3.58, white spots are detected all over the captured space. Black spots are distinguished as well. It is still not clear if the black spots are carbides or the footprint left by the impurities removed during the polishing. However, the black spots could be carbides as they appear in the grain boundaries, just as they are lying in figures 3.58, 3.59 and 3.60.

As it was mentioned in previous pages, the white spots could possibly be heavier metals agglomerated when the metal is cooled. In order to obtain a finer capture of the possible heavy metals, the SE detector was used to capture the same picture as with PDBSE. Both figures can be examined right below, 3.58 and 3.59. Some other pictures were taken so as to get a deeper analysis. They are presented in figures 3.60 and 3.61.

Carbides are also displayed in figure 3.59 and 3.61 when SE detector was used.

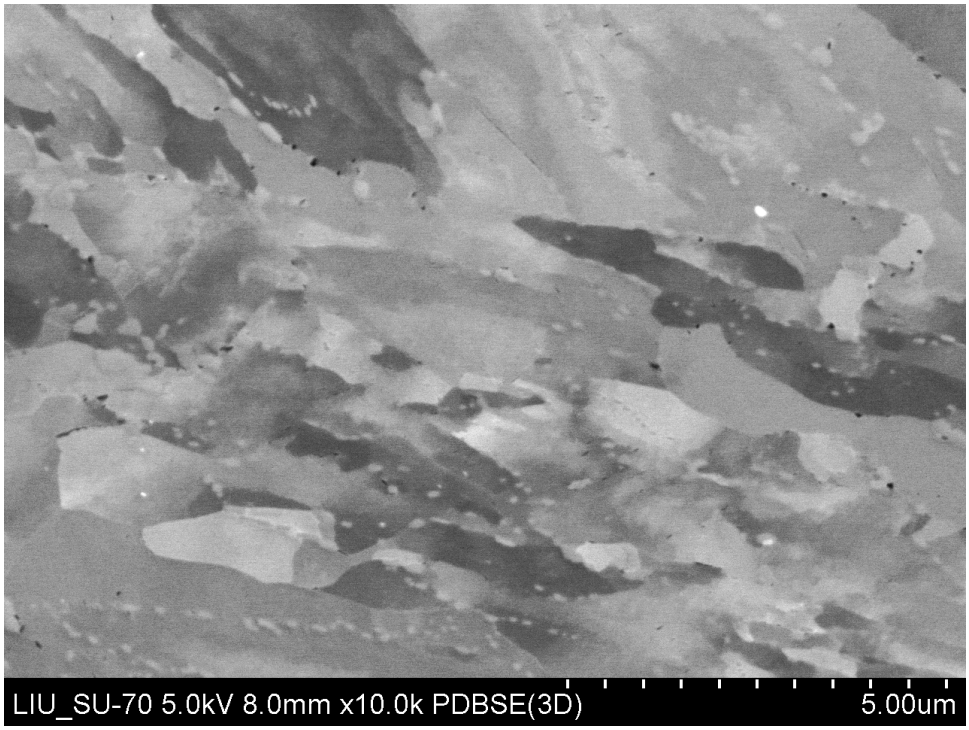

Figure 3.58 Picture of the inside of the VSR specimen in tangential direction, 10K magnifications

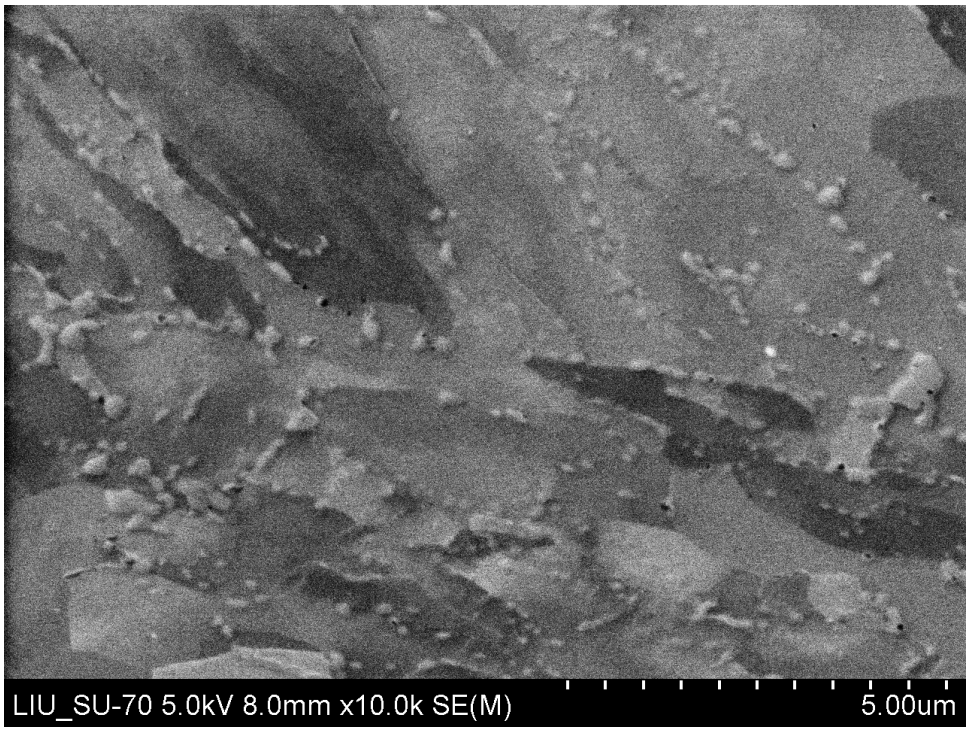

Figure 3.59 Picture of the inside of the VSR specimen in tangential direction, 10K magnifications, SE method

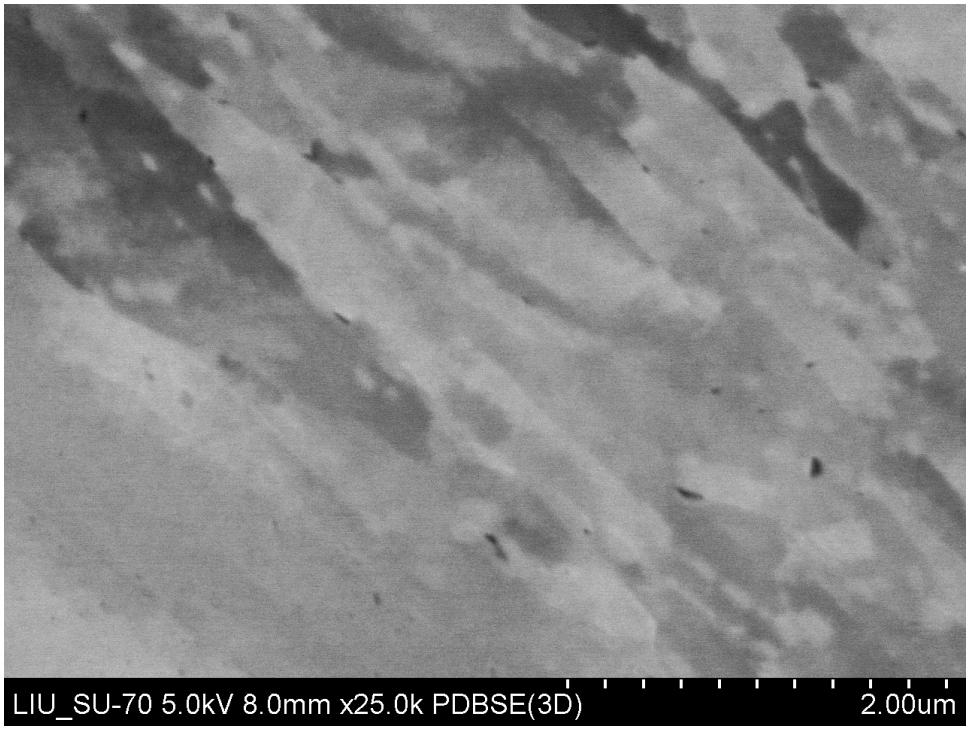

Figure 3.60 Picture of the inside of the VSR specimen in tangential direction, 25K magnifications

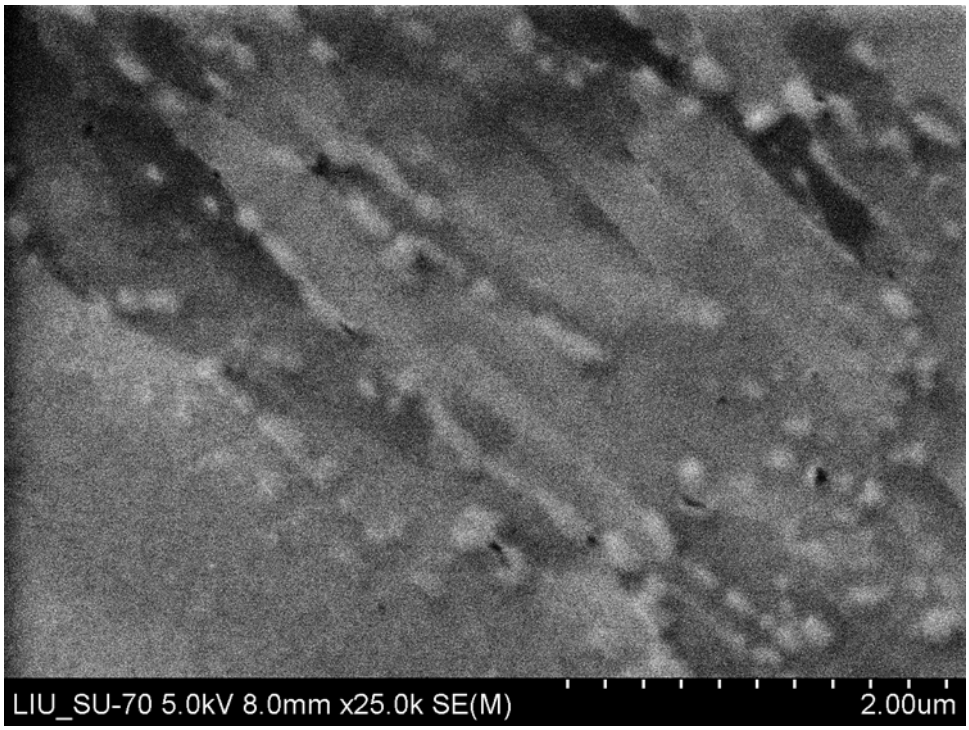

Figure 3.61 Picture of the inside of the VSR specimen in tangential direction, 25K magnifications, SE method

High magnification pictures, figures 3.62 and 3.63, were taken in order to get a finer measure of the spot's size if there was an interest.
Taking a view to the black spots of the figure 3.62, it becomes less clear the statement performed about the carbides. Using a high magnification, it is shown that some spots are not exactly in the grain boundaries.

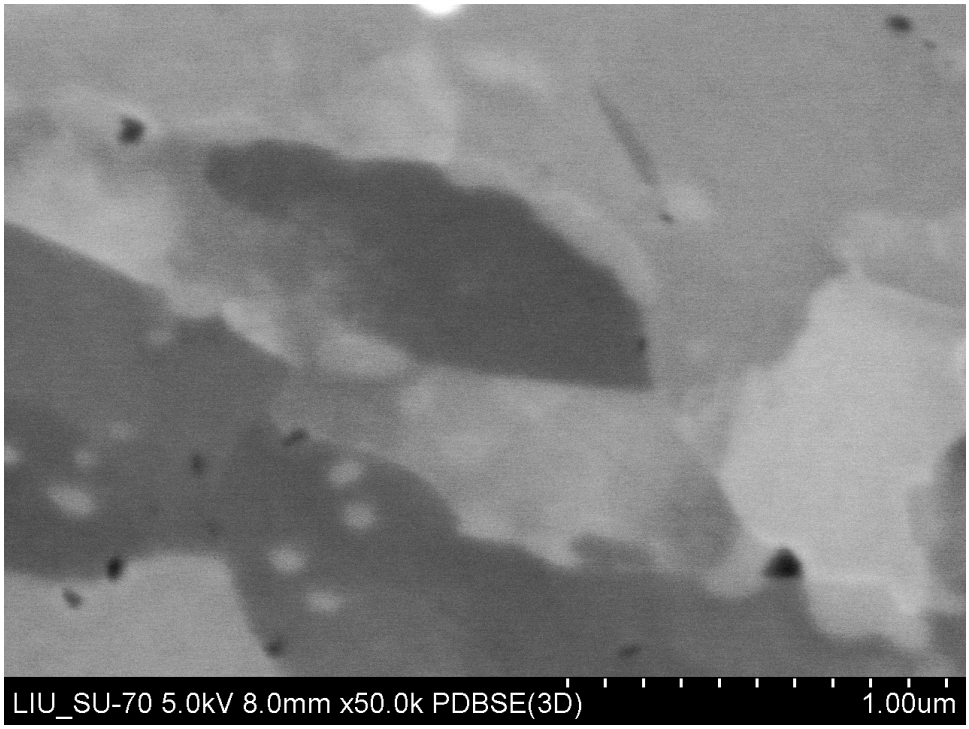

Figure 3.62 Picture of the inside of the VSR specimen in tangential direction, 50K magnifications

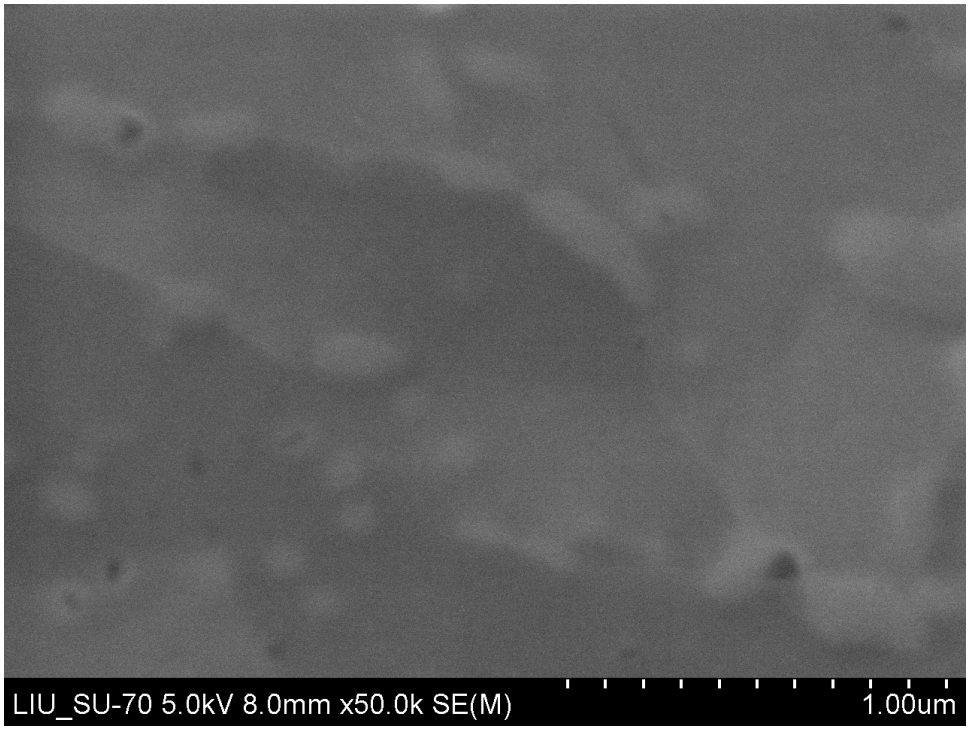

Figure 3.63 Picture of the inside of the VSR specimen in tangential direction, 50K magnifications, SE method

3.3.4 Discussion

Lengthwise the report, an analysis and a comparison of the microstructure peculiarities was carried out, so a short and precise conclusion will follow.

In both microscopes, it was displayed the explicit difference between the radial and tangential direction's microstructure. The thin deformation layer and the tangential bending discerned can be easily detected in all the pictures along the report.

The last remarkable point in this report is the difference spotted in the Heat Treated grain size and orientation comparing to the machined and the VSR ones. The conclusion gathered is that the heat treatment substantially varies the material properties. Furthermore, the white spots amount was increased with the heat treatment process.
To conclude this microstructure analysis, mention that no great differences were found between the machined and the VSR microstructures.

3.4 HARDNESS TESTING

3.4.1 Introduction

In this part of the project, the measure of the hardness of the specimens will be performed. By it, a sense of the variation of the microstructure hardness by applying the different treatments will be analysed.

The aim of the hardness testing is to measure the resistance of the surface of a material to be penetrated by a constant load. There are three hardness measurement methods: *scratch*, *indentation*, and *rebound* [12].
The most common method is the indentation method as it is simple, cheap and a non-destructive way to measure the hardness. Tensile strength can also be estimated [12]. It is the one exercised in this project.

All over the years, the hardness testing has been improving. Nowadays it is based on a small indenter, which is forced against the surface of the material in specific conditions of velocity and load. The way of measuring the hardness is to measure a specific length of the indentation that varies with the method. Once the length is set, it is related with a scale of hardness. The softer the material is, the bigger and deeper the indentation comes forth and the lower the value of the hardness results [12].

Different techniques could be applied for the testing and the choice would be carried out depending on the material analysed. The most common tests are Brinell and Rockwell [11].
In the Rockwell method it is possible to combine different indenters and loads in order to be able to analyse any material or alloy even the hardest and the softest ones. The indenters can be diamond or steel spherical balls [12].

The Vickers and Knoop tests are micro-hardness tests. The term micro-hardness refers to the micro-loads applied on the indenter. As it is shown in the table 4.2, this type of indenter is a small diamond pyramid. The loads are smaller than in the Rockwell and Brinell tests. They are often below 1 kgf, that equals 9'81 N. These techniques are useful when a small specific part of the specimen have to be measured. The small indentation has to be measured in assistance of a microscope. The load value (P) is then converted into a harness scale (see table 4.2).

A polishing has to be executed before the hardness testing due to flaws on the surface [7]. Commonly, Knoop and Vickers methods are declared as HK and HV respectively [11][12].

In the table 4.1 it is shown the different types of tests.

Table 4.1 Different types of tests [11].

Test	Indenter	Max. Loads
Brinell	Ball of 10 mm	3000 kg
Brinell	Ball of 10 mm	500 kg
Rockwell A	Diamond cone	60 kg
Rockwell B	Ball of 1/16 ''	100 kg
Rockwell C	Diamond cone	150 kg
Rockwell D	Diamond cone	100 kg
Rockwell E	Ball of 1/8 ''	100 kg
Rockwell F	Ball of 1/16 ''	60 kg
Vickers	Diamond pyramid	10 kg
Knoop	Diamond pyramid	500 g

Table 4.2 Hardness equations for the different hardness tests [12].

Test	Lateral View	Upper View	Load	Hardness
Brinell	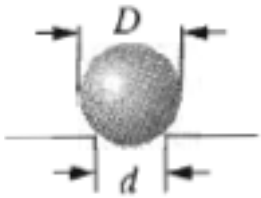	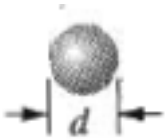	P	$HB = \frac{2P}{\pi D\,(D - \sqrt{D^2 - d^2})}$
Rockwell	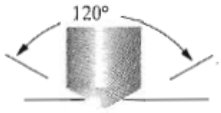		P	
Vickers	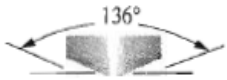		P	$HV = 1'854\,\frac{P}{{d_1}^2}$
Knoop	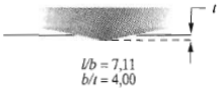	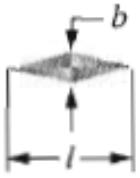	P	$HK = 14'2\,\frac{P}{l^2}$
Note: P is given in kg and D, d, d_1 and l are given in mm.				

Brinell and Rockwell methods are the most common ones. There are tables relating tensile strength with both of them. In case one of them is needed, it is not necessary to perform a new test; there is a table where the different methods can be converted. Nevertheless, it is not a reliable technique; the figure shown below could differ depending on the material type and its characteristics [12].

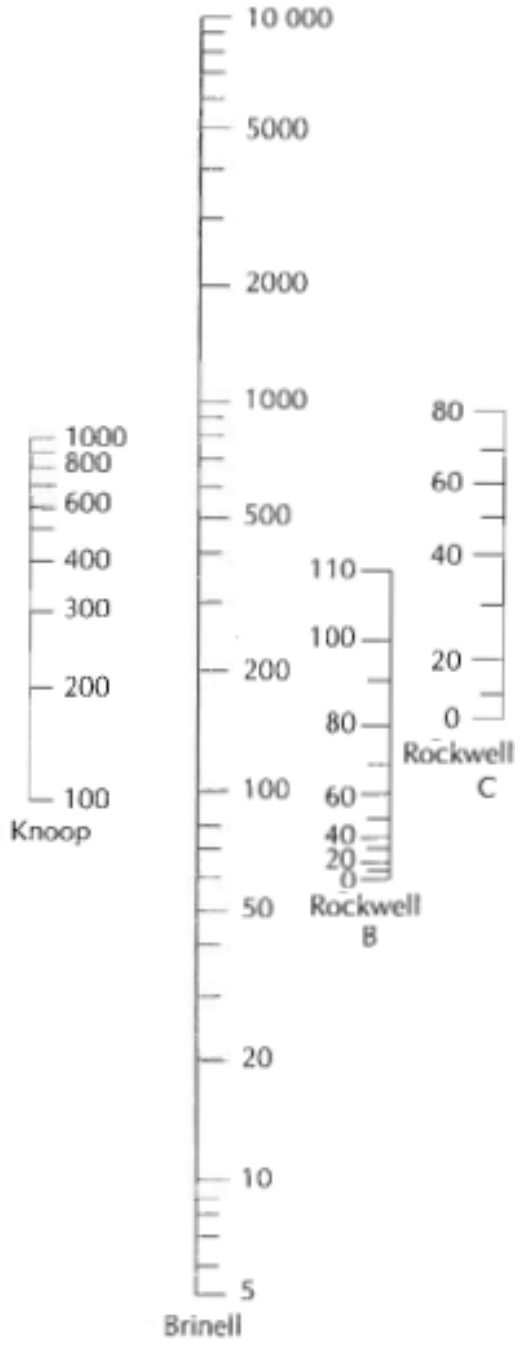

Figure 4.1 Converter between different hardness scales [12].

3.4.2 Vickers hardness testing

3.4.2.1 Introduction

There are some facts to take into account when performing a hardness testing. The indentation will deform the surrounding area and alter its properties. In order to avoid misinterpretations, there is a standard rule about prescribing a certain distance between multiple indentations [13]. As picture 4.2 shows below, the indentation has to be spaced with at least 3 times the length of the previous indentations diagonal and the first indentation has to be placed more than two and half times the indentations diagonal distance from the edge [13]. Besides, there is another rule that states that the minimum diagonal length should be 20 μm in order to ensure an accurate reading of the indents [13].

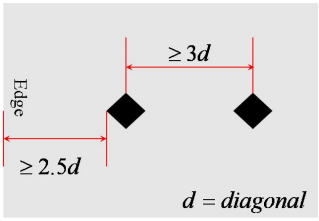

Figure 4.2 Indentation rules.

3.4.2.2 Conversion table

In both Vickers and Knoop methods there is a conversion table where the outcome hardness measurement depends on the load applied.
By taking some hardness measurements with different loads to a sample specimen for both methods, a conversion table was accomplished for this specific project. The real hardness of the specimen is 706 HV. Therefore, a great measurement error of the hardness can be output if a low load is selected for the analysis.
Additionally, in table 4.3, it is shown the different Vickers and Knoop values related to their indentation diameter.

Table 4.3 Indentation diameters of the sample specimen's analysis

HK	DIAMETER (μm)	HV	DIAMETER (μm)
1128.2	11.3	793.8	4.8
937.0	19.5	783.7	7.7
830.6	29.2	768.1	11.0
772.8	42.9	756.4	15.6
726.1	62.6	755.3	22.2
728.0	76.6	747.3	27.3
709.7	100.1	729.7	35.7
701.9	142.4	719.8	50.8

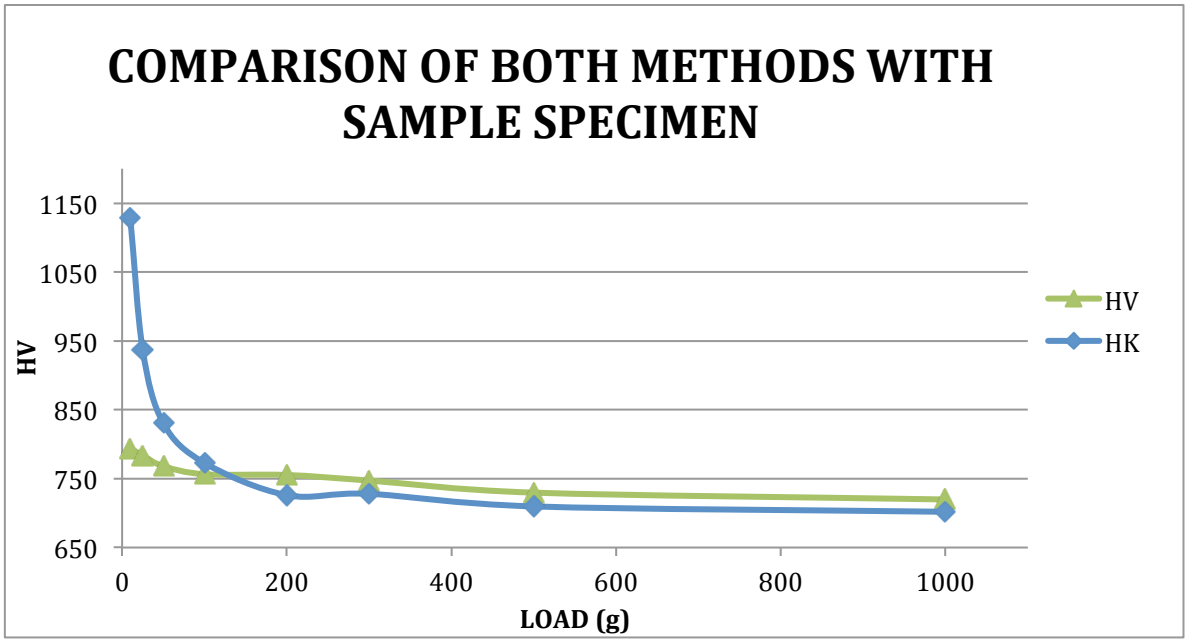

Figure 4.3 Vickers and Knoop method measurements with different loads

3.4.2.3 Vickers testing results

For an accurate measurement of the hardness variation along the depth of the ring, three different measures were performed in each specimen. Right after, an average of them was calculated in order to get an idea of the hardness along the depth.
To get a clear idea of the procedure of the measurements performed, an image of one of the specimens will be shown below.

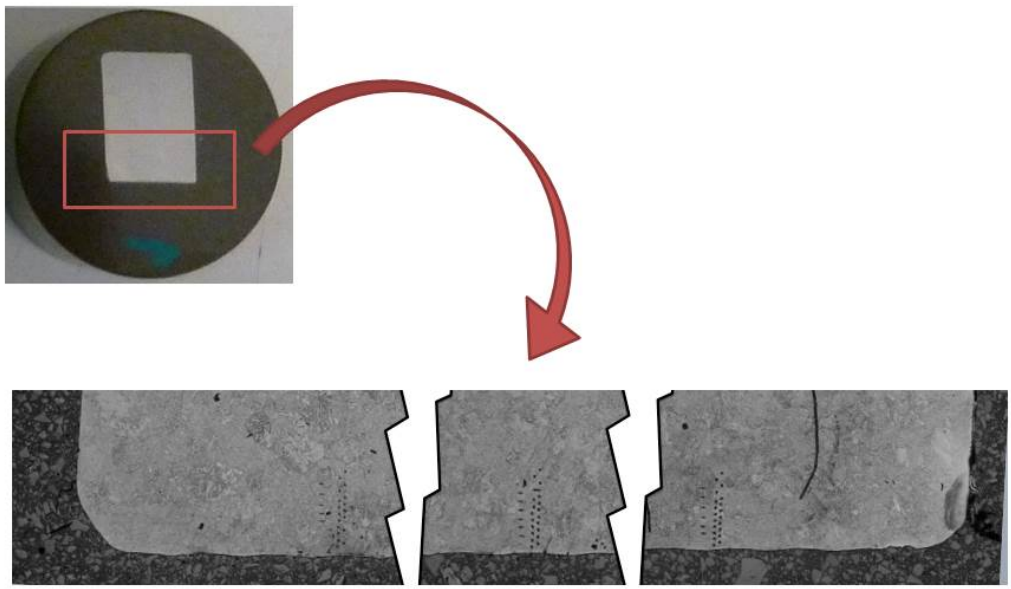

Figure 4.4. Detail of the indented lines.

Something to take into account is that the interesting section for the hardness analysis is the share around the edge of the surface of interest. This fact implies that the indentation size has to be as small as possible so as to follow the rule that states a two and a half times distance from the edge. Otherwise, the measurement cannot be trusted. As the other rule mentioned above states, the length of the diagonal of the indentation has to be greater than 20 μm to get a grant result. With the load selected for this project, 25 g, a hardness measurement error will be committed as it was shown in figure 4.3 and also because of the diagonal length. In consequence, the aim is to study the fluctuation of hardness along the depth of the specimen's surface. The real value of the hardness value of each specimen will be exposed at the end of this analysis.

3.4.2.3.1 Machined ring

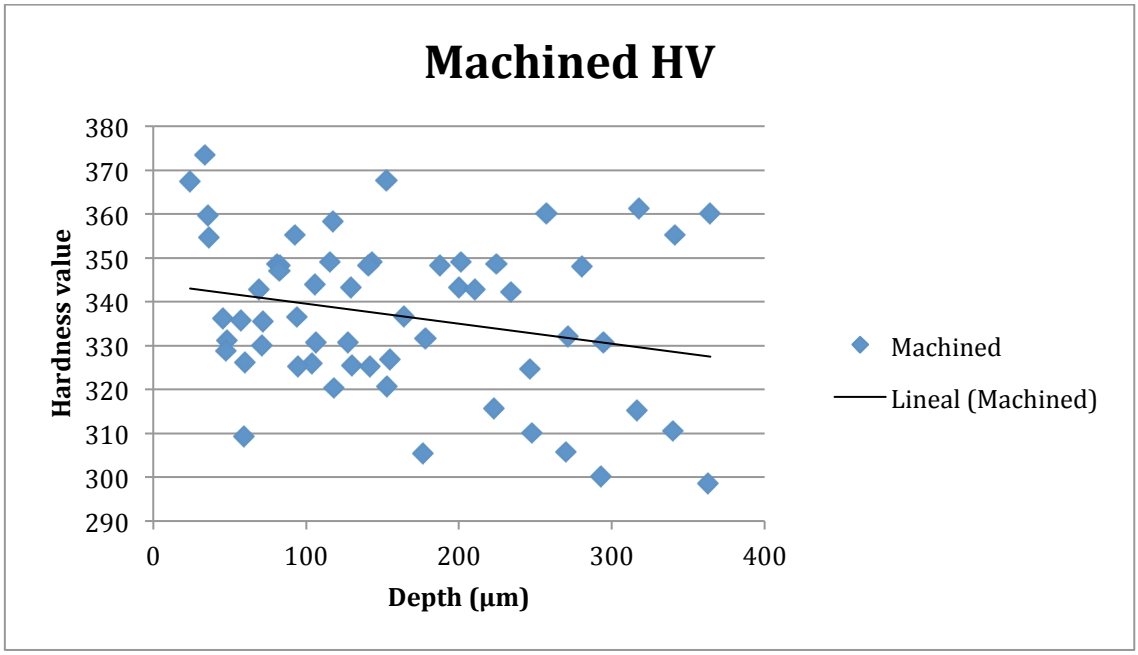

Figure 4.5 Vickers hardness testing measurements in the machined ring.

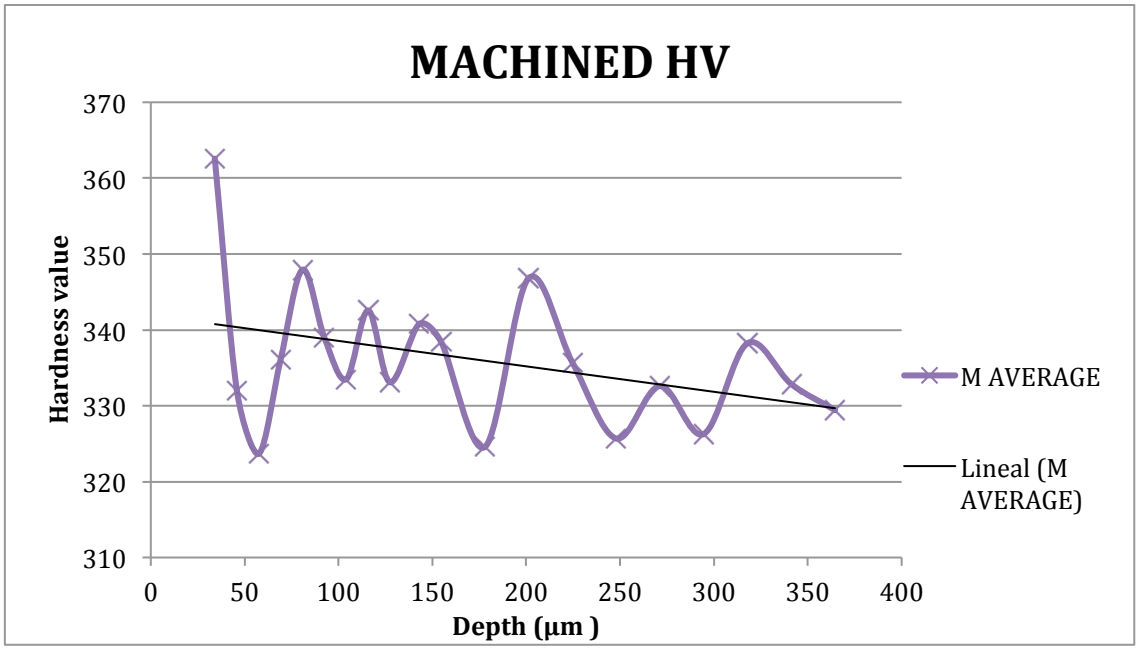

Figure 4.6 Average of Vickers hardness measurements.

As it is displayed in the figure 4.4, the machined ring has different hardness values for each depth. The reason is that the microstructure varies in different parts of the specimen's section analysed. The martensite is not homogeneous all along the surface and the variation of the hardness also depends on which part of the grain is hit by the indentator. The hardness of the grain boundary is higher than the middle part, so different values will come up depending on the indentation position as figure 4.6 shows below.

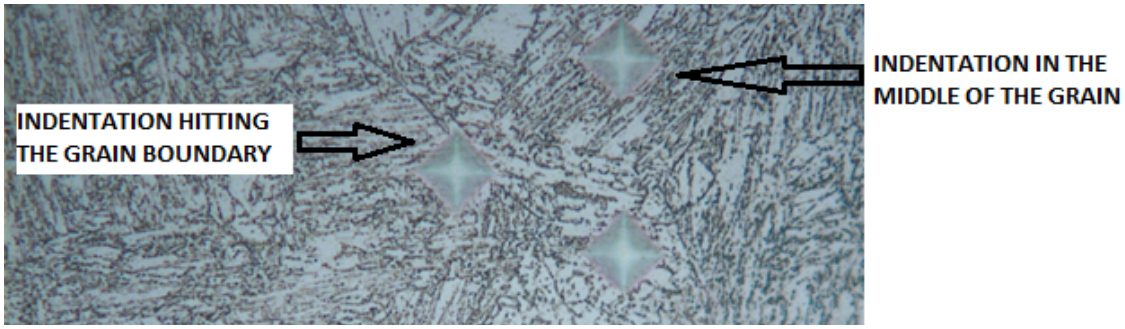

Figure 4.7 Different Vickers indentations.

As it is displayed in Figure 4.4, the measured values have a greater difference on deeper measurements. The ones closer to the surface have ever so little variation between them. The trend of all the measured values decreases from about 340 to 330 HV.

The average graphic, displayed in figure 4.5, was created by performing a middle value for each depth of the three lines generated for the hardness testing. It shows the same trend as the points displayed just above, in figure 4.4; a slightly decreasing trend that varies from 340 to 330 HV when the depth is increased.

The range of variation of the curve exposed in the figure 4.5 is from325 to 350 HV. For the contrary, the points displayed in figure 4.4 have a similar range in low depths but, when the depth is increased, a greater hardness value difference could be noticed.

3.4.2.3.2 Heat Treated ring

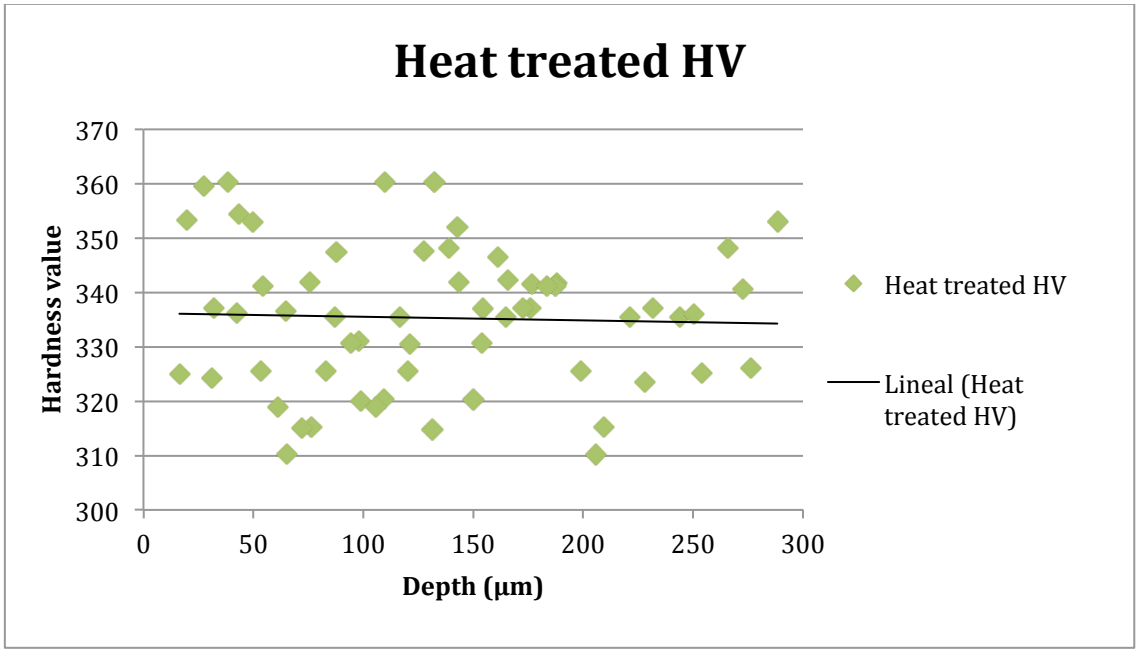

Figure 4.8 Vickers harness testing measurements in the Heat Treated ring.

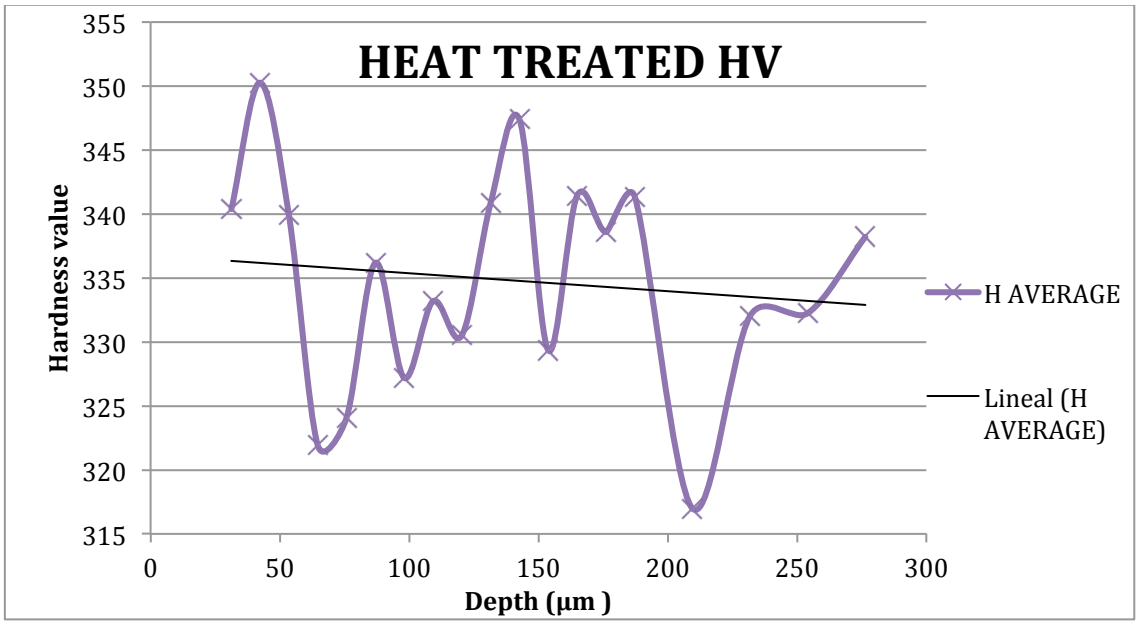

Figure 4.9 Average of Vickers hardness measurements.

As it is set put in figure 4.7 aloft, the measurements do not differ substantially when the depth is increased. It is clear that both the points and the average trends

do not diminish greatly, instead, their trend curves decrease less than 5% of the total hardness.
This particular behaviour of the Heat Treated ring shows that the heat treatment hardens the whole ring but the total hardness is not higher than the machined ring one.

3.4.2.3.3 Vibratory Stress Relieved ring

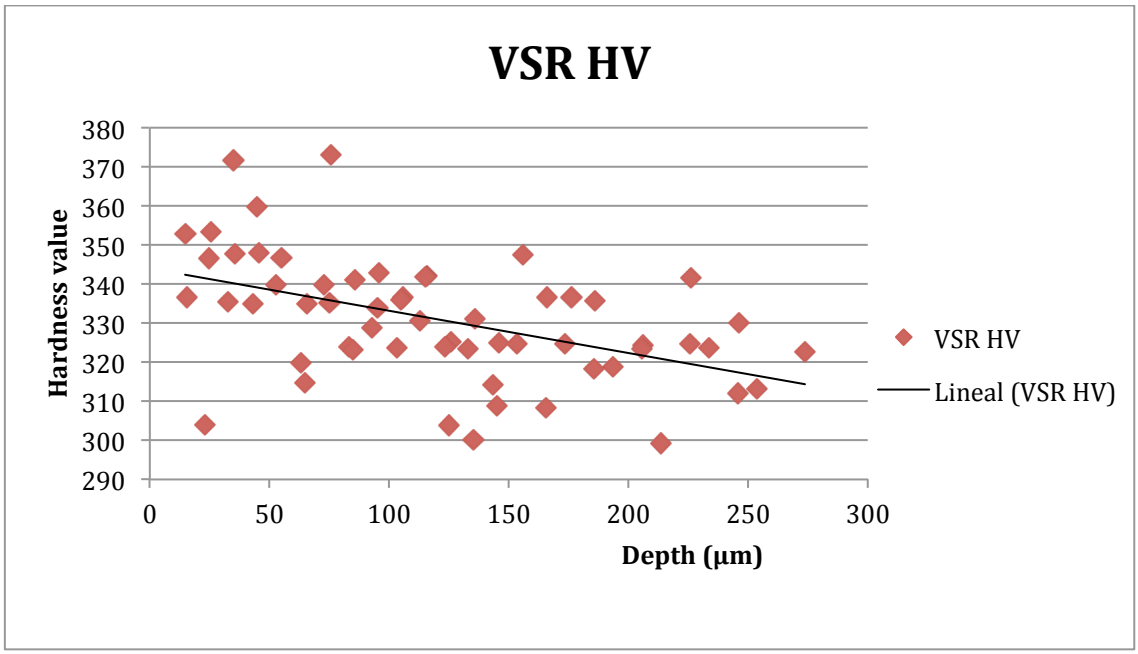

Figure 4.10 Vickers harness testing measurements in the VSR ring.

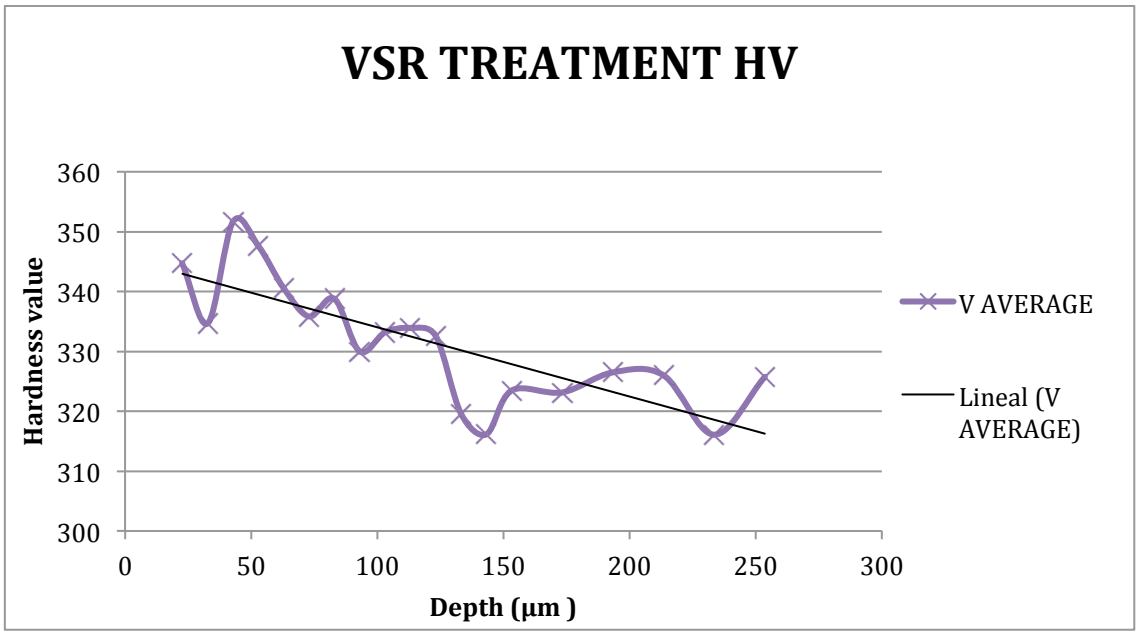

Figure 4.11 Average of Vickers hardness measurements.

As it is displayed in figure 4.9, the data obtained for the Vibratory Stress Relieved ring is quite homogeneous and the hardness values decrease substantially as the

depth increases. Both the average trend and the measurements trend perceptibly decrease from about 345 to 315 HV.
A clear fall of the hardness appears in the ring after the VSR treatment.

3.4.2.3.4 Comparison of the average hardness of the rings

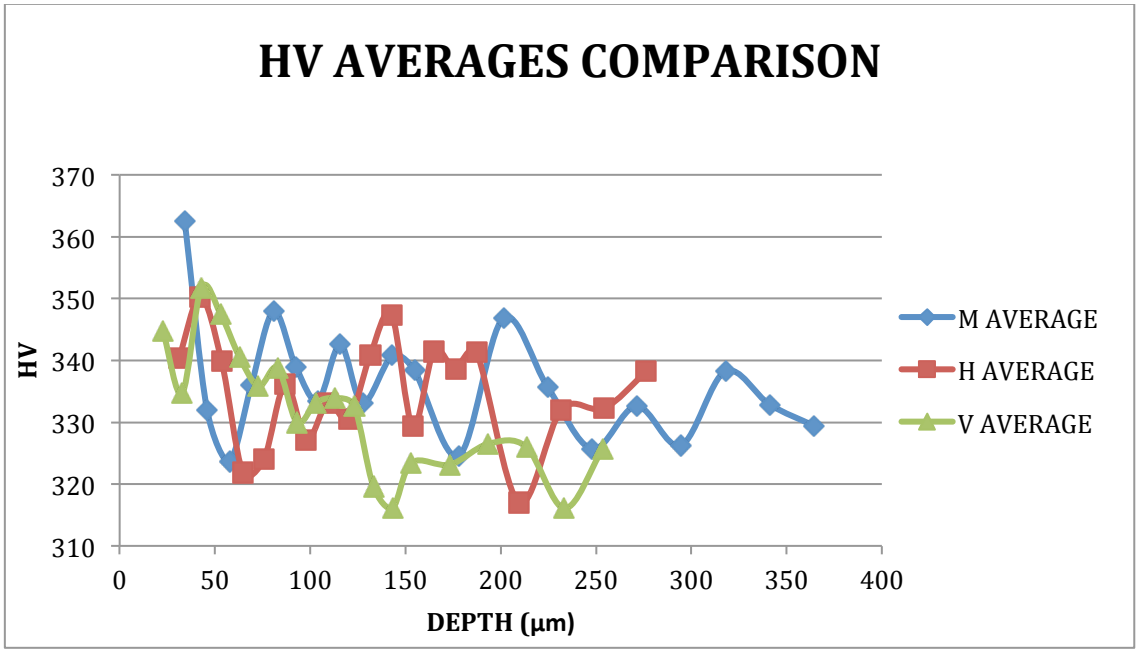

Figure 4.12 Average Vickers measurements comparison.

With the data obtained, it is clear that, in the portion of the specimen closer to the surface, the highest value captured belongs to the machined ring. As the average has been executed with just three different values, the result is not as reliable as it should be, so this is just an approximation. Besides, some measuring or statistical errors can also appear.

All along the surface, both the heated and the machined curves have equal trends and the vibratory one has lower values once the depth gets greater than about 120 µm.

3.4.2.4 Real hardness values

As it has been explained previously, the value of the hardness itself cannot be trusted in consequence of the size of the indentations. In order to know the real value of the hardness, some indentations have been performed randomly with a load of 300g in each specimen. The results are shown right below in figure 4.12:

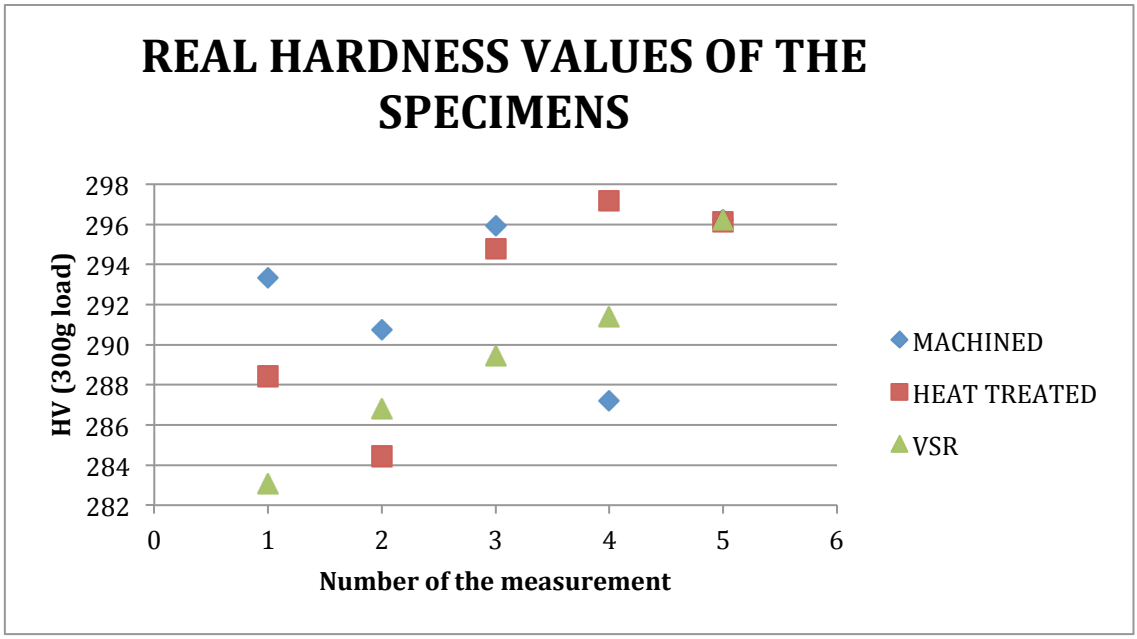

Figure 4.13 Hardness values of each specimen with a 300 g load

The results of the average performed for the values outcome of each ring are the following:

- Machined ring: 292.688 HV
- Heat Treated Ring: 292.186 HV
- VSR Ring: 289.382 HV

3.4.3 Knoop hardness testing

3.4.3.1 Introduction

Vickers and Knoop methods can be both useful as they have different properties and characteristics. Right after, some comparisons will be made clear in order to understand why the Knoop method was executed as well.

- The Knoop indenter penetrates about half as deep as the Vickers making it suitable for hard and brittle materials [12].
- The Knoop test is more sensitive to surface conditions [12].
- The error reading the Knoop indentations is smaller than the Vickers indentations because Knoop's diagonal is three times longer than Vickers diagonal [12].
- As Knoop and Vickers methods have different geometry of the indenters, the Vickers test is used for rounded areas whereas Knoop test is used for elongated areas [12].

It can be appreciated, in the graphics of the Vickers method, that the first values are not very close to the surface, so it is not possible to analyse the very surface of the ring with the named method. In order be accurate in the analysis of the hardness of the surface, the Knoop method will be executed as it is a great alternative to measure the specimen closer to the surface. As it could be appreciated in the picture below, an advantage can be taken to the fact that Knoop indentation has a pretty different diagonal size. It means that, while following the rule of having a diagonal greater than 20 μm, it is possible to get close to the surface since two and a half times the distance of the smaller indentation is not a big distance and a small load could be chosen.

The aim is to measure the hardness of a layer of 5μm on the very surface. The rule of keeping the small diagonal of the indentation two and a half times far from the edge couldn't be fulfilled because of the tiny size of the layer. Therefore the data obtained cannot be trusted. The purpose of graphics that will follow is to get an idea of the hardness slope between the layer and the surrounding area.

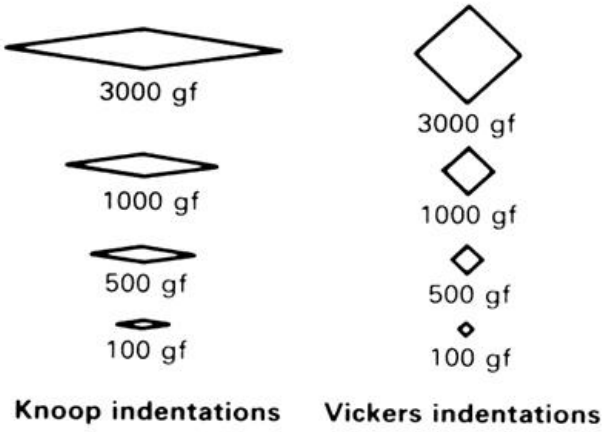

Figure 4.14 Difference between Knoop and Vickers indentations [13].

3.4.3.2 Results

In order to get results of the Knoop testing, random measurements were performed all along the surface of each specimen so as to get a general idea of the hardness variation with the depth of the specimen. The hardness of each indentation is displayed in the graphics below.

3.4.3.2.1 Machined ring

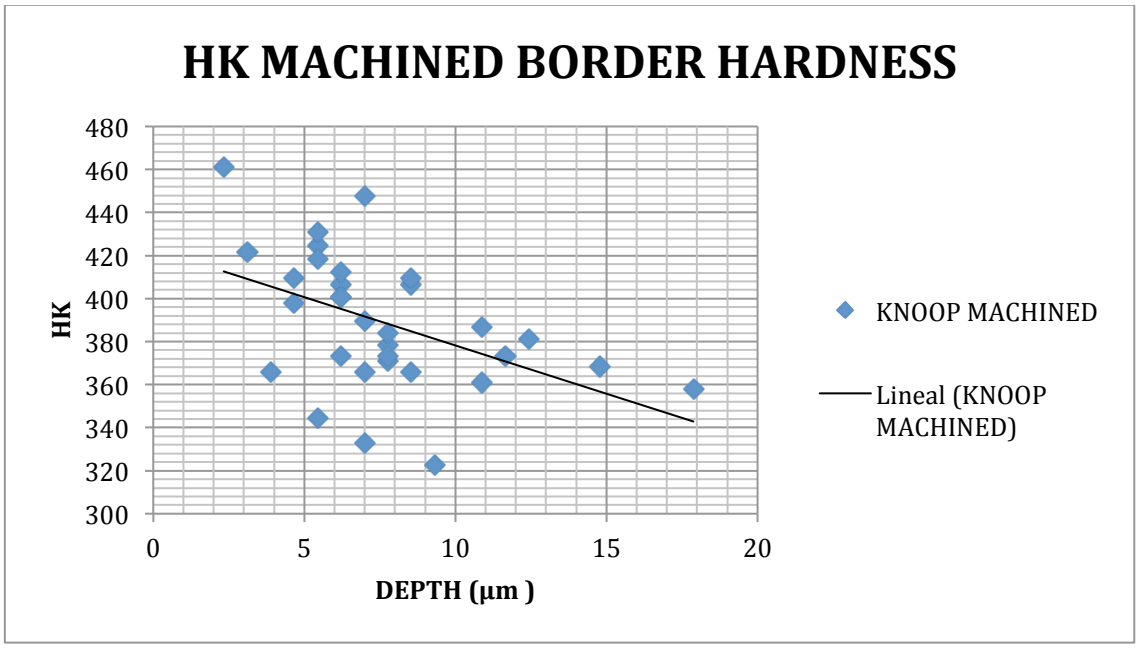

Figure 4.15 Knoop hardness test measurements in Machined ring.

Taking a view to the results accomplished, a clear diminish of the hardness as the depth increases is noticed in the figure 4.14.
Furthermore, a great difference of the hardness value in the same depth of the specimen is easily noticeable.

3.4.3.2.2 Heat Treated ring

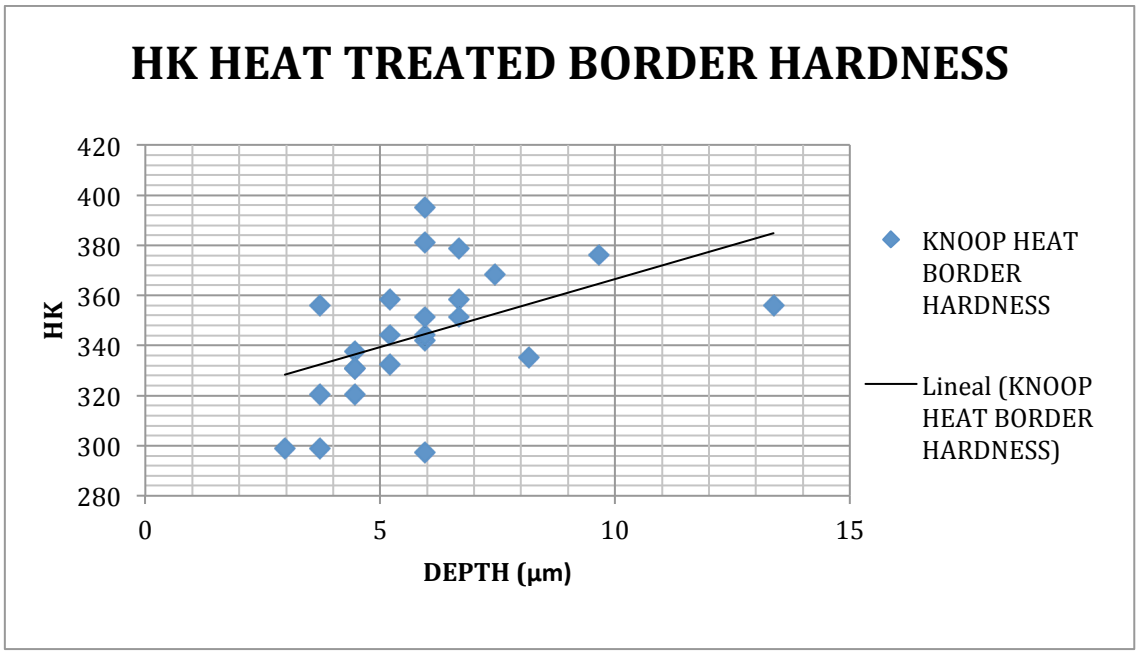

Figure 4.16 Knoop hardness test measurements in Heat Treated ring.

The trend of the Heat Treated ring hardness along the depth of the specimen is an increase of the hardness as the depth increases.
The different values of the hardness for each depth are quite homogeneous.

3.4.3.2.3 VSR ring

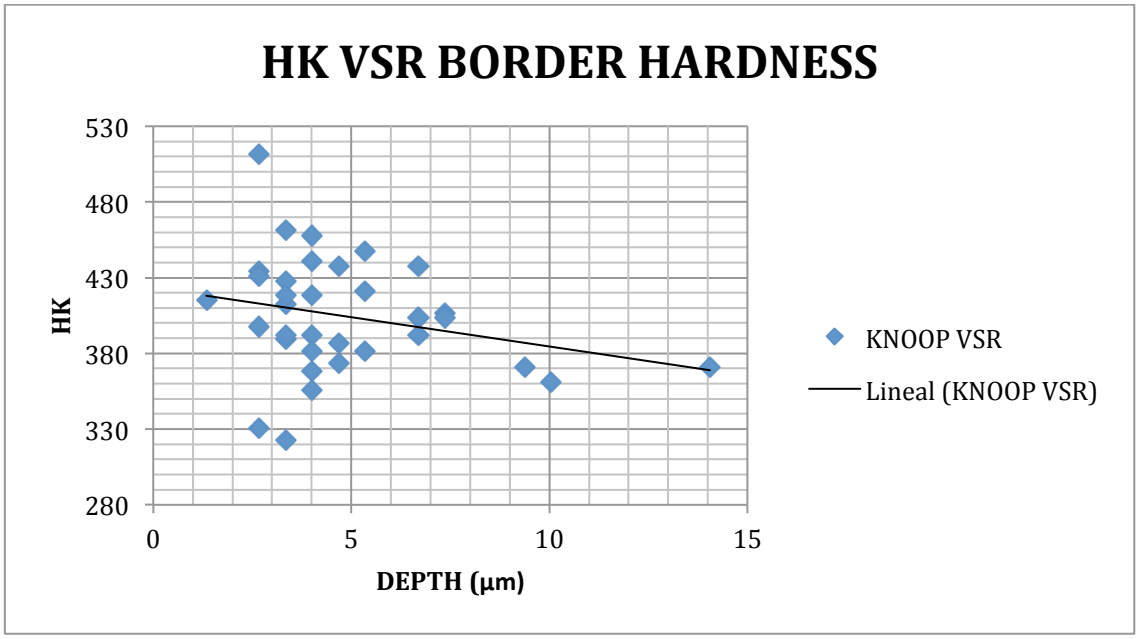

Figure 4.17 Knoop hardness test measurements in the VSR ring.

As the graphic above shows, there is no clear tendency of a fluctuation of the hardness with the depth in the very surface. The decreasing tendency shown in figure 4.17 comes forth once the depth is greater than the layer.
The difference of the hardness values for each depth is quite wide and grows smaller as the depth grows bigger.

3.4.4 Comparison of both methods

3.4.4.1 Results the comparison of each ring

3.4.4.1.1 Machined ring

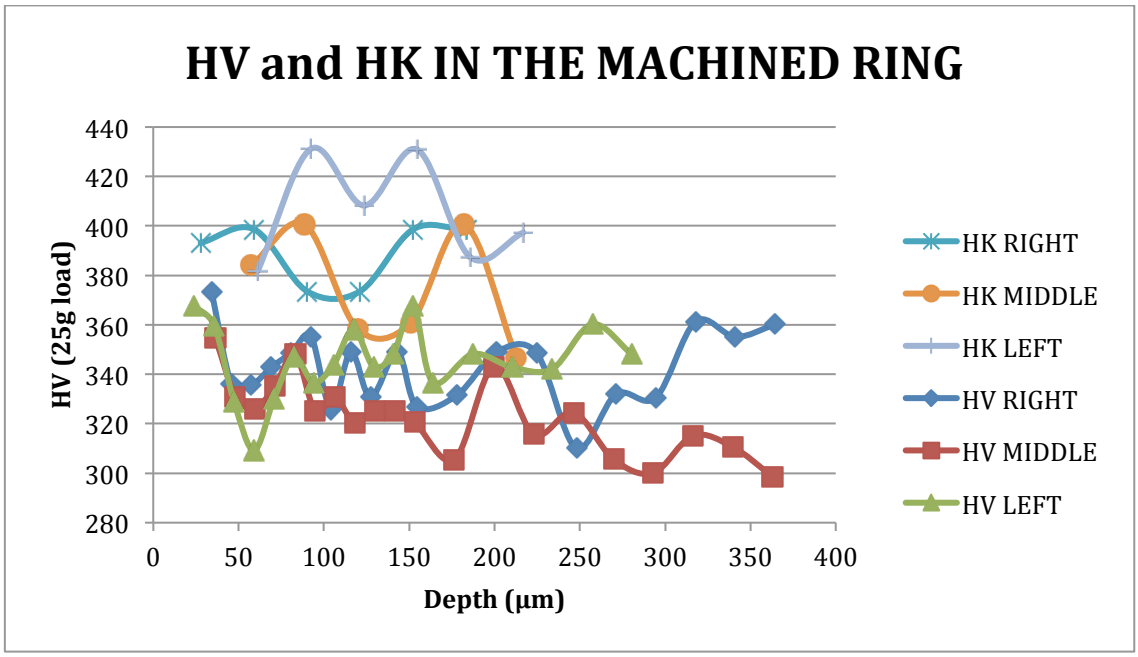

Figure 4.18 Comparison of both methods in the Machined ring.

Taking a view to figure 4.17, the machined ring shows that the Knoop test values executed have higher values in comparison to the Vickers testing.

The Vickers testing accomplished has almost the same trend on the three measured lines and they are totally contained among around 300 and 370 HV. Knoop test, in contrast, has a wider range of values and not a clear trend.

3.4.4.1.2 Heat Treated ring

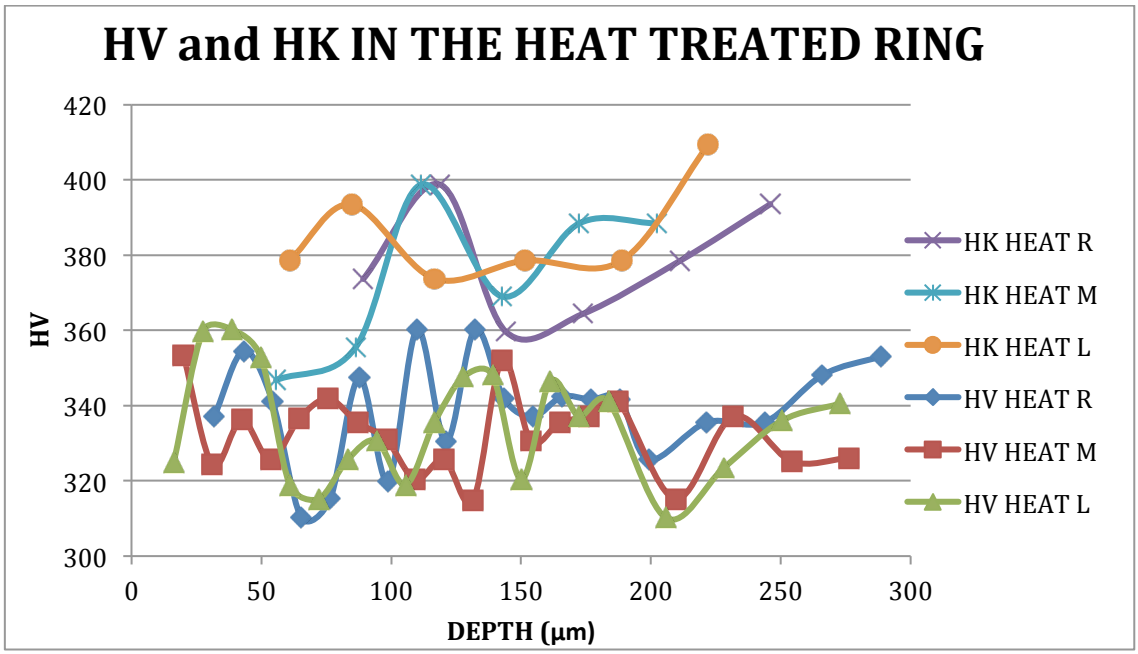

Figure 4.19 Comparison of both methods in the Heat Treated ring.

In the case of the Heat Treated Ring, the Vickers testing presents almost the same trend and the values are enclosed between 315 and 360 HV, meanwhile the Knoop test has higher values, reaching hardness values of 410 HK. The Knoop test values are located in the same range of hardness and all of them have higher values than the Vickers one.

3.4.4.1.3 VSR ring

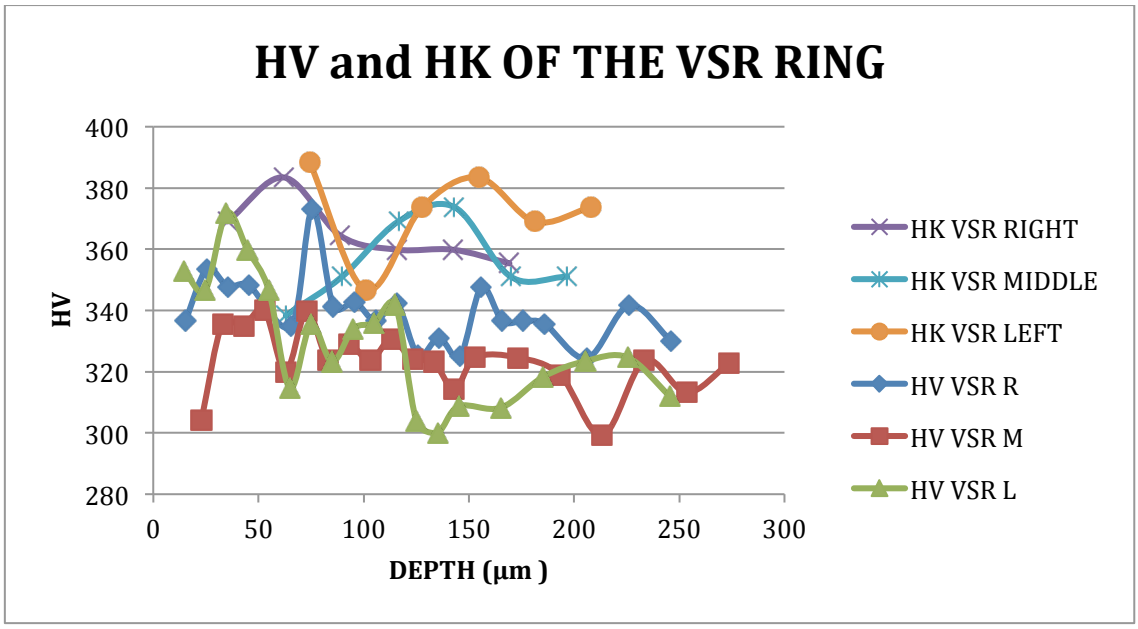

Figure 4.20 Comparison of both methods in the VSR ring.

The conclusion of the analysis of the VSR ring is the same as in one Heat Treated. The Knoop measured hardness presents greater values than the Vickers one in the three lines analysed.
Another fact to take into account is that the Vickers results have the same trend, but the Knoop values are unstable.

3.4.4.2 Comparison of both trends of each ring

The following three graphics represent the average carried out in the three different specimens with both Knoop and Vickers methods.

3.4.4.2.1 Machined ring trends

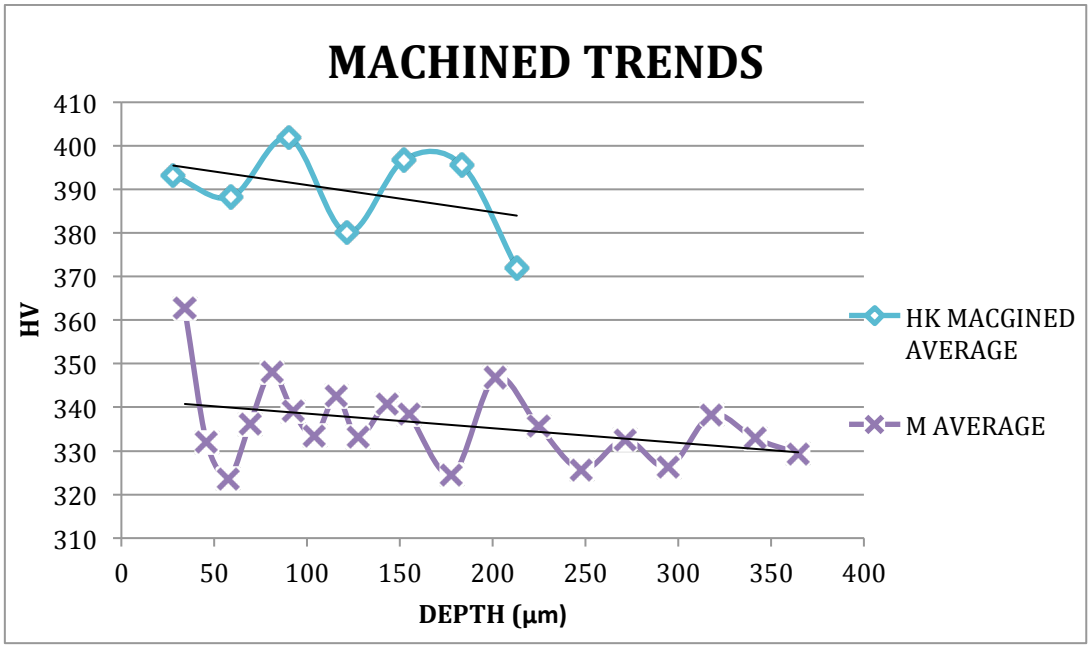

Figure 4.21 Average comparison of both methods in the Machined ring.

3.4.4.2.2 Heat Treated ring trends

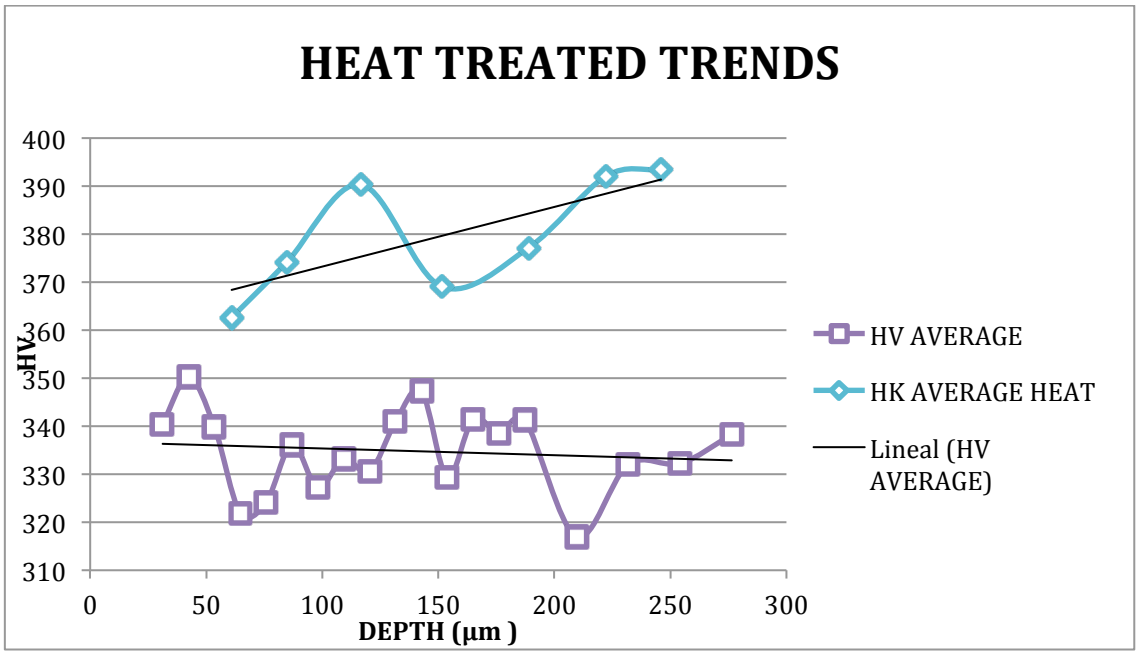

Figure 4.22 Average comparison of both methods in the Heat Treated ring.

3.4.4.2.3 VSR ring trends

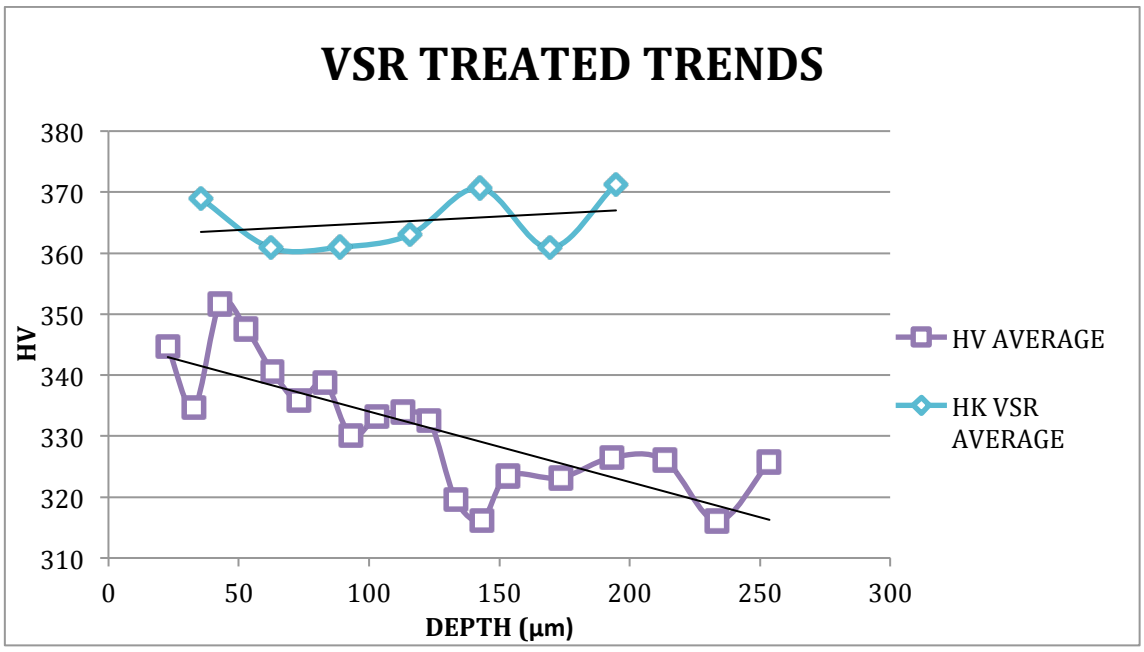

Figure 4.23 Average comparison of both methods in the VSR ring.

3.4.4.2.4 Analysis of the results

It is clear that, in every graphic, Knoop test provides higher hardness values than the Vickers method. As it is stated in the first part of the hardness testing, with low load values of the indentations, the hardness measurement error is quite high and it differs substantially between the Knoop and the Vickers methods.

Not just an important contrast of the hardness value was outcome, but also a slightly different trend of both methods was noticed in all of the rings.

Both trends in the machined ring diminish when the depth is increased. In the Heat Treated ring, in contrast, the Knoop analysis shows that the hardness increases with the increase of the depth, while the Vickers test shows a quite stable hardness all along the measured depth.

To conclude the comparison of both Knoop and Vickers tests analysis, it is clearly displayed a slight increase of the hardness measurement in the VSR ring with the increase of the depth in the Knoop test, even though the Vickers results show a trend decrease.

3.4.5 Discussion

Taking a view to the analysis performed, the conclusion is that both methods cannot be compared. The hardness range varies substantially and a fluctuation of the trends could be appreciated in all the rings.

The reason of the comparison was to be sure that the hardness value of the Knoop method in the edge of the specimens couldn't be compared to the Vickers test, it will only be considered the fluctuation of the hardness with the depth, not the value itself.

First, an analysis of the Vickers test results will be executed.

In the original ring, the machined one, a decrease of the hardness trend with the increase of the depth was observed. A wide range of hardness values was outcome when performing the test, though.
By analysing the Heat Treated ring, a homogeneous hardness was detected. The absolute value of hardness was not higher than the machined ring. However, there was no decrease of the hardness along the studied surface. This behaviour could be in consequence of the tempering applied right after the machining.
The VSR ring showed the same trend as the machined ring but a greater decrease of the hardness was noticed. Besides, the VSR hardness values were more homogeneous than the other two ring ones.
The behaviours explained above could be understood taking a view on the average curves of each ring shown in figures 4.5, 4.8 and 4.10 respectively.

The real hardness values exposed in part 3.4.2.4, show that the three rings have the same hardness values on the rings, even if the hardness on the edge differs amongst them.

As it was exposed in the Knoop method analysis, the aim was to inspect if the layer shown in the microstructure pictures had a different hardness than the rest of the ring.
The conclusion arisen was that the machined ring had a decrease of the hardness, so the layer had actually an alteration of the properties comparing to the rest of the ring.
The Heat Treated ring had, even if it was an unexpected behaviour, an increase of the hardness value along the layer depth.
The VSR ring trend does not show much alteration along the layer examined.
Nevertheless, the hardness values obtained cannot really be trusted, as it was not possible to keep the two and a half times distance from the edge to the middle of the indenter told in the rules of the method performance. Besides, atypical results could be found due to measure or statistical errors or flaws on a small piece of the specimen. Additionally, the part of the grain hit in the indentation could make a quite different hardness results. Therefore, by the results obtained, an idea of the possible behaviour could be gained, whereas it is not feasible to get a certain conclusion by performing this kind of macroscopic methods.

3.5. CUTTING THE NEW RINGS

3.5.1 Introduction

The new rings were sent by Siemens A.B. They have a bigger size, closer to the original rings one. It implies that the idea of which is the best method to relieve residual stress could have a more realistic analysis and, arising from the study accomplished, a more reliable conclusion could be performed.
The same tests will be run and, furthermore, a comparison between each pair of rings will be carried out.
Before the new rings were cut, two strain gauges were installed on the rings in order to know the strain relieved during the cutting process. These values will be analysed in the following pages.

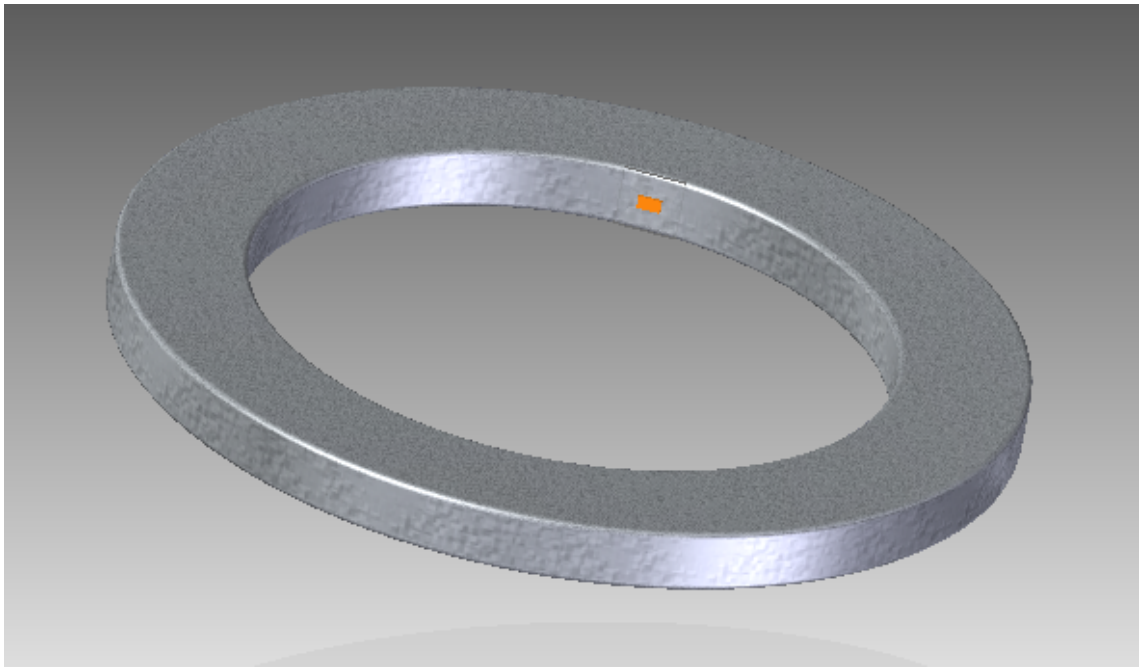

Figure 5.1. Strain gauge located on the inside surface of the ring.

3.5.2 Spark cutting method

The spark cutting method, technically called electric discharge machining (EMD), is based on cutting the desired piece in the shape required by applying electrical discharges [14][15].
The piece is inserted in a dielectric liquid and the sparks are to appear between two electrode current discharges. The aim is to remove material by reducing the distance between the two electrodes set up for the flow of the current. Once the distance is short enough, the intensity of the electric field in the volume between the electrodes becomes greater that the strength of the dielectric, which breaks, allowing current to flow between the two electrodes [14]. Both piece and wire material is removed, so it is necessary to replace the wire to maintain a constant cutting conditions [14][15].

3.5.3 Analysis of the data

3.5.3.1 Ring 1

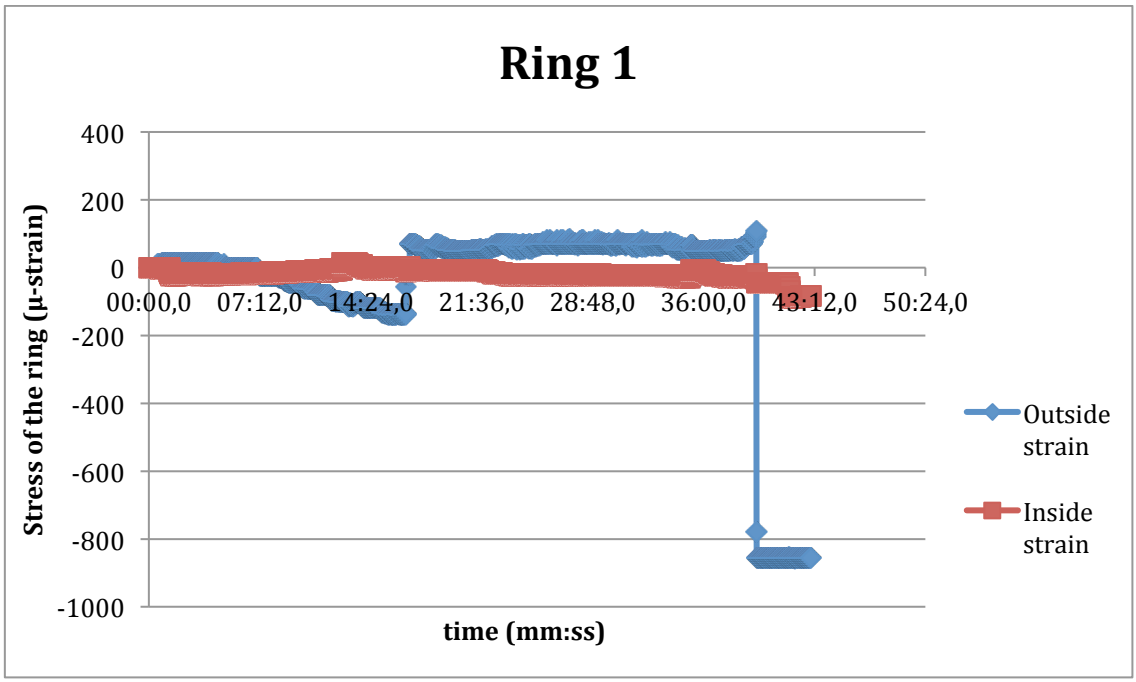

Figure 5.2. Data from the cutting of the Ring 1

In the figure displayed above, figure 5.2, it is shown the two cuts performed to Ring 1. The first 16 minutes of the cutting process belong to the first cut carried out. During this process, the ring suffered compression stress. This behavior could be caused by the relief of the residual stress within the ring. Besides, the fact that there was less surface cut than uncut could entail this kind of stress relief as well.
After 16:40 minutes of the cutting time measured, the second line starts to be crosswise from the inside part. The outside strain gauge, located on the outside surface, started to record tensile values over 70 µ-strain. The measured values confirm quite stable tensile stress relief during the whole cut.
Some high compression values appear at the end of the graphic, after the minute 39:27. The reason for them to appear is that the ring had so much residual stress and, when the cut was carried out, compression stress was relieved and it was necessary to hit the piece that was supposed to fall apart.
The inside strain gauge, located on the inside surface, shows more stable and low values. The reason could be that, for the first cut, there is no stress relief in the inside surface as it consumes less energy for the ring to expand the outside surface. Taking a view to the second cut, carried out from the inside, a relief of the residual stress appeared, implying that the gauge captures compression strain values as the figure below shows.

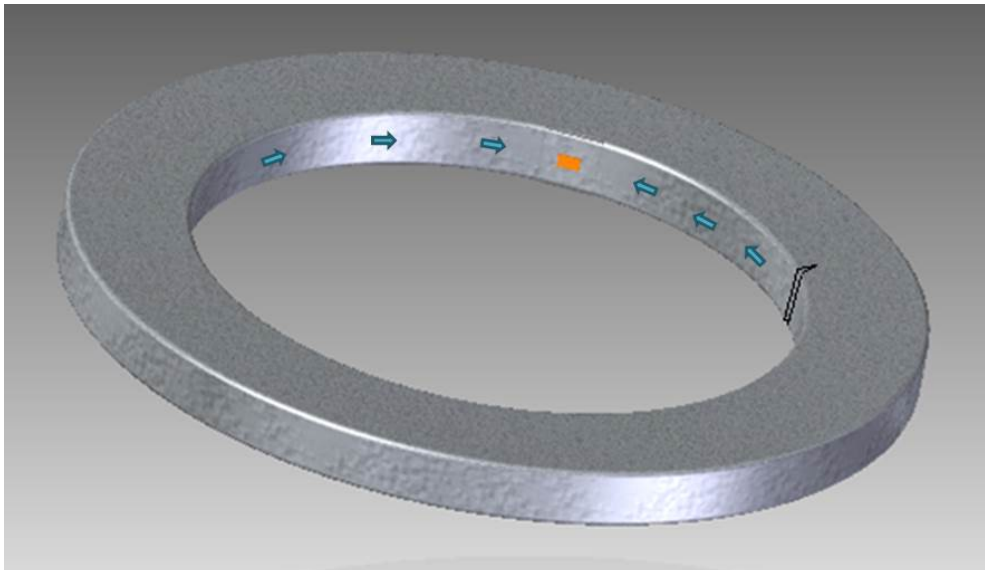

Figure 5.3 Gauge's measure explanation when cutting from the inside

The final hit to release the cut piece also influenced in the inside gauge, as the data shows in the graphic above.

3.5.3.2 Ring 2

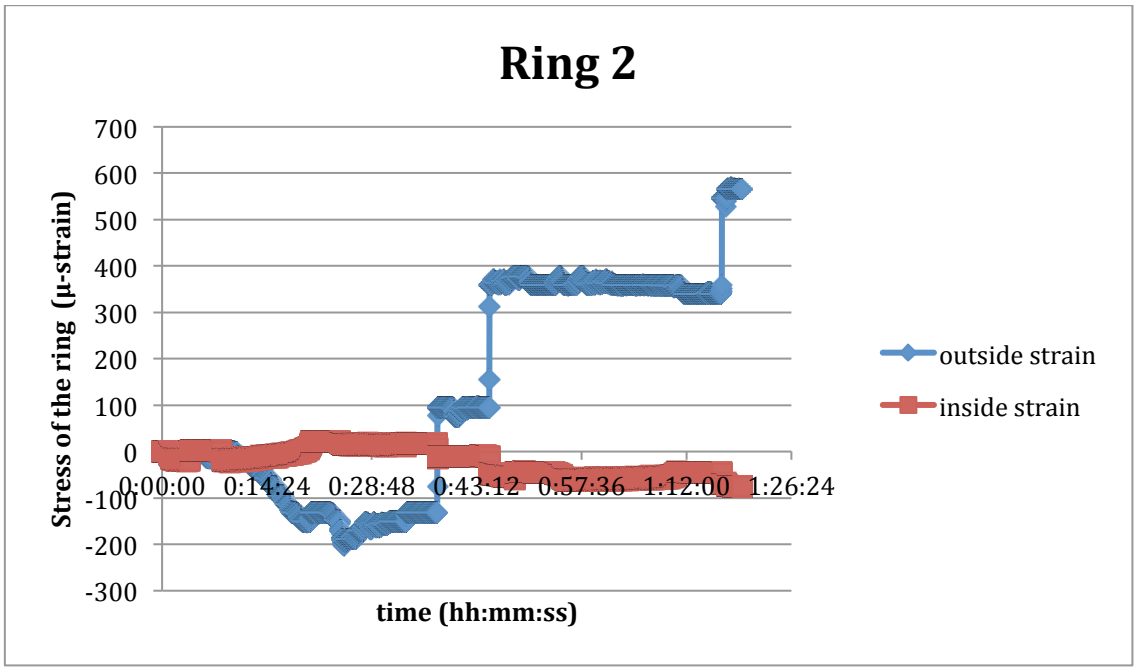

Figure 5.4 Data from the cutting of the second ring.

While the cutting of Ring 2 was performed, a problem took place. The cut started on the outside surface and, as a consequence of the stress relief pressure applied by the ring, the wire broke twice. In order to finish the cut, the process had to start from the beginning two times more. That is the reason of why the cutting time for the little piece took longer than the other two rings. Besides, the water supply was not enough so the technician had to fill the tank up. This procedure also delayed the cutting process.

Similar values to the first ring were recorded by the inside strain gauge. The values are almost constant until the minute 36, when the stress relieved in the ring provokes the trend change, from tensile stress to compression stress behavior.
On the other hand, the outside strain gauge displays the ring's behavior quite sharp. At first, compression stress takes place. After reaching a peak of 190 μ-strain in the minute 25, compression stress starts decreasing until the first stop takes place. Once the machine starts cutting again, tensile stress relief takes place as a consequence of the stress relief on the whole ring.
Some high stress values appear at the end of the process since this ring had also to be hit by a hammer.

3.5.3.3 Heat Treated ring

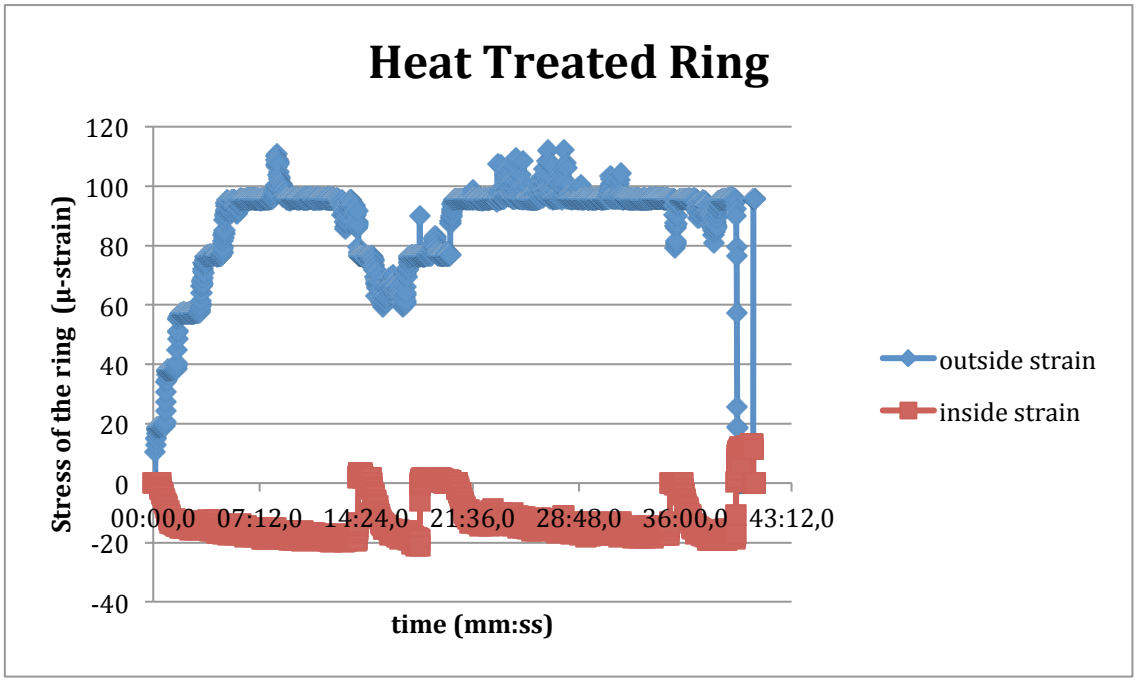

Figure 5.5 Data from the cutting of the Hear Treated ring.

Taking a view to the figure of the Heat Treated ring, it is easily noticeable that the outside strain gauge did not record compression values at any moment of the cutting process. Besides, the values are almost constant, around 100 μ-strain. A valley could be appreciated between the minutes 13 and 20. The reason of the decrease of the stress relief is that one cut was finished and the second one started right after.
The inside strain gauge measurement shows constant values as well. The range is between 5 and -20 μ-strain. There are two peaks and one valley between the minutes 13 and 20. As it was explained right above the reason is the end of the first cut and the beginning of the second one.
The same problem happened at the end of the cutting process, it was necessary to hit the piece in order to be able to remove it from the whole ring.

3.5.4 Discussion

As it was explained before, the aim was to measure the strain values of the ring during the cutting process. It could be used to know if stress was relieved in the ring. To get an idea of how the ring handles the mentioned process, a look to the graphics shown above could be taken.
Getting a closer view of Ring 1, it is noticed that the maximum value of stress relieved was 136 μ-strain of compression stress, whereas during the second cutting line, the maximum strain value recorded was just 76 μ-strain of tensile stress. A clear fact is that the values recorded by the outside strain gauge are much higher than the results obtained by the inside strain gauge. This phenomenon is caused due to the cutting direction, performed from outside to inside part of the ring. Besides, it could be appreciated that, when the cutting line is almost bored, the strain gauges record the highest values of stress relieved. It could be due to the fact that the cut section is much smaller than the whole ring and higher values of strain are gathered in the remaining section.
The Ring 2 results are not as clear as the Ring 1's due to the problem explained earlier about the wires' breaking off. However, it is possible to acquire an idea about the behavior of the ring. As in the first ring, the inside strain gauge does not record high stress relief during the process. The high values obtained were collected by the outside strain gauge. The explanation for the behavior found could be that the time between the stops was larger than in the other rings, so the conditions of the ring could change in that time.
In the Heat Treated ring, the values filed were different than the other rings ones. First of all, it was found that they were lower, reaching peaks of 108 μ-strain in the outside strain gauge and -20 μ-strain in the inside one. As it was mentioned already, the outside strain gauge did not record compression values during the whole process. Making a comparison with the other two rings, a totally different behavior was noticed. The first two rings filed compression values on the beginning of the cutting process. Moreover, the inside strain gauge only recorded tensile strength values after each leap of the curve. It is quite difficult to get any straight conclusion with the graphic obtained, as it does not follow a trend related to the cut carried out.

3.6 HOLE DRILLING

3.6.1 Method background

The Hole Drilling is a mechanical method that measures the magnitude and direction of the principal stresses by performing a semi- destructive technique [16]. It consists in drilling a small hole in the material and record the measurements of a gauge glued on the piece's surface. It is an uncomplicated technique to carry out the stress relief analysis. As it is an easy to install and cheap method, it is widely used [16].

The Hole Drilling is based on the theory of elasticity. It is considered that the ring has uniformly distributed stress on the surface. By executing a hole on the surface, the stress is relaxed in its surroundings. The local strains on the surface are modified and measured by the strain gauges installed on the surface [17].

The steps fulfilled in this method are:

1. The strain gauges installation.
2. The drilling process.
3. The strain measurements.
4. The measurement analysis.

3.6.1.1 Strain gauges installation

The gauges used to measure are strain gauges of residual stress of the company Micro-Measurements©, with a k factor of 1,3.

The rings which are to be analysed have a rough surface, as it can be appreciated in figure 6.2. It implies that, once the gauge has to be glued on the surface, too much glue will be stagnated between the gauge and the surface. As a result, the gauges would record the strain of the relaxation of the glue instead of the one in the ring. To solve the roughness of the surface, a rough polishing was carried out in order to obtain a slip surface. The problem this procedure entails is that, by polishing the surface, the stress that it is supposed to be relieved with the Hole Drilling is partially relieved by the polishing. The solution chosen was to install two different gauges in opposite sides of the ring to analyse the difference between the stress relief after the polishing and the original surface. One of them was polished previous to the Hole Drilling, whereas the other one was not treated. However, all the rings were cleaned using a mixture of acetone and isopropanol so as to remove all the surfaces' impurities.

As the previous parts display, the important directions are radial and tangential directions. In consequence, the strain gauges were located in a way that records the stresses in those two directions. The gauge number one is located in tangential direction and number two in radial direction. The gauge number three is placed in 45º between both directions. An image was placed right below to make this explanation more clear, in figure 6.1.

Figure 6.1 Strain gauge used and detail of the hole performed

The steps followed to allocate the strain gauges were:

1. Cleaning the rings' surface.
2. Polishing one of the surfaces until it has no flaws.
3. Applying glue in the bottom of the strain gauge.
4. Applying catalyst in the bottom of the strain gauge.
5. Press the strain gauge with a special paper and keep the pressure for a few minutes.
6. Welding the wires in each welding part of the strain gauges.

Once the strain gauge is perfectly fixed, the next step lies in connecting the wires from each rosette grid to three separate channels of a strain-measuring machine. The instrument has to be balanced in order to achieve initial zero readings for each grid.

3.6.1.2 The drilling process

The first step of the Hole Drilling test is to place the ring in the right position. Using an optical microscope with a scale inside it as a guide, the centre of the gauge's mark is located in the very centre of the microscope's scale. Additionally, the Hole Drilling machine has to be levelled as the ring lays so as to perform a vertical hole.

Once every part is correctly placed, the strain gauge's wires are welded to the equipment used for the values' recording. Right after, the equipment is balanced and initialized before the hole making process is started.

Once the ring is placed in the right position, the microscope is replaced by the drilling machine, shown in figure 6.1.Helped by a micrometre, the drill starts going down. It is a manual process and it has to be stopped once the drill touches the strain gauge's surface. In that very moment, the value recording machine is settled as zero and the drilling process starts. The method used for drilling is the one which, while the drill goes deeper by turning the micrometre around, the drill has to be turned as well, 185˚ in this case. The drilling process is very simple. The first millimetre is the depth of interest as the greater changes take place in it. As a consequence, the depth drilled each time will be 40µm. The procedure is to turn the micrometre around as the same time that the drill is also turned around 185˚. Each time a new depth is carried out, the drilling turn will change directions. After each drill, a couple of minutes have to be waited until the strain values get stable. The reason is that, while drilling, some friction appears and, as a consequence, the strain gauge is heated up and the value cannot be trusted. Once the value shows constant in the machine, it is filed and the next depth could be carried out. Once a flat tendency is noticed in the values output, the drilling could be stopped.

Figure 6.2. Drilling machine and details of the drill

3.6.1.3 Gathering information

The equipment measured the results obtained from the gauges. The results are presented in the figures below. The measurements are compared in the pictures with the theoretical value of the Uniform Stress Method, which considers that the residual stresses are uniform with depth from the specimen surface.

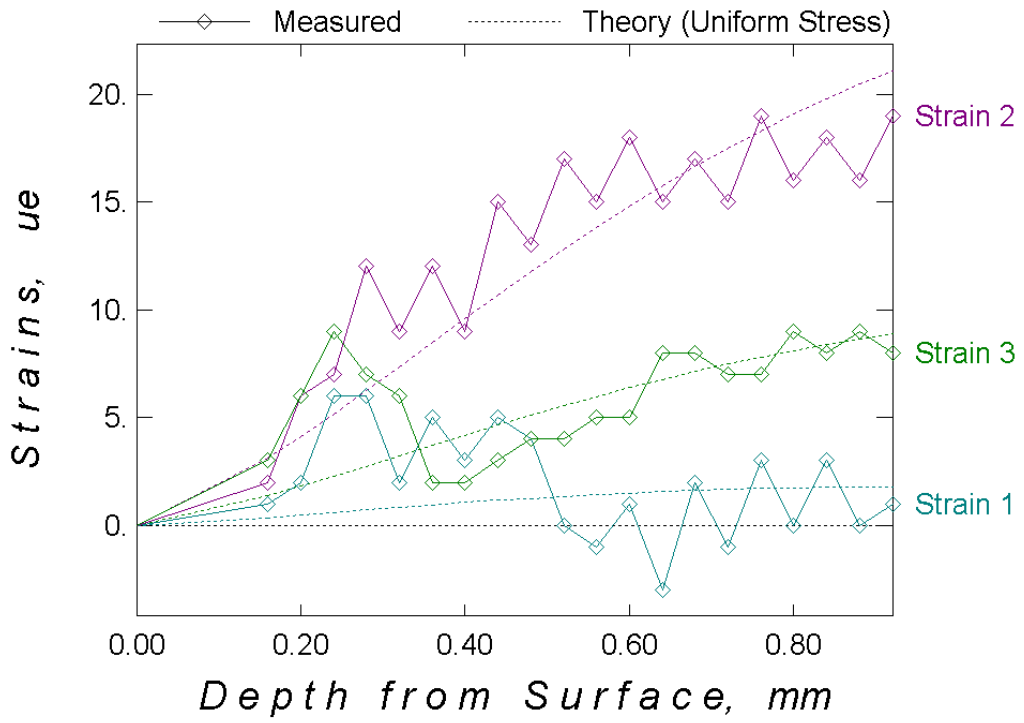

Figure 6.3. Data from the Hole Drilling of the unpolished surface of the Heat Treated ring.

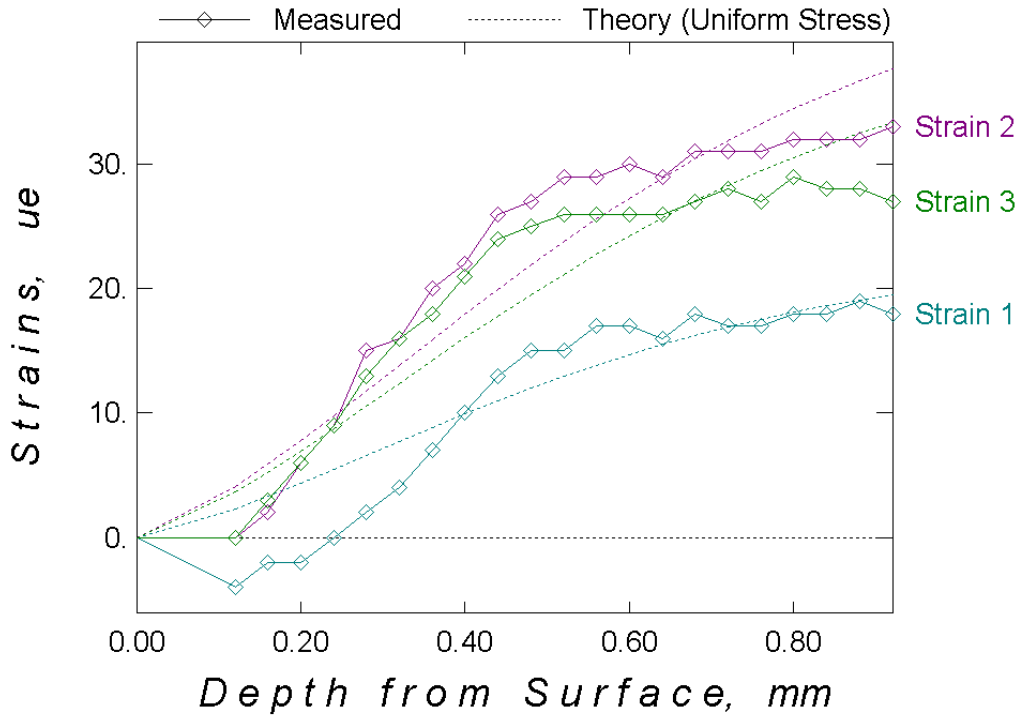

Figure 6.4. Data from the Hole Drilling of the polished surface of the Heat Treated ring.

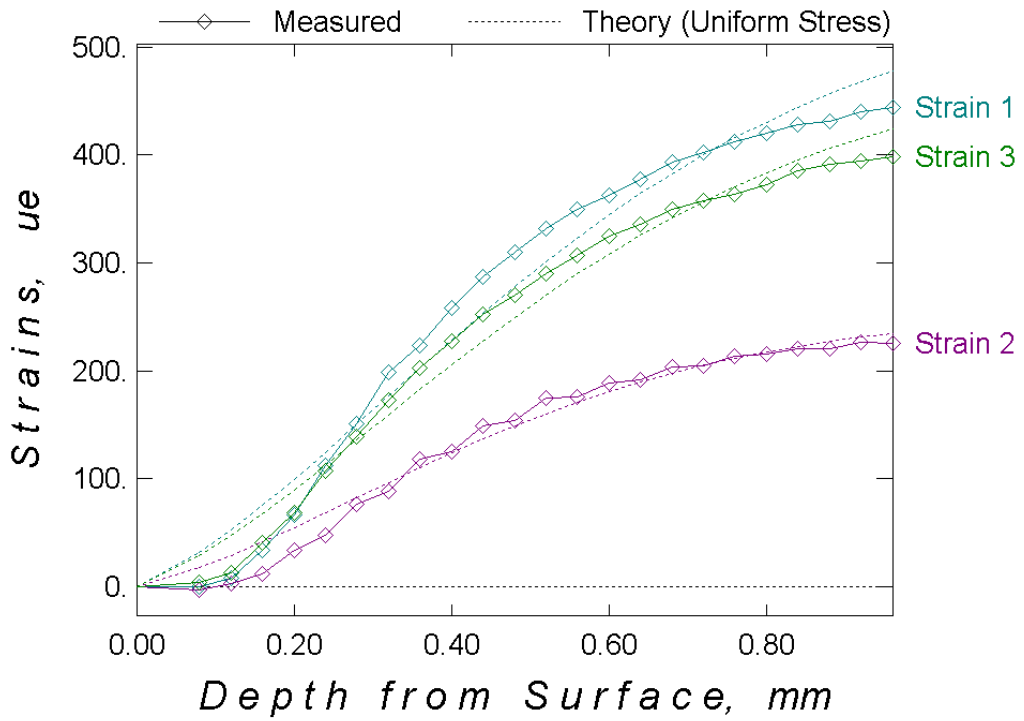

Figure 6.5 Data from the Hole Drilling of the unpolished surface of the ring 1.

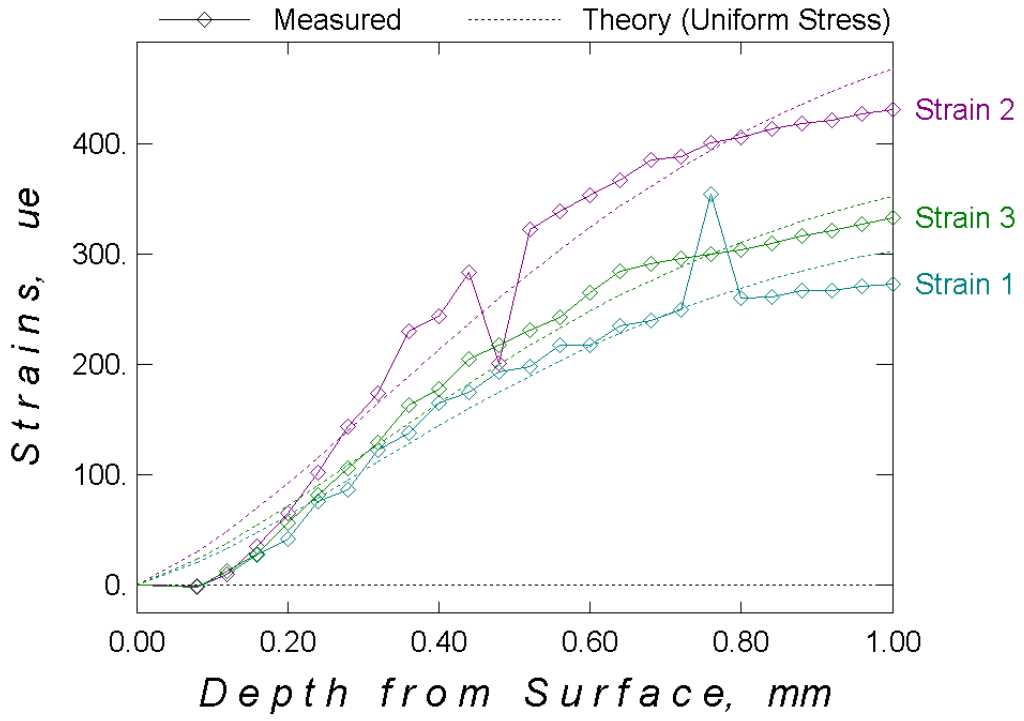

Figure 6.6 Data from the Hole Drilling of the polished surface of the ring 1.

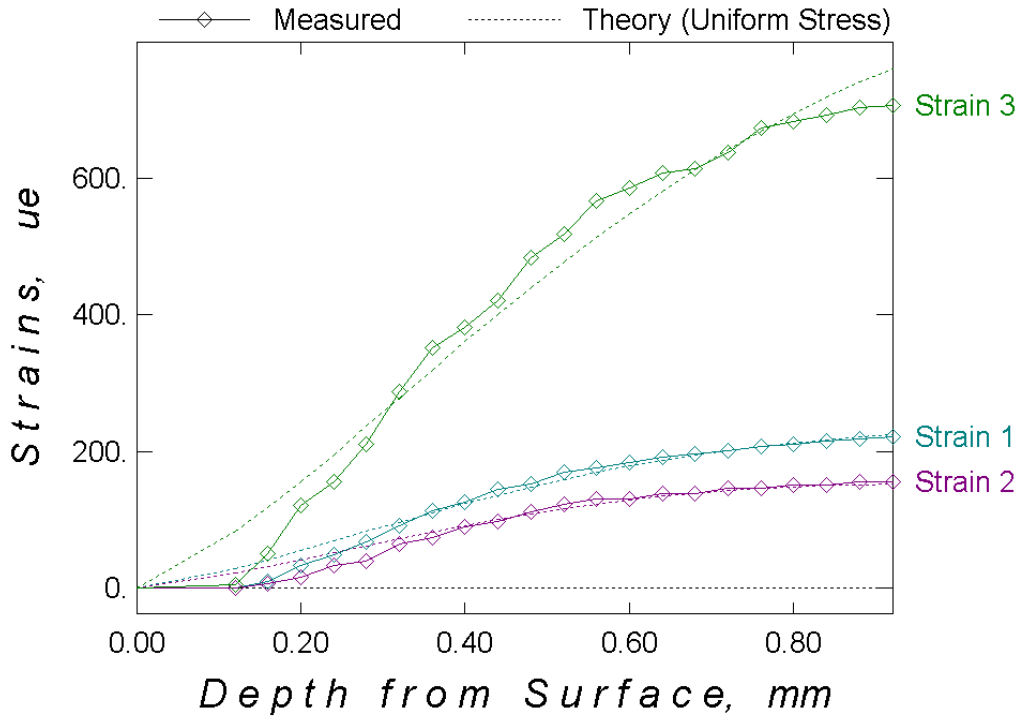

Figure 6.7 Data from the Hole Drilling of the unpolished surface of ring 2.

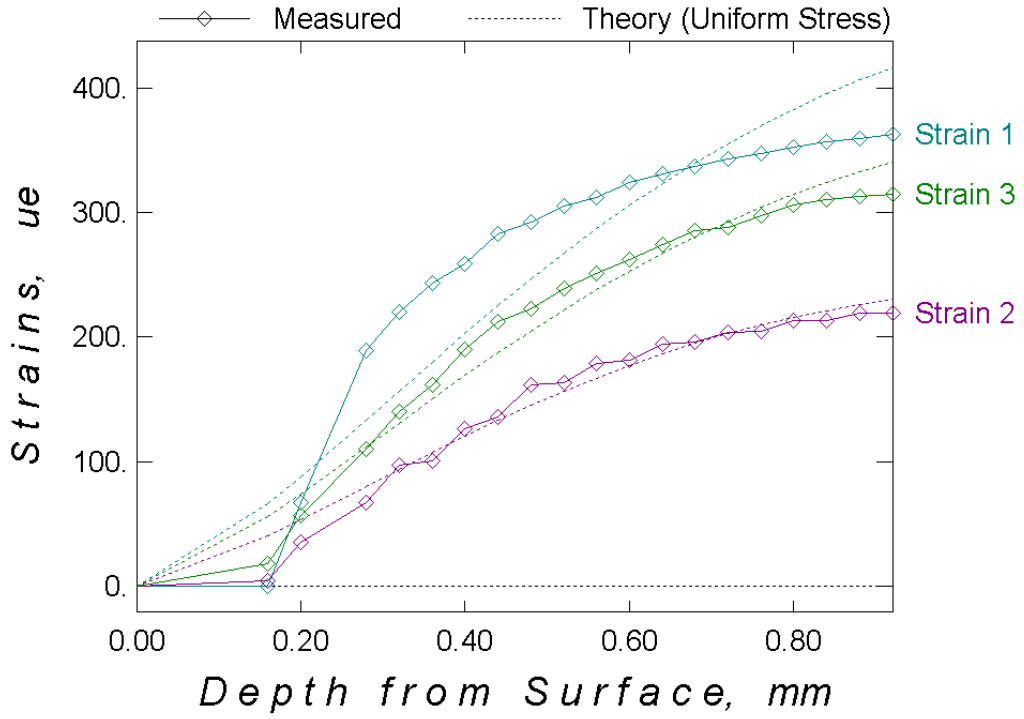

Figure 6.8 Data from the Hole Drilling of the polished surface of the ring 2.

3.6.2 Results of the stress relief

3.6.2.1 Results obtained

The calculation of the stress relief on the rings was carried out by the Integral Method hypothesis. This hypothesis considers a separate evaluation of residual stress within each increment of depth selected during the Hole Drilling measurements [18].
The results are presented in the figures below. They represent the maximum and minimum stress relief and the stress in X and Y direction (tangential and radial direction respectively) related to the depth.

3.6.2.1.1 Heat Treated ring

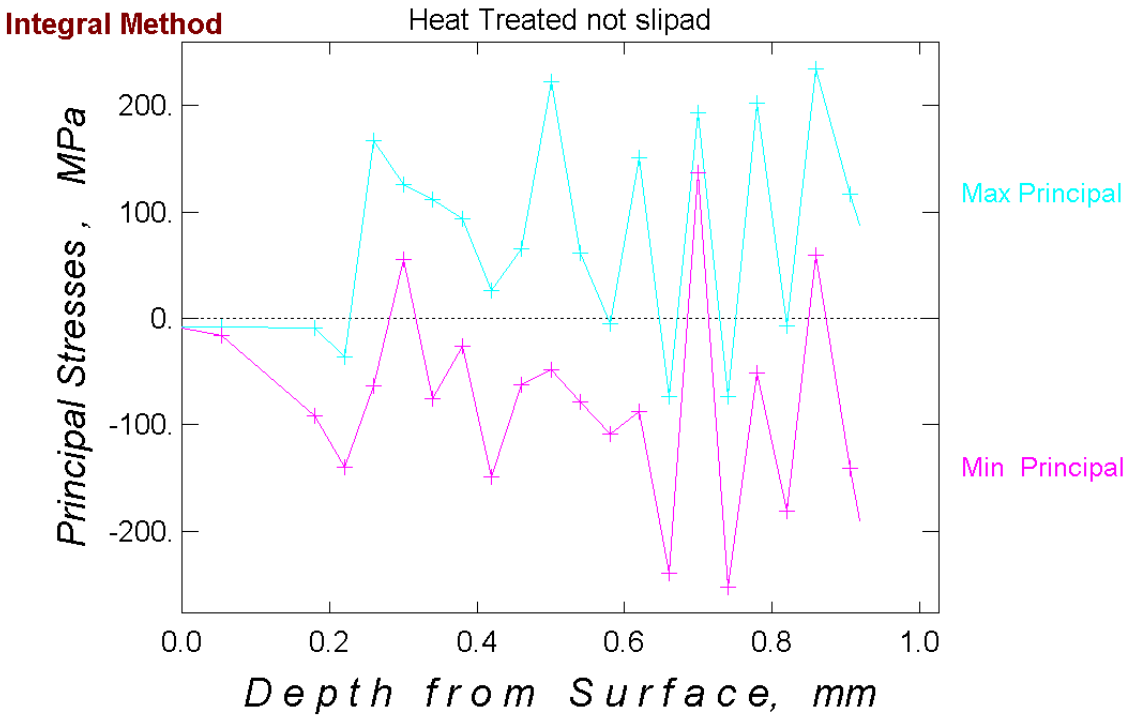

Figure 6.9 Principal stresses from the Hole Drilling of the unpolished surface of the Heat Treated ring.

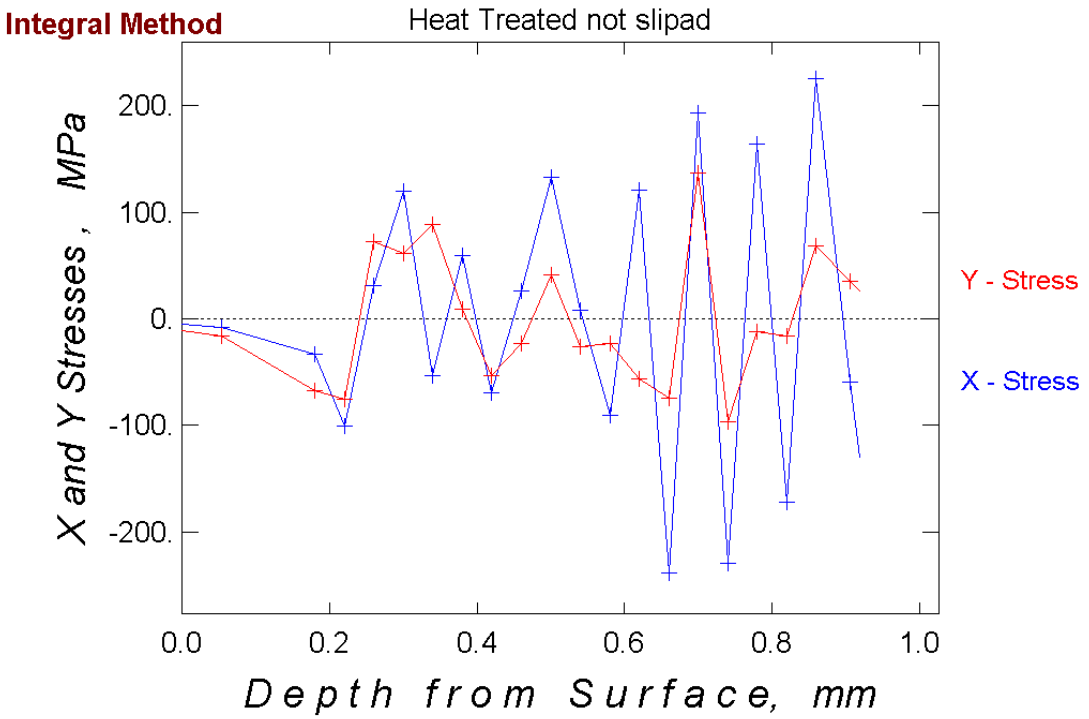

Figure 6.10Tangential and radial stresses from the Hole Drilling of the unpolished surface of the Heat Treated ring.

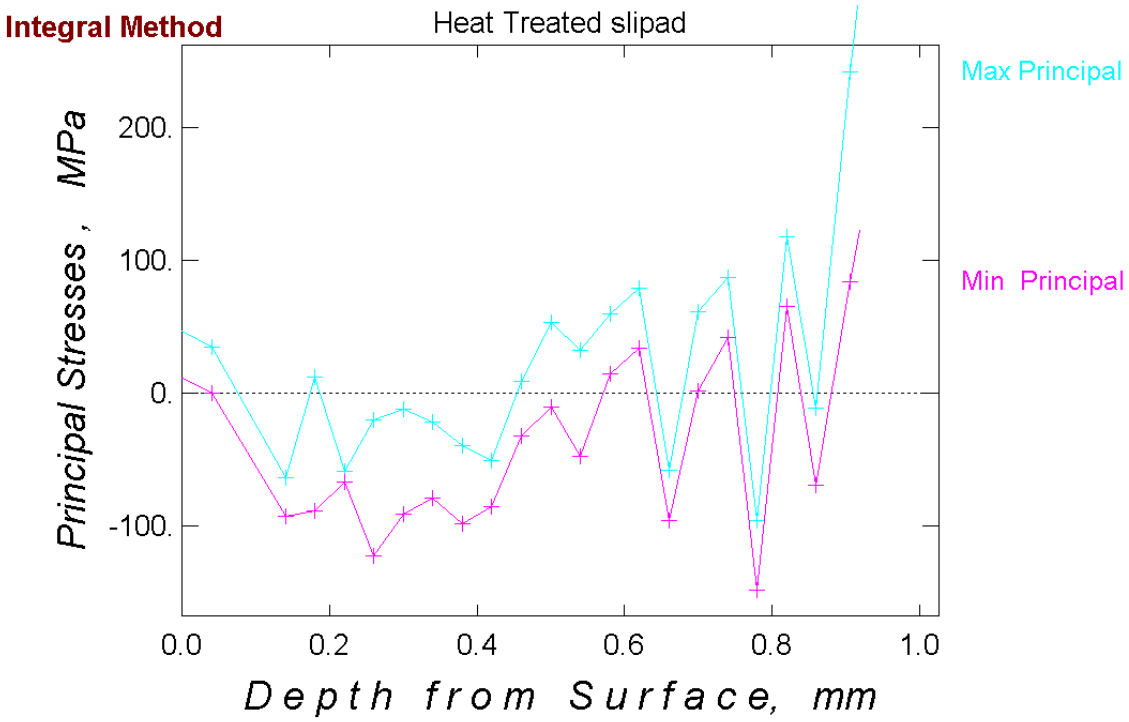

Figure 6.11 Principal stresses from the Hole Drilling of the polished surface of the Heat Treated ring.

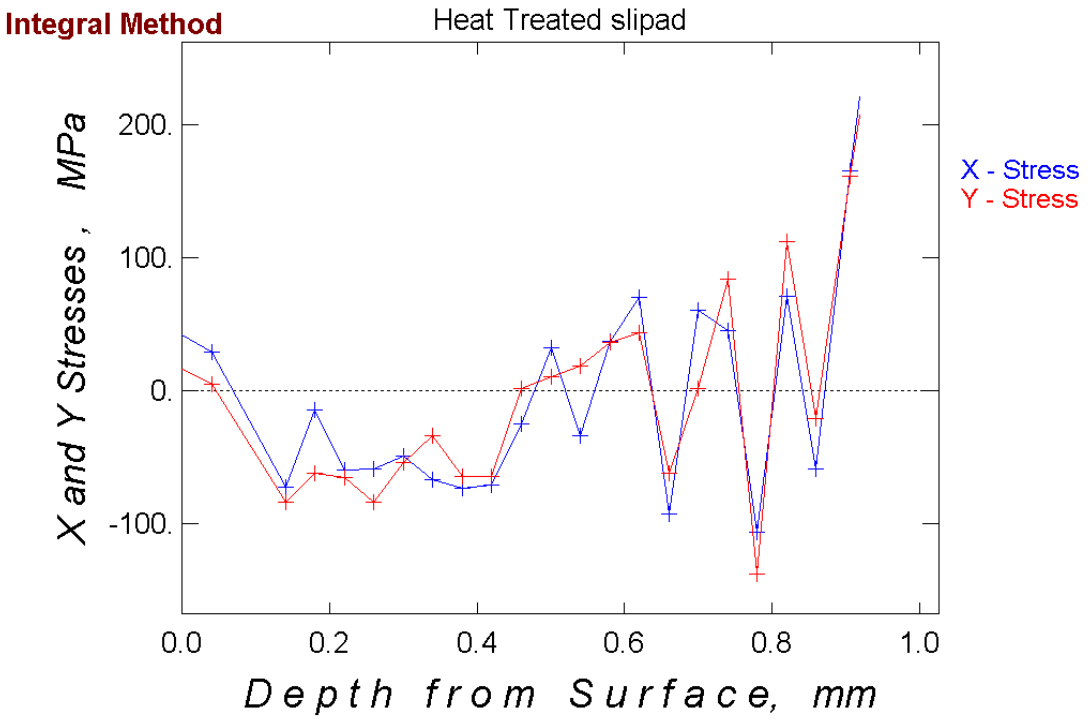

Figure 6.12 Tangential and radial stresses from the Hole Drilling of the polished surface of the Heat Treated ring.

3.6.2.1.2 Ring 1

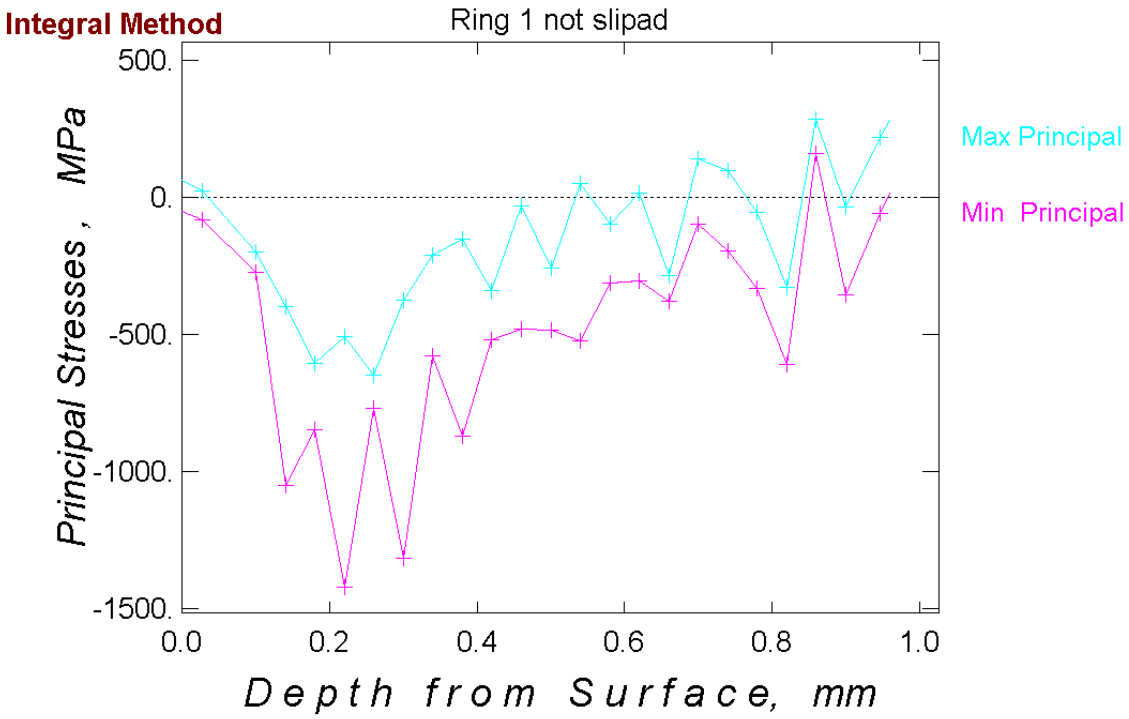

Figure 6.13 Principal stresses from the Hole Drilling of the unpolished surface of the ring 1.

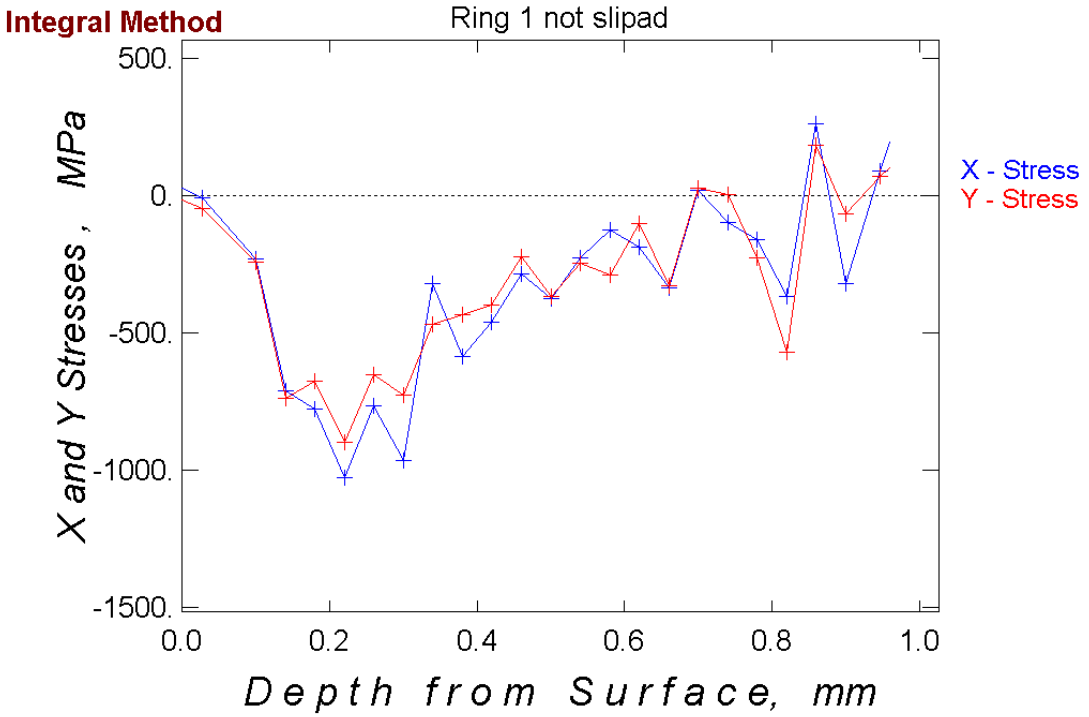

Figure 6.14 Tangential and radial stresses from the Hole Drilling of the unpolished surface of the ring 1.

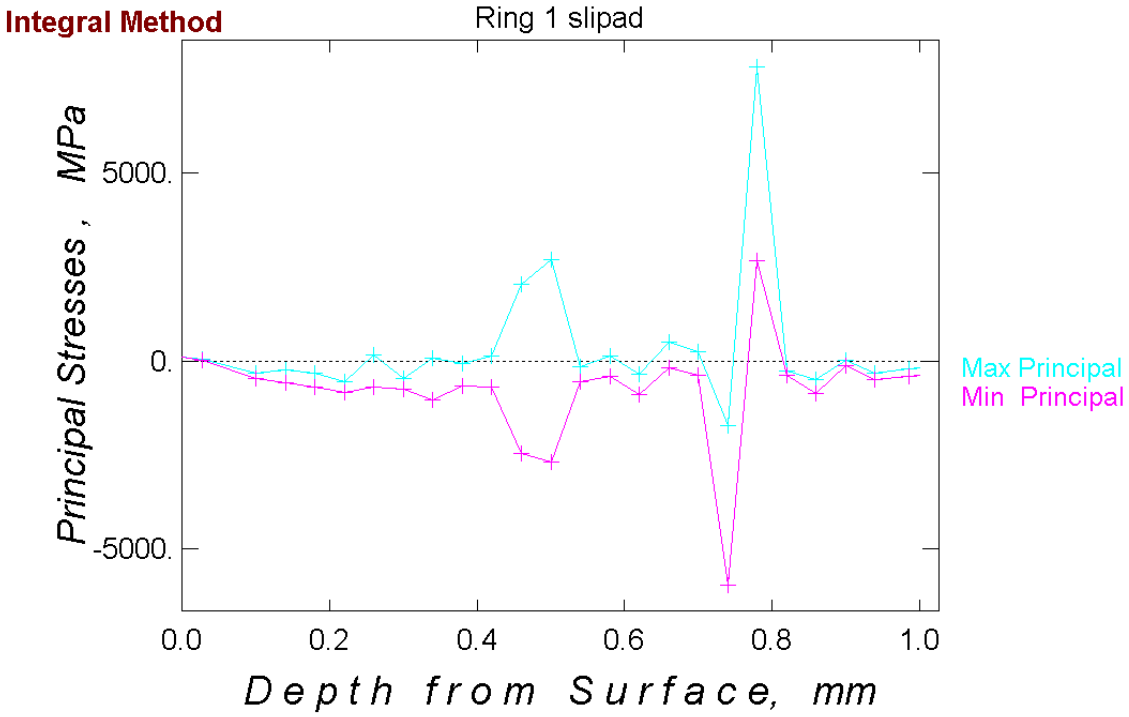

Figure 6.15 Principal stresses from the Hole Drilling of the polished surface of the ring 1.

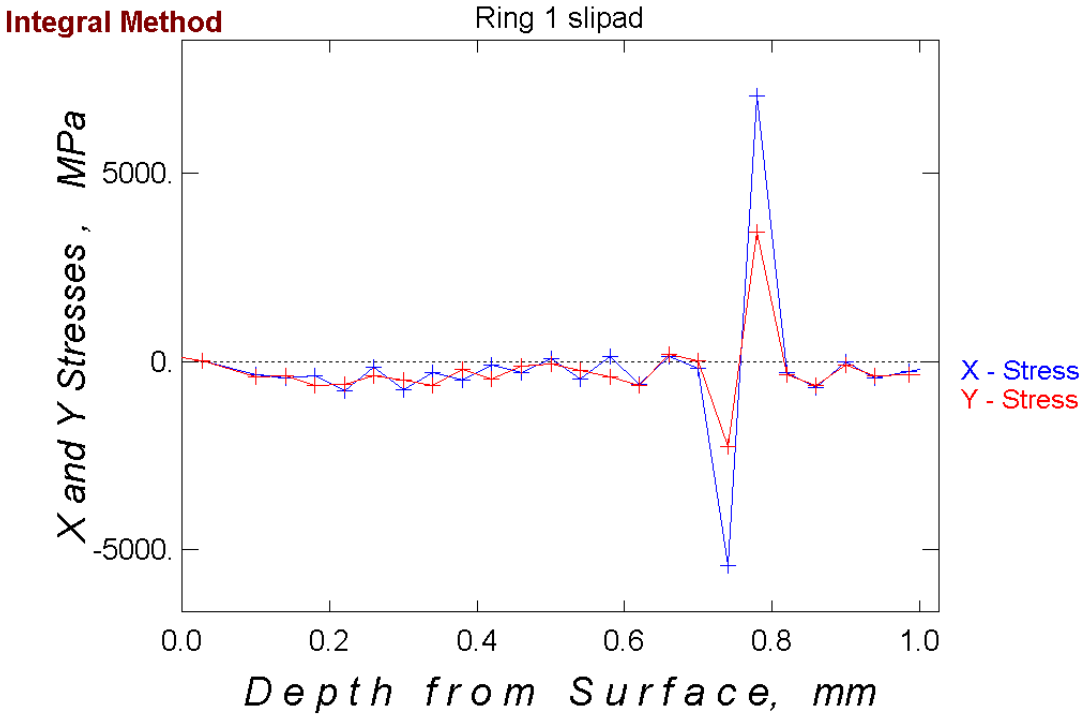

Figure 6.16Tangential and radial stresses from the Hole Drilling of the polished surface of the ring 1.

3.6.2.1.3 Ring 2

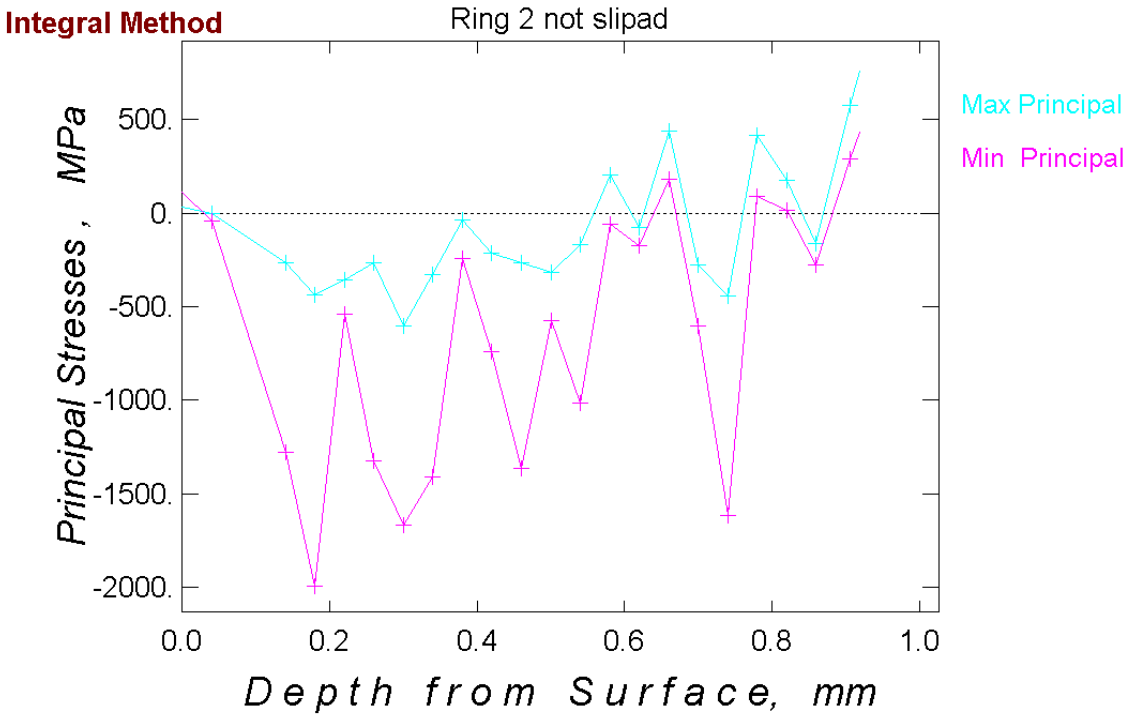

Figure 6.17 Principal stresses from the Hole Drilling of the unpolished surface of the ring 2.

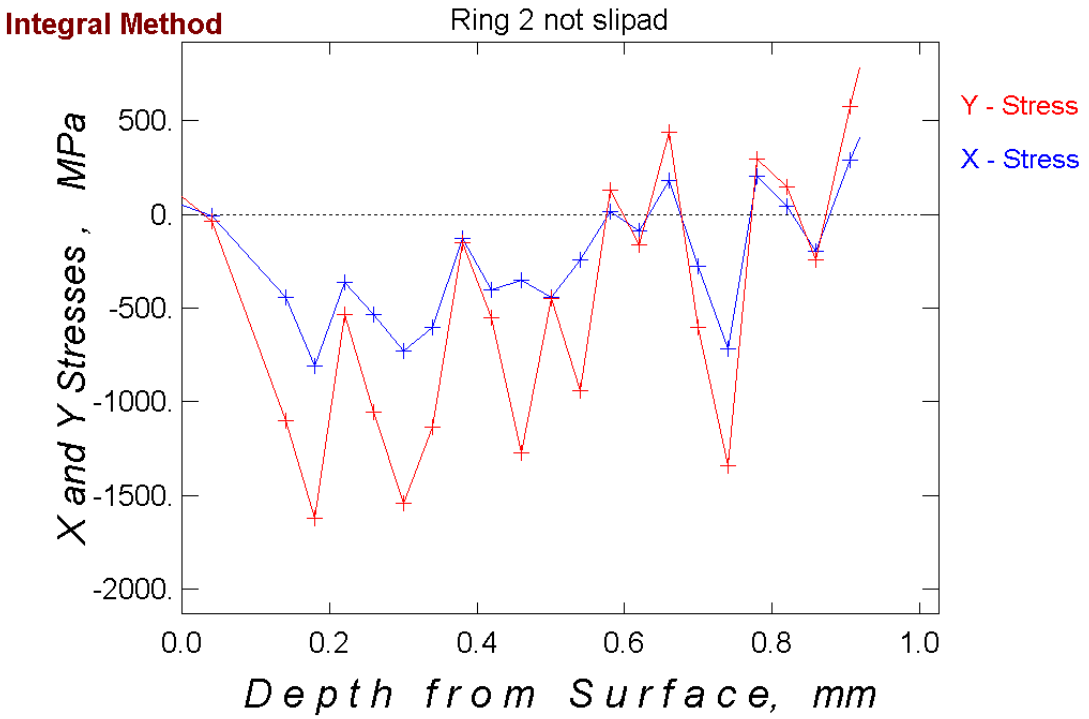

Figure 6.18 Tangential and radial stresses from the Hole Drilling of the unpolished surface of the ring 2.

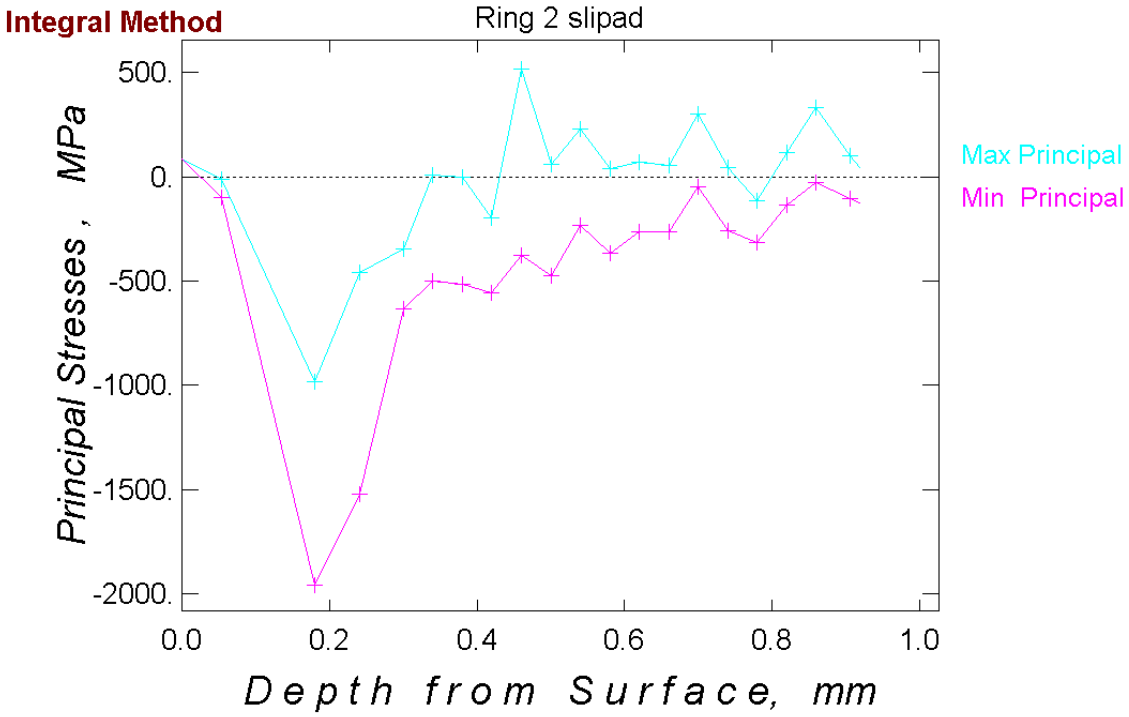

Figure 6.19 Principal stresses from the Hole Drilling of the polished surface of the ring 2.

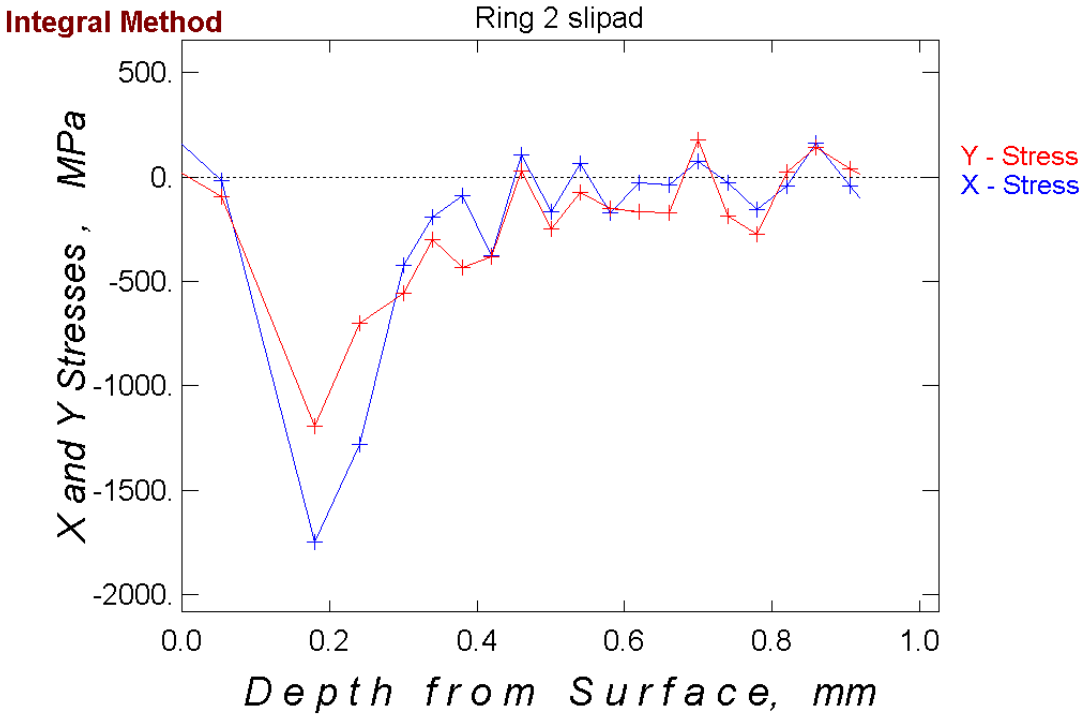

Figure 6.20 Tangential and radial stresses from the Hole Drilling of the polished surface of the ring 2.

3.6.2.2 Average results

With a simple glance to the graphics, it can be appreciated that the values obtained with the test performed are not reliable. They are very oscillating along the depth and they don't show any tendency. It could be caused by many circumstances. For instance, the method used. As it is an integral method, each measurement has influence on the surrounding values. Besides, another factor which could affect is the depth drilled in each measurement, which was very low (0,04 mm). Therefore, a clear conclusion cannot be achieved from these graphs.
In order to avoid these matters, the action executed was to take sets of three values and calculate their average. The obtained results are presented in figures 6.21 to 6.32.

3.6.2.2.1 Heat Treated Ring

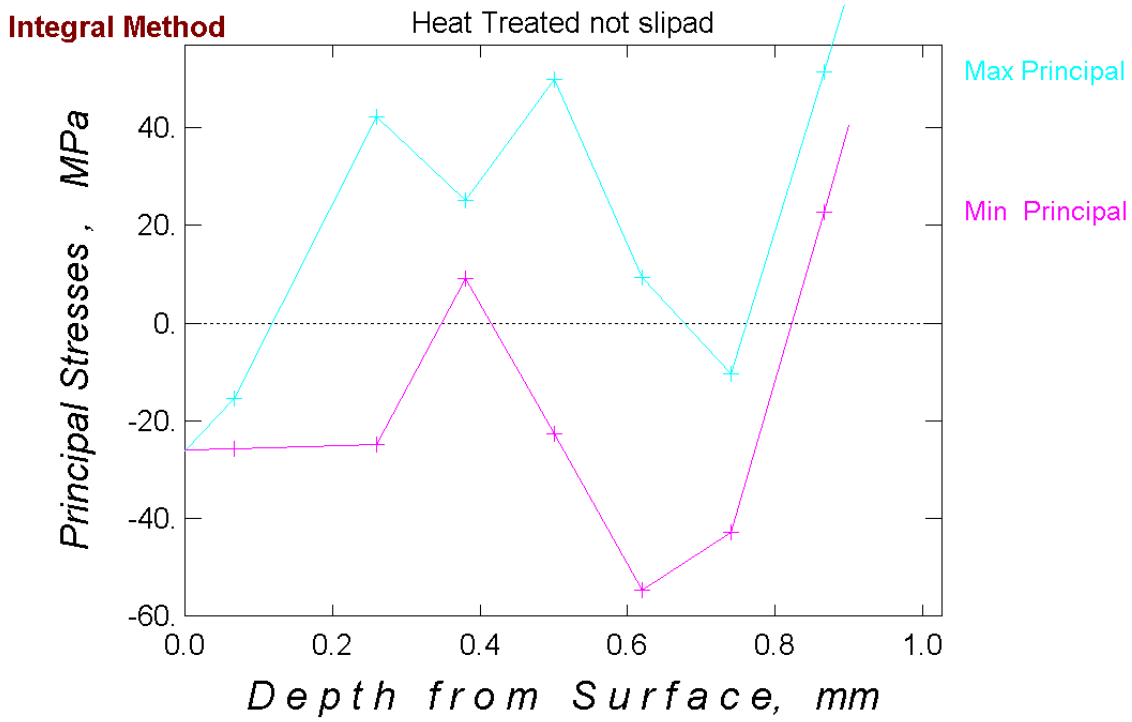

Figure 6.21 Principal stresses from the Hole Drilling of the unpolished surface of the Heat Treated ring.

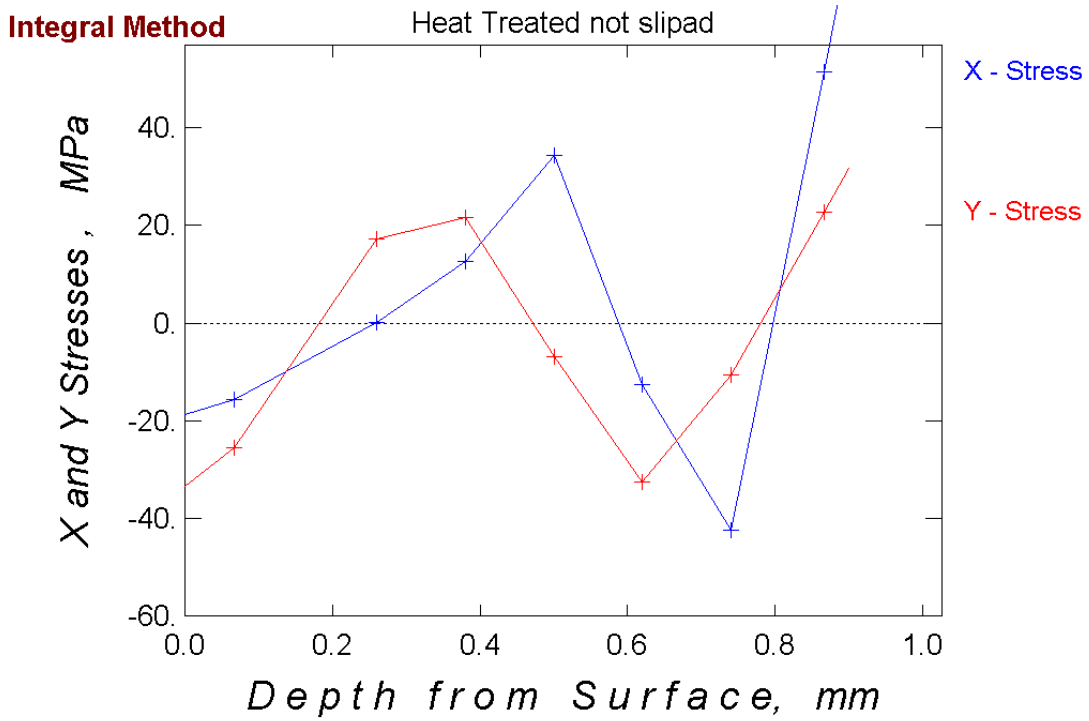

Figure 6.22 Tangential and radial stresses from the Hole Drilling of the unpolished surface of the Heat Treated ring.

This first pair of figures, 6.21 and 6.22, show that compression stress appeared in the ring's surface. In depths from 0.2 mm to 0.5 mm, the compression tress is converted to tensile stress. Once the tensile stress peaks are reached, values start decreasing again to a new compression stress peak and the relieved stress starts to

decrease until tensile stress is arisen at 0.8 mm deep. Two facts to mention are that both tensile and compression stresses appear fluctuating all along the hole performed and that the measured values of the stress relieved are quite low in the measured depth.

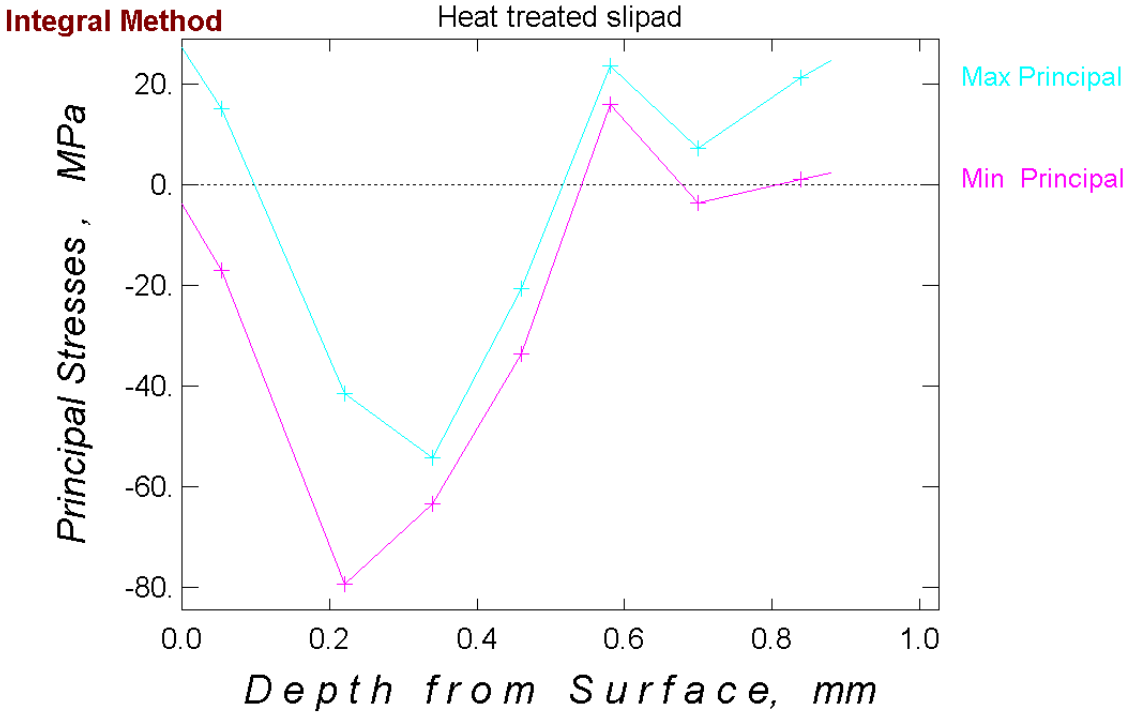

Figure 6.23 Principal stresses from the Hole Drilling of the polished surface of the Heat Treated ring.

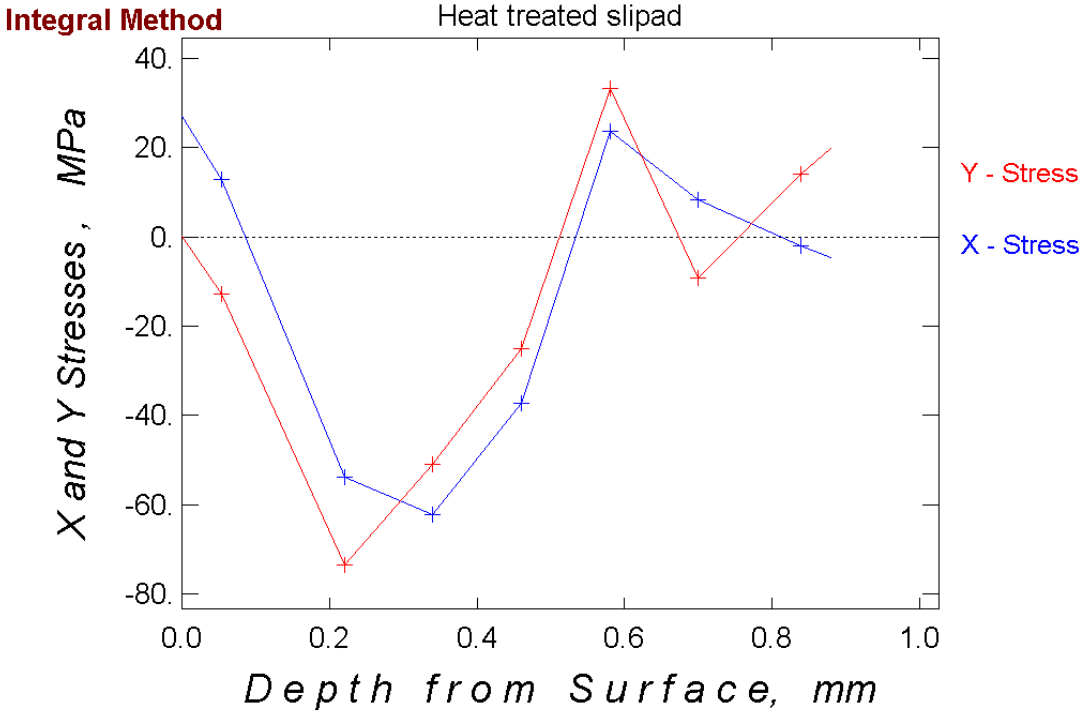

Figure 6.24 Tangential and radial stresses from the Hole Drilling of the polished surface of the Heat Treated ring.

In figures 6.23 and 6.24 it can be appreciated that a similar behaviour is displayed between tangential (X) and radial (Y) stresses. Anyway, the tangential stress starts with a tensile strength relief and goes to compression rapidly until more or less 60MPa in about 0.3 mm deep. Right after, the compression stress starts decreasing until tensile stress appears again in about 0.5 mm deep. Once 0.6 mm depth is reached, tensile stress starts to decrease and a tendency around 0 MPa enters the picture. On the other hand, the radial stress starts showing a value of 0MPa on the very surface and keeps the tangential direction tendency all along the measurement performed.

3.6.2.2.2 Ring 1

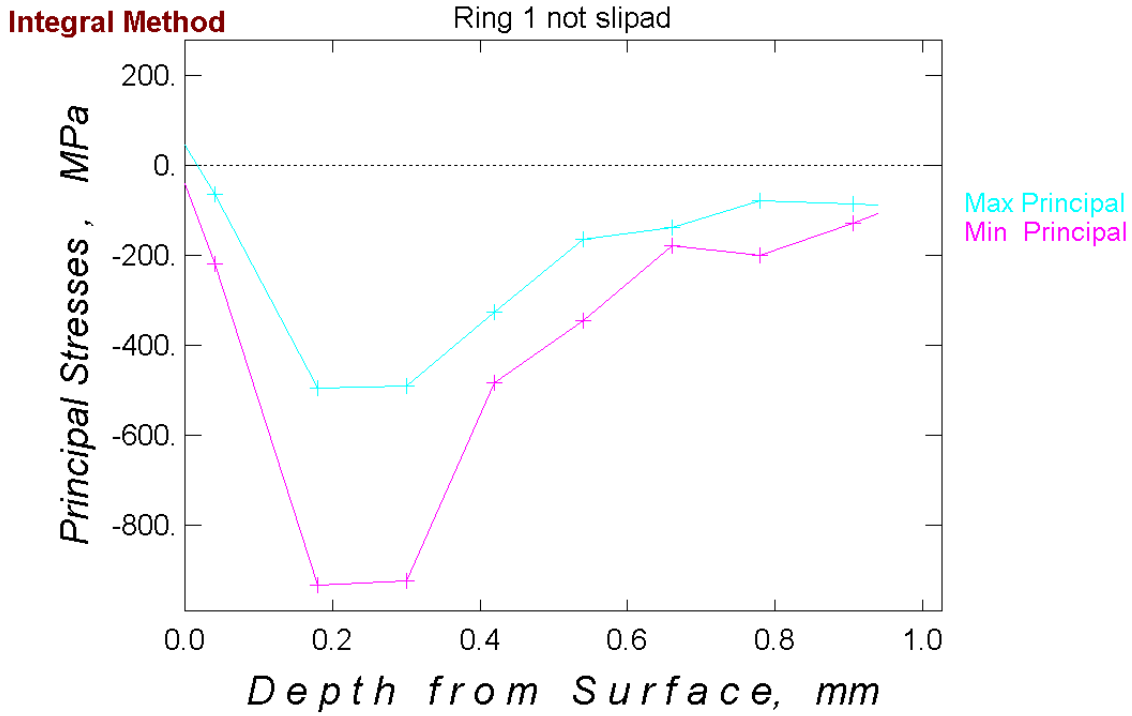

Figure 6.25 Principal stresses from the Hole Drilling of the unpolished surface of the ring 1.

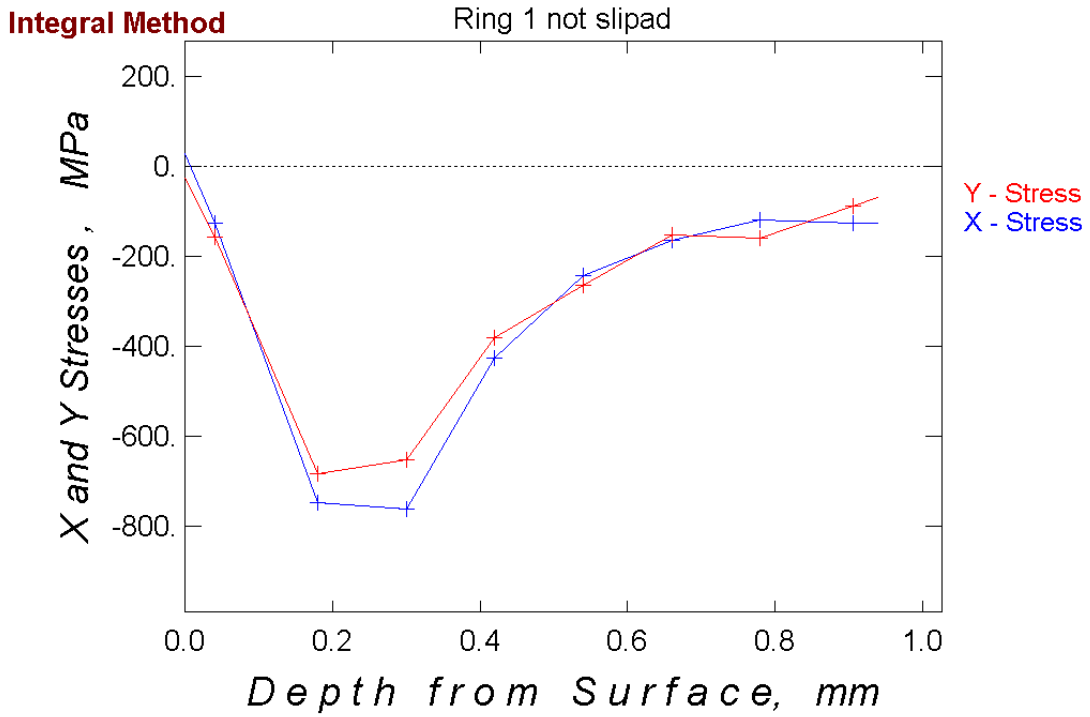

Figure 6.26 Tangential and radial stresses from the Hole Drilling of the unpolished surface of the ring 1.

Figures 6.25 and 6.26 show the Ring 1's behaviour. Taking a look to these graphics, some facts were found evident. First, mention that both directions have equivalent tendencies. Second, notice that there is no tensile stress relief, when the hole is performed, just compression stress comes forth. Third, mark that unusual high

values appear in the whole experiment. Fourth, spot that the tendency is not around zero. Even in 1mm depth, there is still stress relief. Finally, it can be detected that the maximum compression stress appears between around 0.2 and 0.3 mm and that, instead of having a peak as the rest of the holes performed, it is stable along these depths.

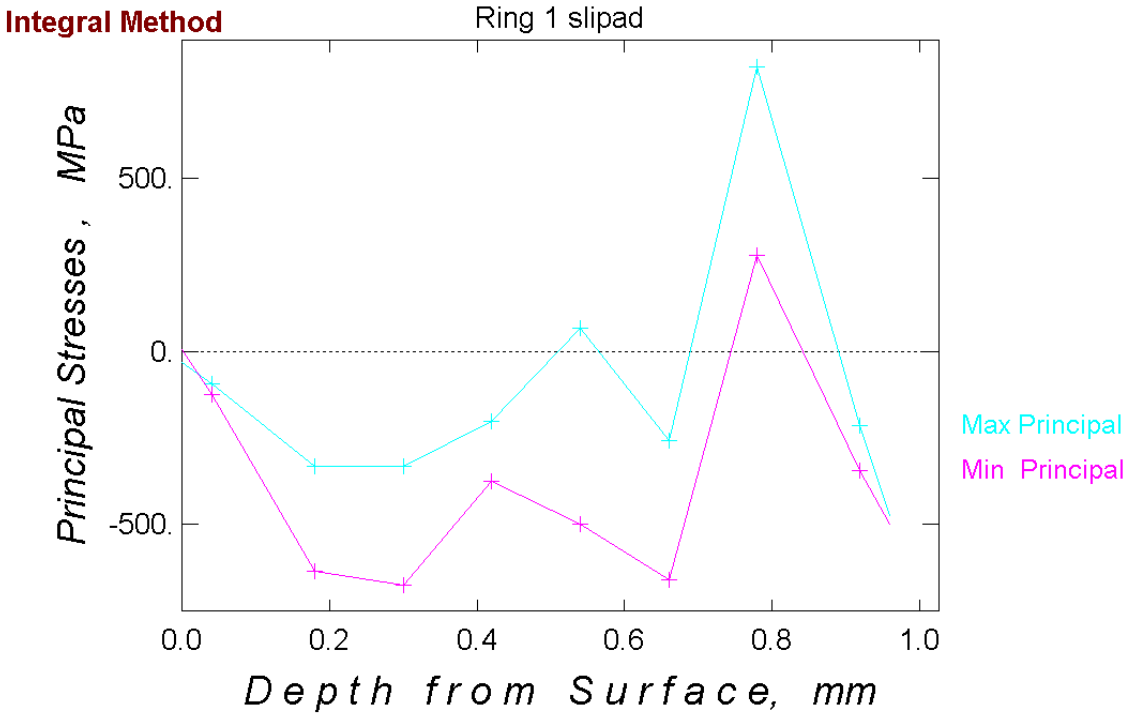

Figure 6.27 Principal stresses from the Hole Drilling of the polished surface of the ring 1.

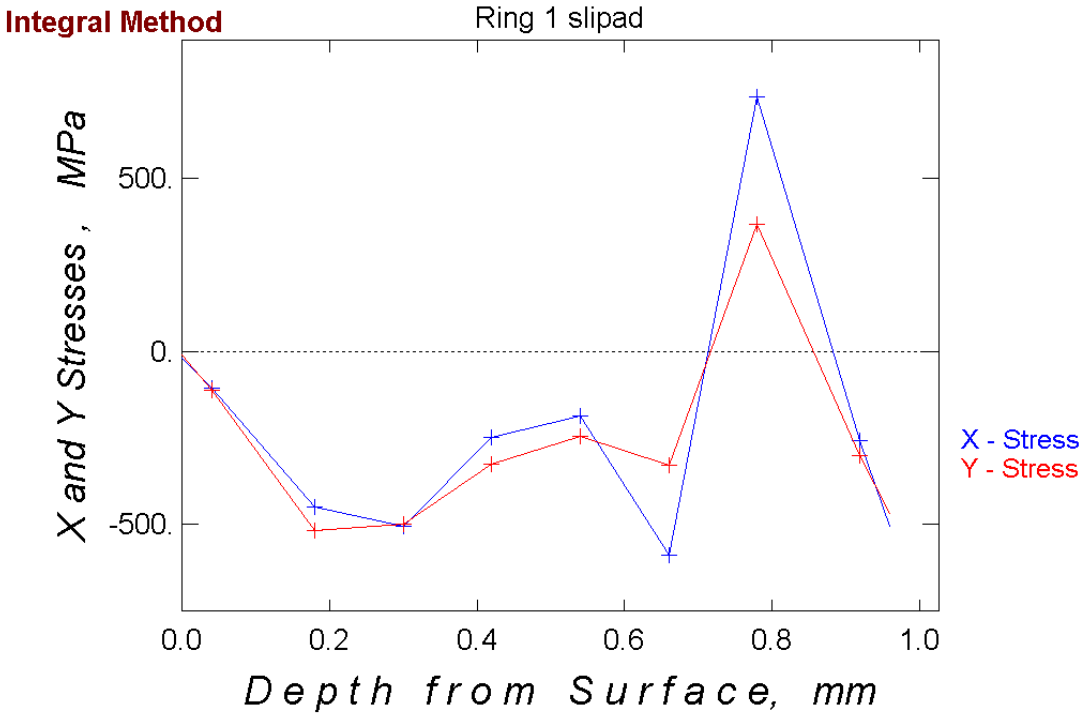

Figure 6.28 Tangential and radial stresses from the Hole Drilling of the polished surface of the ring 1.

Figures 6.27 and 6.28 display the stress relief of the polished surface of Ring 1. At first, the behaviour of the two curves is quite similar to the non-polished surface of this ring. It starts a compression stress relief with a peak between 0.2 and 0.3 mm and, right after, it starts decreasing. Once a depth of 0.5 mm is reached, an opposite behaviour can be noticed. The compression stress relief starts increasing again and, as soon as it reaches a peak in about 0.7 mm, it starts to decrease until a peak of tensile stress is found in 0.8mm. A high fluctuation was spotted after 0.5 mm.

3.6.2.2.3 Ring 2

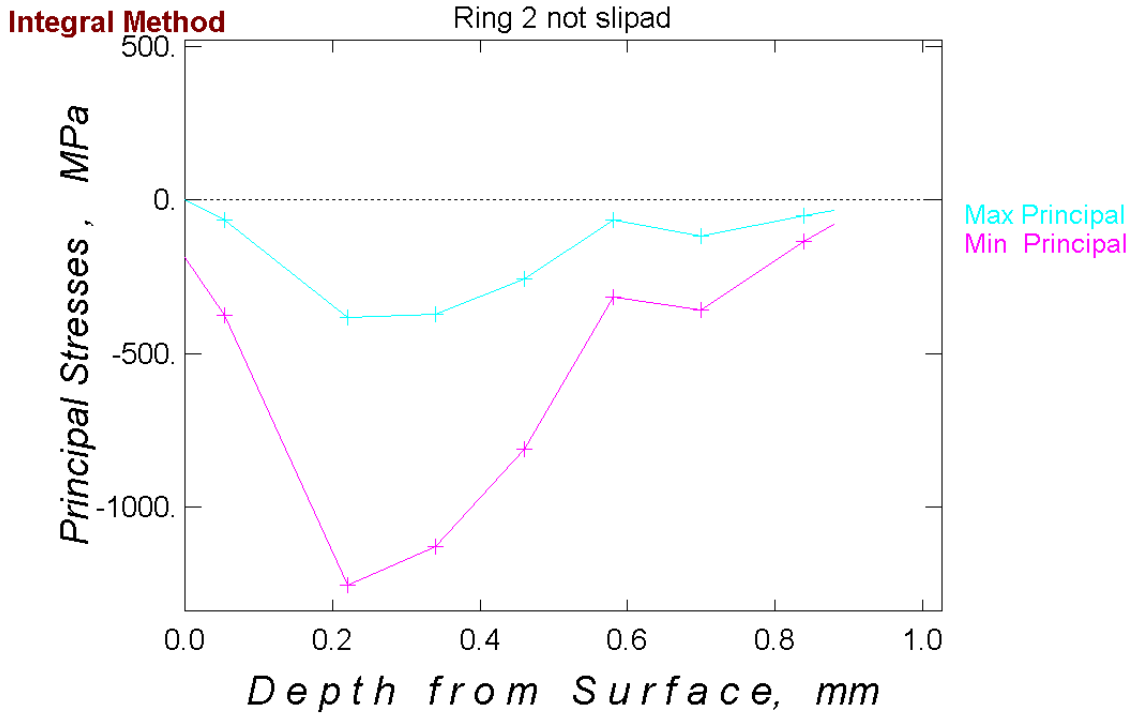

Figure 6.29 Principal stresses from the Hole Drilling of the unpolished surface of the ring 2.

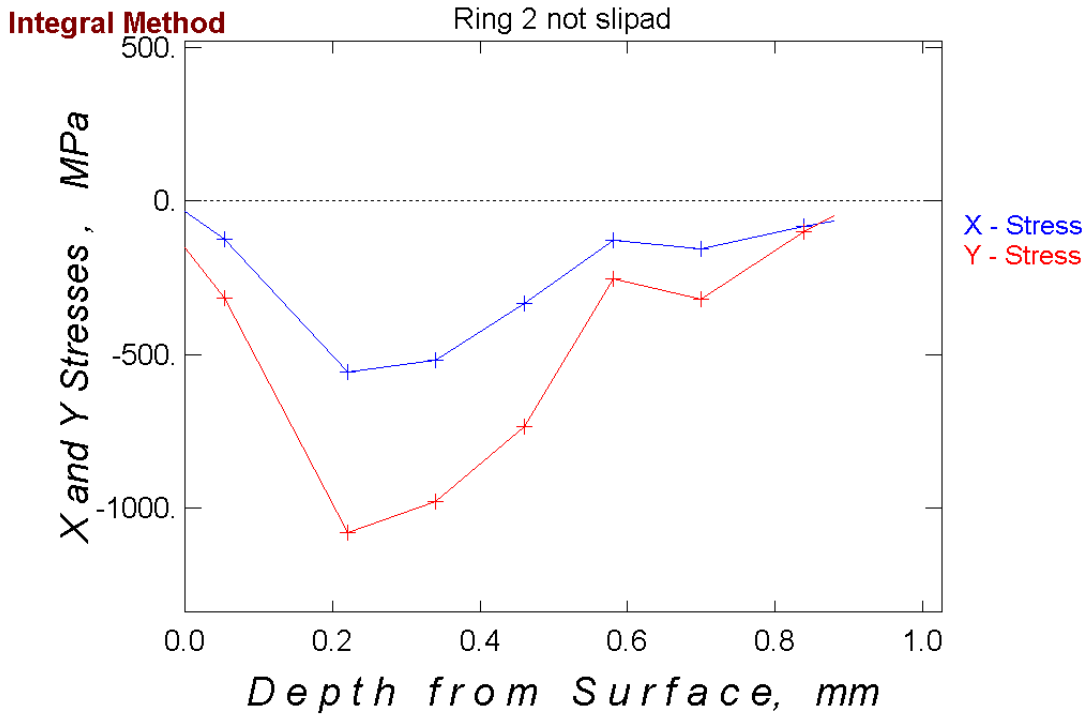

Figure 6.30 Tangential and radial stresses from the Hole Drilling of the unpolished surface of the ring 2.

Figures 6.29 and 6.30 display the original surface experiment carried out in Ring 2. Both directions, radial and tangential, show just compression values, equal trends and different values all along the measured depth. More stress is relieved in radial direction than in tangential. Too high values of stress were noticed in the direction

mentioned. Analogous compression peaks are found in 0.2 mm deep and also a tendency of 0MPa when a depth on 1mm is reached.

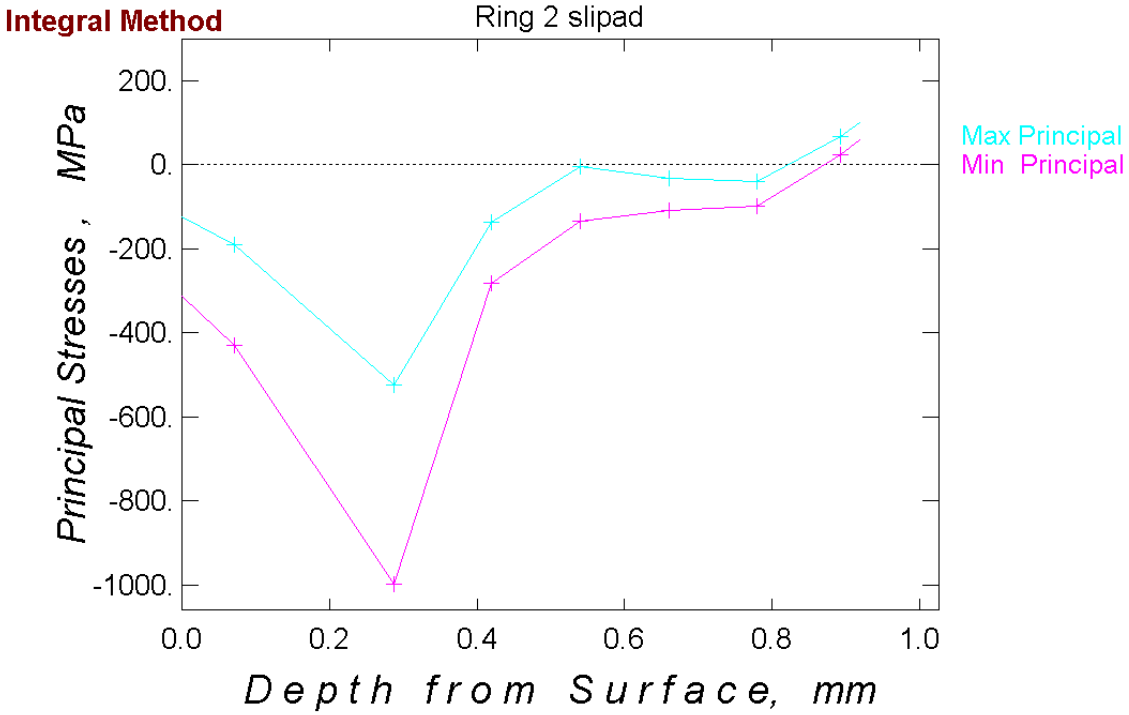

Figure 6.31 Principal stresses from the Hole Drilling of the polished surface of the ring 2.

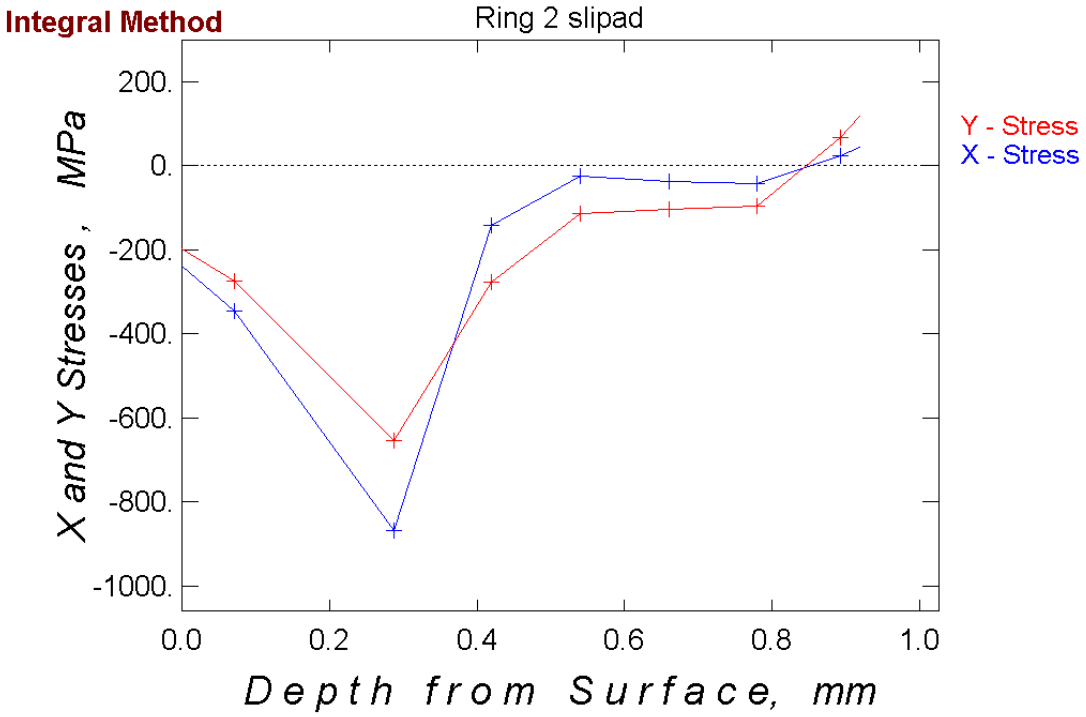

Figure 6.32Tangential and radial stresses from the Hole Drilling of the polished surface of the ring 2.

Right above, 6.31 and 6.32 figures present the polished surface experiment carried out in Ring 2. It is noticeable that both directions have similar values, quite high

stress relief results. A sharp peak is shown in around 3 mm deep and another remarkable fact is that there are stress relief values even in the surface. The results start with 200MPa of compression stress and decrease until the mentioned peak is reached. In a depth slightly higher than 0.8 mm, compression stress becomes tensile stress. As the other rings behaviour, there is a non-stress relief tendency when the depth comes to 1mm.

3.6.3. Discussion

First a comparison of the two different methods, polished and unpolished surfaces, of each ring will be carried out and, afterwards, a comparison of the three rings will be executed.

In rings 1 and 2, similar tendencies were found between the polished and the unpolished surfaces. The only peculiarity to mention is the fluctuation of the Ring 1 in the last half part of the curve in the polished surface experiment. Instead, in the Heat Treated ring there is no analogy between the two curves. They both have different behaviours and tendencies. However, the values' range is more or less similar.

When a glimpse is taken to all the graphics displayed above, some conclusions can be held. The values recorded of the stress relief on the Heat Treated ring are essentially lower than the ones recorded in the other two rings. The cause is that the second heat treatment executed to that ring relieved a high percentage of the residual stress stored in the machining, as it can be appreciated taking a view to the values of the machined ring.
Comparing the results of the experiments carried out in rings 1 and 2, two remarkable facts were detected. First, the stress value on the surfaces differs around 200MPa, and second, that the Ring 2 displays higher values of stress relief around the compression stress in depths of 0.2mm.

An unascertained circumstance observed is that the rings received by Siemens A.B weren't named in a way to recognize the three types of rings. In order to be able to solve the problem, an analysis of the difference of the rings 1 and 2 will be carried out. As the great value on the surface of the Ring 2 displayed and the higher values recorded in the peak mentioned right above, the conclusion states is that the machined ring is the one named as Ring 2.

3.7 X-RAY TEST

3.7.1 Introduction

In previous pages, a description of the residual stress is given. Residual stress can be measured with the X-Ray Diffraction method. It is based on "the fact that the spacing of the atomic planes in a crystalline material is altered by stress and that spacing can be determined by the measuring the angular position of a diffracted X-Ray beam" [1]. The variation of this spacing is a strain from which the stress can be determined.

This method is widely used. It is because it's a fast and non-destructive way to measure the stress. However, the most common use of this method is to determine the stress at the surface. The reason is that the service failure usually is initiated at the surface, a knowledge of the surface residual stress is sufficient for most applications. If information about the subsurface is needed, material must be removed in order to expose the subsurface to the X-Ray beam. In that case, the method will become destructive [1].

A destructive analysis was performed in this project. In order to examine the profile behaviour, several layers were analysed. The procedure is based on removing a layer of material once the previous one has been analysed.

3.7.2 Results

The analysis was executed in tangential direction. A view will be taken to the graphics and, right after, a comparison of the stress relieved with the X-Ray method and the Hole Drilling technique will be carried out. The studied depth has been 250μm so as to get an idea of the behaviour of the rings and the differences between them. Furthermore, error bars are displayed in the graphics below.

3.7.2.1 Heat Treated ring analysis

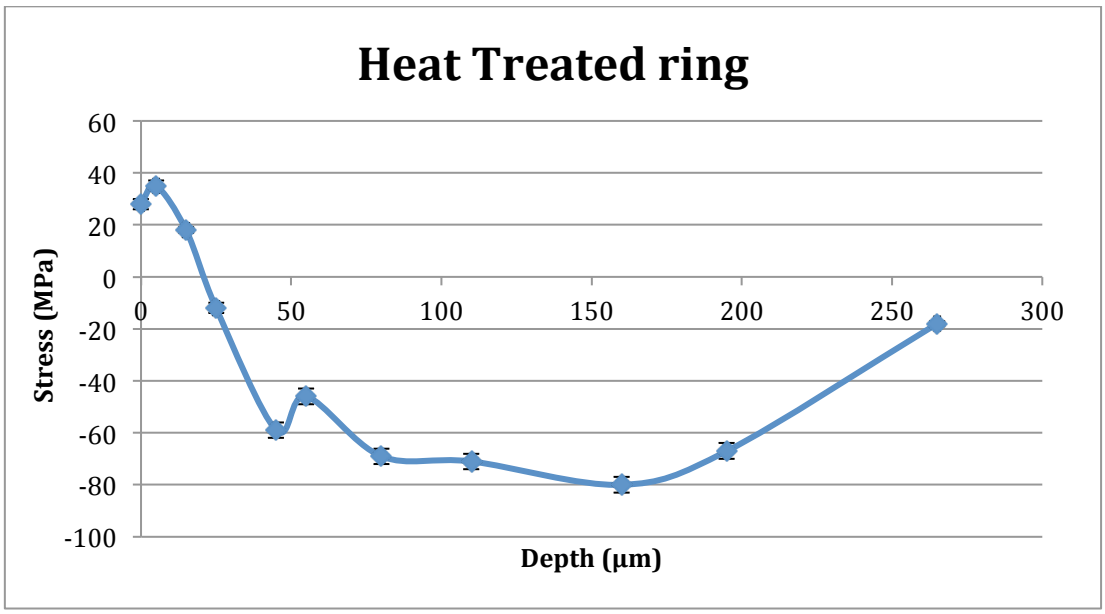

Figure 7.1 Heat Treated ring results in tangential direction

The graphic above, 7.1, shows the stress relieved with the X-Ray analysis in tangential direction. First, mention that the values' range is fairly small. The results show that the surface relieves tensile stress and that it starts decreasing until around 25 µm depth is reached. The next measurements obtained belong to compression stress relief. The data acquired show that the maximum stress relieved is 80 MPa of compression stress. The trend of the stress relieved could be close to 0MPa when a higher depth is reached.

3.7.2.2 Ring 1 analysis

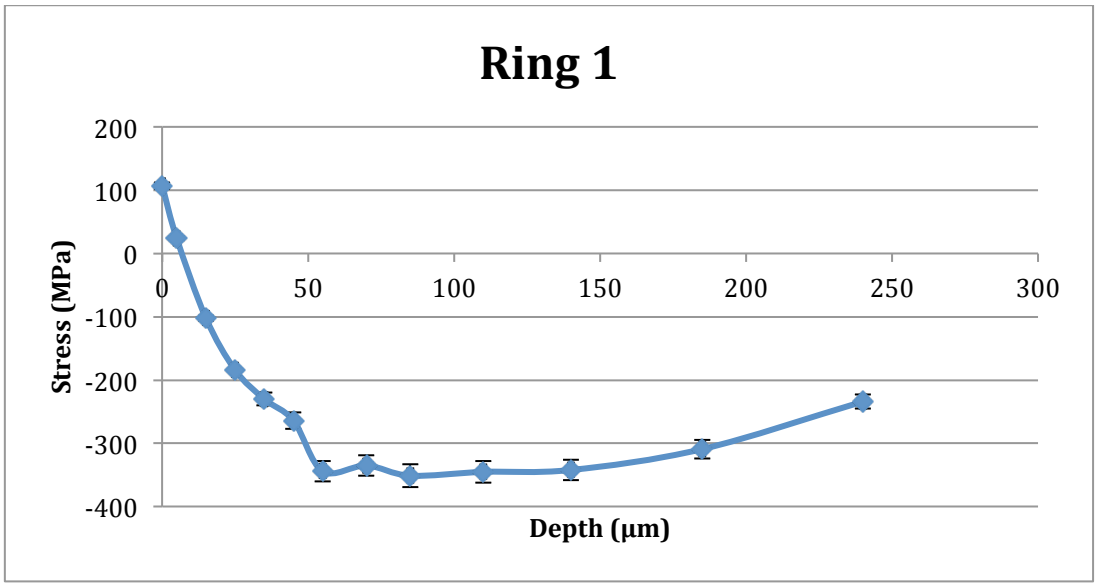

Figure 7.2 Ring 1 results in tangential direction

Figure 7.2 shows the values obtained when Ring 1 was analysed. It can be appreciated that, in the surface, the tensile stress value is a little bit higher than 100 MPa. The value measured starts going down rapidly until a compression stress peak is reached. The values recorded in depths between 50 and 150 μm are around 350 MPa of compression stress. The tendency analysed could reach a value of 0MPa but in a quite higher depth.

3.7.2.3 Ring 2 analysis

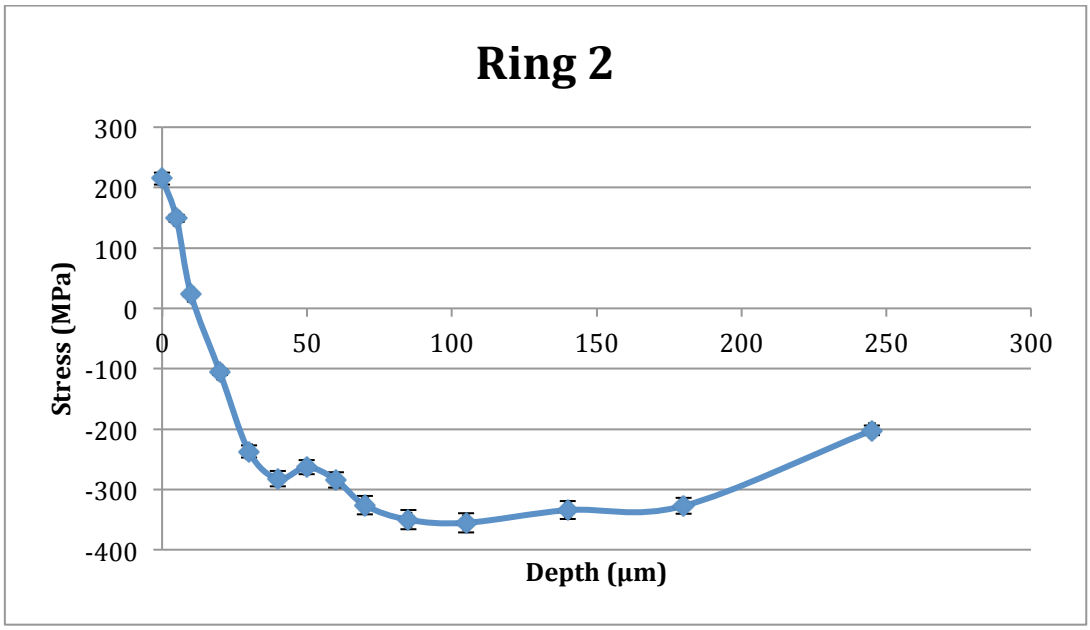

Figure 7.3 Ring 2 results in tangential direction

The graph displayed right above, 7.3, shows a similar behaviour to the previous one, 7.2. The surface stress value matches more than double, 215 MPa in Ring 2 but equal trends were observed. In figure 7.3, the lower values recorded start in around 80 μm and last until around 180 μm have been analysed. Same tendency to 0MPa was detected, perhaps in a higher depth.

3.7.2.3 Graphs comparison

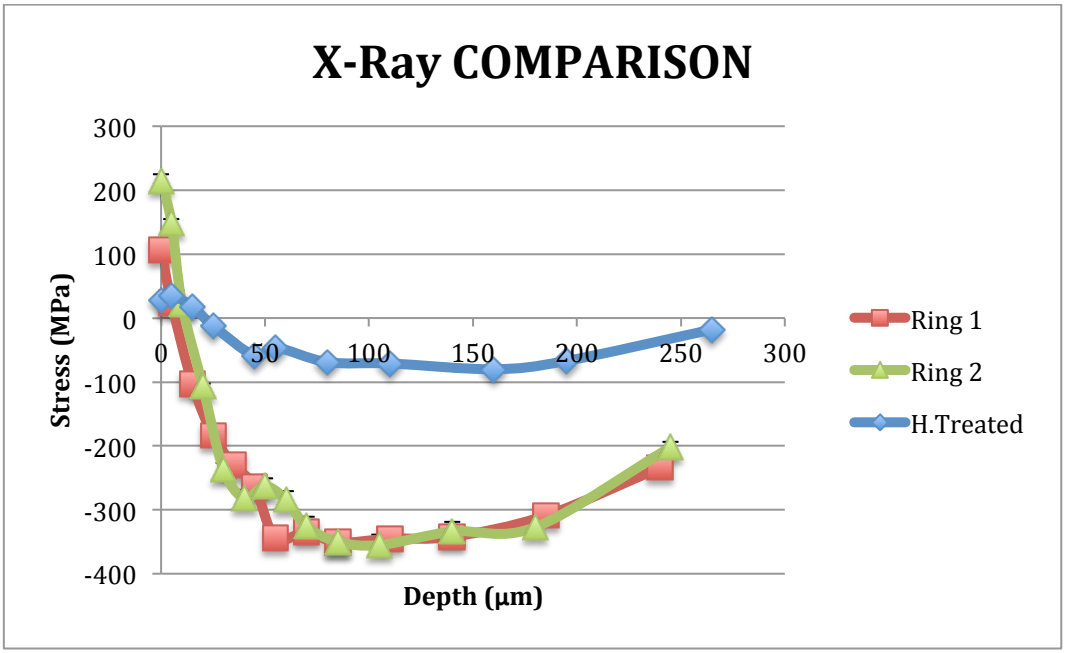

Figure 7.4 The three rings comparison in tangential direction

Just a quick glance to the graphic shown above, 7.4, presents the great difference between Rings 1 and 2 and the Heat Treated ring. The only advantage of making the ring vibrate to relief stress can be observed on the surface. In the small rings previously analysed, a difference between the VRS and the Machined rings could be perceived. However, this new X-Ray analysis shows that no real contrast can be spotted between them.

3.7.3 Discussion

By analysing the graphics of the X-Ray test, some points could be brought out. First, emphasize that the Heat Treated ring has considerably lower values all along the measured depth, a lower value of stress on the surface and a close value to 0MPa, -20 MPa, when the depth of 250 µm is acquired. The highest value reached is -80 MPa, instead of the -355 MPa obtained in Ring 2.

Rings 1 and 2 do not differ substantially. They both have equal trends and similar values. A difference to point out is that the Ring 2 surface value is twice greater than the one obtained from Ring 1. The range of maximum compression stress values recorded has equal lengths but, in Ring 2, starts in a large depth. The last difference to mention is that both rings have quite despair values on the last measurement. Ring 1 measures -234 MPa and Ring 2 has -202MPa of stress relieved.

A similarity to mention is that the three rings start with a positive value of tensile stress and rapidly switch to compression stress. It is maintained during the whole measurement executed.

3.8 COMPARISON OF THE HOLE DRILLING TECHNIQUE AND THE X-RAY TEST

3.8.1 Introduction

The stress relief of the rings was analysed by the two methods explained in previous pages. In order to get an idea of the accuracy of two different surfaces used in the Hole Drilling technique and the technique itself, a comparison of the results obtained will be executed right below.

3.8.2 Discussion

3.8.2.1 Heat Treated ring

Figures 6.22 and 6.24 display the non-polished and polished surfaces respectively in the Hole Drilling test carried out. Figure 7.1 shows the tangential direction analysis carried out with the X-Ray machine. When the three graphics are compared, it can be plainly seen that figure 6.22 differs totally to the other two graphics. Figures 6.24 and 7.1 present equivalent trends. They both start in around 30 MPa of tensile stress and reach 80 MPa of compression stress in 200 μm. the difference between them lies in the fact that the X-Ray test brings up compression stress values in a closer layer to the surface than the Hole Drilling technique.
The fact that the non-polished surface is totally different could be in consequence of the roughness of the surface and the interference of the glue in the strain gauge's measurements. As the values appeared to be quite low, the interference could have a high influence in the outcome results.

3.8.2.2 Ring 1

Figures 6.26 and 6.28 display the non-polished and polished surfaces respectively. Figure 7.2 presents the tangential direction analysis accomplished with the X-Ray machine. Taking a view to the three graphics, a clear similarity between their trends can be considered. Figure 7.26 shows pretty high values of stress relief but, the other two display very similar values down to 200 μm. The greater contrast between figures 6.28 and 7.2 is that the surface value differs quite substantially. The Hole Drilling Technique shows a value of 0MPa in the very surface and, on the opposite, the X-Ray test presents a value of 107 MPa of tensile stress.

3.8.2.3 Ring 2

Figures 6.30 and 6.32 display the non-polished and polished surfaces respectively. Figure 7.3 presents the tangential direction analysis completed with the X-Ray machine. When the Ring 2 is analysed, the opposite similarity appears. Figures 6.32 and 7.3 are the ones that have equivalent tendencies and ranges. The X-Ray test shows a value of 215MPa on the surface meanwhile, in the Hole Drilling test

results, there is no tensile stress on the surface. The polished surface of Ring 2 shows, in figure 6.30, a completely dissimilar values' range and also a high compression stress in the surface. The influence of the adhesive could be a reason of the strange behavior. However, the stress outcome values are rather high to advertise the interference.

5. DISCUSSION

In this point of the report, a brief discussion will be executed as discussions were already drawn up in each test performed.

Every test executed brings up the same conclusions. First, mention that both X-Ray tests and the Hole Drilling test show that the Heat Treated ring has lower values of residual stress. The VSR ring values are similar to the machined one.
Second, notice that the microstructure analysis, the hardness test and the FWHM value analysed in the first X-Ray analysis show a higher modification on the properties of the Heat Treated ring. No substantial differences were found between the Machined and VSR ring microstructures.
Besides, the Vickers hardness test shows disparate behaviours on the rings. The Heat Treated ring has a homogeneous hardness along the measured surface while the Machined ring slightly decreases and the VSR ring does it quite noticeably. The Knoop hardness test shows that the Machined ring possesses a harder layer on the edge, while the Heat Treated ring has an increase of the hardness with the depth. The VSR ring does not show much alteration along the layer examined.

To conclude, it should be remarkable the fact that the Hole Drilling test performed is not completely reliable. As the values were very fluctuating, new graphics with sets of three values had to be implemented. Even the new graphics were still not enough accurate solutions to get a clear conclusion. The X-Ray method is more reliable technique to analysis the rings' behaviour.

6. CONCLUSSION

The aim of this project was to analyse which of the methods studied had a greater residual stress relief. Every test carried out point that the heat treatment is the most adequate technique to reduce the mentioned stress. Acceptable difference was detected to state that the Heat Treated ring had less residual stress than the VSR treated ring.

As was mentioned in the scientific context, 40% of the residual stress could be relieved with the VSR technique. It also was mentioned that the stress relief was dependent on the vibratory amplitude so perhaps the amplitude used in that ring was not the appropriate one.

To conclude, it would be brought out that, conceivably, an analysis of the mechanical properties of the Heat Treated ring could be executed in order to get a clear sense of the variation of properties suffered with the heat treatment. Considering those factors, a clear idea of the consequences of the variation of the properties could be compared to the residual stress relief.

Holding both considerations, the most reasonable solution could be selected.

7. REFERENCES

[1] Stress Measurement by X-Ray Diffraction-SAE J784a, Society of Automotive Engineers, INC., 1971.

[2] C. A. Walker, A.J. Waddell and D.J. Johnston: Vibratory stress relief- an investigation of the underlying processes, 1995.

[3] A. S. M. Y. Munsi, A. J. Waddell and C.A. Walker: The influence of Vibratory Treatment on the Fatigue Life of Welds: A Comparison with Thermal Stress Relief, 2001.

[4] G.-C. Luh and R. –M. Hwang: Evaluating the Effectiveness if Vibratory Stress Relief by a Modified Hole-Drilling Method, 1998

[5] M. C. Sun, Y. H. Sun, R. K. Wang: The vibratory stress relief of a marine shafting of 35# bar steel, 2003.

[6] Y. P. Yang: Understanding of Vibration Stress Relief with Computation Modeling, 2007.

[7] Metals handbook, Ninth Edition, Volume 9, American Society for Metals, 1985.

[8] Günter Petzow: Metallographic Etching, American Society for Metals, 1978.

[9] A. Puskar: The use of high-intensity ultrasonics, Amsterdam, Elsevier Scientific Publishing Co. (Materials Science Monographs. Volume 13), 1982.

[10] R. Norman Weller, John M. Brady and William E. Bernier, Efficacy of ultrasonic cleaning, Journal of Endodontics, Vol. 6, No 9, 1980.

[11] Donald R. Askeland, The science and engineering of materials, third edition, 1998.

[12] William D. Callister Jr., David G. Rethwisch: Materials Science and Engineering: An Introduction, 2010.

[13] www.struers.com (consulted 04/10/2013)

[14] Dagobert William Rudorff: Apparatus and Method for cutting materials, 1950.

[15] W.J. Gray and F.H. Spedding: A Technique for cutting and Polishing Small Metal Spheres, Institute for Atomic Research and Department of Metallurgy, Iowa State University, VOLUME 40. NUMBER 11, 1969.

[16] Prof. –Ing. B. Scholtes: Residual Stress Analysis of Components with Real Geometries Using the Incremental Hole-Drilling Technique and a Differential Evaluation, Kassel University, 2007.

[17] Technical note: Measurement of Residual Stresses by the Hole-Drilling Strain Gage Method, Micro-Measurements ©, document number: 11053, 2010.

[18] Vangi, D.: Residual stress evaluation by the hole-drilling method with off-center hole: An extension of the integral method, Journal of Engineering Materials and Technology; Journal Volume: 119, 2009.